SIMU Programme
supported by the
European Science Foundation

NEWSLETTER

ISSUE 1

Editor: Dónal Mac Kernan
Centre Européen de Calcul Atomique et Moléculaire
Ecole Normale Supérieure de Lyon,
46 Allée d'Italie, 69364 Lyon Cedex 07, France

Tel:00-33-04-72728632   Fax: 00-33-04-72728636   email: dmack@cecam.fr

The SIMU programme aims at building cooperation across Europe in the field of computationl physics and chemistry of condensed matter, with particular emphasis on the development of novel computational techniques to perform multiscale molecular simulations.

URL: http://simu.ulb.ac.be/

Contents

I

Preface

We are launching this, the first issue of the *SIMU* Newsletter, to contribute to the general aim of the *SIMU* programme: namely, to provide support to the scientific community, which recognises itself via the goal of developing new simulation techniques to meet the challenges of bridging scales in molecular simulations of condensed matter.

Why a newsletter? We feel that there is a need for more information to flow among us. Information on the very existence of the programme (some of you who endorsed the proposal submitted two years ago to *ESF* may have forgotten what it is all about!), information on the activities which are being planned at this time (workshops, tutorials etc...), on the activities which might be proposed in the future, information also on the different groups that participate: who they are, what they do, how they work, etc... We really would like that this newsletter to become a forum for discussion, so as to have in common a knowledge and understanding useful to others in their work.

We have asked some *SIMU* members to contribute to the newsletter in various ways. The main body consists of articles presenting research related to our "bridging the gap" theme: dissipative particle dynamics, polymer modeling, homogeneous nucleation and electron transfer in biological molecules. The articles we intend to present in future issues need not be original, as the interest of collecting them here comes from the fact that we represent a community with wide interests so that the results described may be unknown to many of us. We will require your cooperation for future articles. The emphasis will rather be on presenting state-of-the-art molecular modeling approaches in different fields to an audience which may not be familiar with the precise physical context but share the concern about the techniques to be used. We also know that writing papers and articles already takes much of our time, and we would rather encourage you to provide us with reports that have already been written at other occasions, but whose distributions have been limited, or papers written for specialised journals, but which may be of general interest.

We also would like to present here some material which is less traditional in the scientific literature. We invited G. Ciccotti to present his thoughts on the importance of the changes that have occurred in physics due to the possibilities offered by a heavy usage of numerics. Similar presentations of personal views are invited from the *SIMU* community. We also want to address some very practical questions, like how to choose a hardware configuration: we present the report of a group having acquired a cluster of PCs. We look forward to receiving comments and reactions from you, possibly with different views and different choices, and we will be glad to relay those reactions in our next issue (we plan two issues a year). There are also sections dealing with conference announcements, interesting URLs on the Web or job offers. Those sections might be very useful in the future, if you feed them with information you have or tricks, addresses etc...you know and wish to share.

This first issue of the newsletter is being sent to you by ordinary mail. Future issues will be put on our web server (http://simu.ulb.ac.be/) from which it will be down-loadable and a notice will be sent to all *SIMU* members. Hard-copies will be sent on request only. Feel free to contact us for positive or critical comments, ideas or suggestions: they will all be welcome.

Michel Mareschal, Chairman of the SIMU steering committee
email: michel.mareschal@cecam.fr

Dónal Mac Kernan, Scientific Assistant to the SIMU programme
email: dmack@cecam.fr

II

SIMU in a nut shell

WHAT is *SIMU* ?

SIMU is an acronym for a programme sponsored by the European Science Foundation (*ESF*) whose full title is :" Challenges in Molecular Simulations: Bridging the Length- and Time-scale Gap". The proposal was submitted in 1998 to *ESF* and has been approved for 5 years, starting in 1999 and ending in 2003. The text of the proposal as well as the list of teams endorsing the programme can be found on our web site (http://simu.ulb.ac.be/).

What is the budget?

The *ESF* programmes are funded "à la carte", according to the number of supporting *ESF* member organizations. *SIMU* is being funded by Belgium (*FNRS*) , Denmark, Finland, France (*CEA* and *CNRS*), Germany (*MPG*), the Netherlands, Italy (*INFM* and *CNR*), Norway, Portugal, Spain, Sweden, Switzerland and the United Kingdom. The total annual budget is around one million French Francs and is meant to support networking activities like short visits, conferences, workshops and tutorials as it was planned in the proposal.

Who is in the steering committee?

The programme is managed through a steering committee: this committee is composed of one representative per country, plus the chairman and a few invited experts: D. Theodorou, D. Frenkel and G. Ciccotti. E. Crespeau, *CECAM* secretary, is also in the steering committee. This committee met twice already: in March 99 and in November 99. Its next meeting will take place in November 2000 to decide the funding of activities for the year 2001.

Who is a member of *SIMU*?

Funding is usually limited to *SIMU* members that are laboratories of funding countries which have endorsed the proposal. The steering committee has decided to have an open policy concerning membership: laboratories whose research is directly concerned with the aim of *SIMU* (development of techniques for bridging the gap) can apply to become members of *SIMU*. They have to write to the committee chairman and to their national representative, presenting their lab and stating how they can contribute to the programme. Labs of countries which are not *SIMU* funders (like Russia, Greece or the United States) can also be associated to the programme. The committee also decided that workshop funding would be decided on solely on scientific criteria, and not on nationality. Acceptance of a participant is the responsibility of the organizer.

What are the *SIMU* activities?

In 1999, four workshops have been proposed within the *SIMU* programme and a similar number is being planned in 2000. Most of the workshops will take place at *CECAM* (in Lyon), taking advantage of the cooperation offered. This is however not at all a mandatory location and workshops can be organized at any other place. Th typical budget is around 50 000 FF, and covers staying expenses of between 20 and 30 participants for a few days. This year *SIMU* is supporting two schools, one in Amsterdam and the other in Manchester. The Amsterdam school took place in January, the Manchester school will be organized at the end of June at UMIST. The *SIMU* support consists of grants for partial financial support of staying and travel expenses. Tutorials are organized in collaboration with *CECAM* in Lyon. Three or four one-week tutorials will be organized this year: participants can apply for grants to cover staying and travel expenses. Short visits can also be funded by the programme. Whereas in the case of workshops, tutorials and schools, support for year 2000 was decided during the committee meeting last November, for short visits, there is an email decision process taking place end of December, end of March and end of June, as well as the November session. Application forms for those funds can be found on our web site. Note that the funding decision depends on a connection existing with the aims of the programme. Note also that such funding can cover meetings of groups who would like to organize TMR networks or similar projects. Finally, two major conferences will be organized during the programme's duration. The first one, "Bridging the time-scale gap", will take place in Konstanz from September 11th till September 15th, 2000. More details on these activities are in the newsletter and on the web site which is regularly updated.

Who can propose activities?

Members are encouraged to make proposals. Workshop proposals forms are available on the web site and they should be sent to the programme chairman before September 30th this year. Proposals will be reviewed by two external experts and sent to the committee members. The committee will then decide in November. Contact the programme chairman or your country representative to see how a proposal can fit within the general programme. Whom to contact?

Do not hesitate to contact directly the programme chairman, Michel Mareschal. You can also contact Dónal Mac Kernan, who is in charge of scientific assistance to the programme.

III

The Computer, Machine of the Dreams of Theoretical Physics

Giovanni Ciccotti
Dipartimento di Fisica,
Università di Roma "La Sapienza",
P. Aldo Moro 2, I-00185 Roma, Italy
email: Giovanni.Ciccotti@roma1.infn.it

The scope of theoretical physics

Modern science was born, at least in principle, the day when humanity decided to liberate itself from the Aristotelian idea of the limits which the condition of being by Nature would impose to our possible activities. For example, it is well known to the historian of science, the argument used by Aristotle to exclude the possibility of automatic machines (in his words, "automata"): if such machines were to exist then slavery would be unnecessary, but slavery is "by Nature" and therefore automata cannot exist. The methodological idea that something unnecessary, or better still, even contradictory with something else cannot exist, is interesting, and in other contexts, even useful. Here, however, it served to define something in principle impossible which was false, and was an ill-omen for human development. The first and most lucid herald of modern science was Francis Bacon, who, although contributing nothing of during to modern knowledge, saw with great clarity what science could do for humanity (making men masters of Nature) and under which condition: submitting mankind to Her own laws. The question obviously becomes a bit more entangled if we try to define what should be those laws, how they should be discovered/invented and what are their limits of validity. There Bacon becomes totally useless, but we can go to Galileo for a few good ideas, or, more generally, to a formalized, or, even more explicitly, mathematical concept of Nature. Contrary to a widespread opinion, held also by physicists, the originality of Galileo is not so much in his insistence on "sensible experiences" (in the words of Galileo the "sensate esperienze" are nothing else than what we call experiments), but in the idea that once the maximum number of "sensible experiences" has been performed, it is necessary to formulate the results mathematically, so that one can derive, by computing, the maximum number of behaviours from the fewest number of principles. The trust that we can place in mathematics guarantees us that, if a consequence is ill-predicted by our model, there are not that many culprits to look for; it is the model which is inadequate. Therefore we must change something in the model, be that simply the change of parameters, or up to the higher level of the general principles, but, in any case, through a relatively linear procedure remaining largely under our control. It is mathematics that plays here the role of protagonist. It is worthwhile to try to understand, therefore, how this happens and why mathematics simplifies so much the search of the error, and, when applicable (we will come back to this shortly), providing so much surety. Yet again, it is Galileo that helps us with a truly amusing and cunning description of the situation. God, Galileo says, knows all possible and imaginable mathematics, while we, poor men, know but a few scraps. Nevertheless, adds Galileo, those few scraps we know as well as Him, for the simple reason that mathematics is "truth" in its purest form, divine. In more modern and less theological terms, we could say that as mathematics is our own creation, and not that of the external nature, it does not have the margin of error that belong to anything which does not stem directly from us. Summing up, the essence of the problem seems clear: if we succeed in representing a large family of phenomena with a few equations, then all of those phenomena are totally under our control, and we may consider ourselves, Bacon-like, to be their masters. That is we can use our knowledge to produce situations different from the ones naturally found, and moreover, to our own advantage. So the question changes, becoming: when is it possible to represent the largest number of phenomena knowable (i.e. the universe) with few equations? In the exact sciences three hundred years have passed during which one has tried to say ALWAYS. In the human sciences, or in any case, as one gradually moves away from the exact sciences, the answer is NEVER, or almost never, or at its most optimistic, a few times. Now the truth is less banal than that, and it is worth discussing in some detail.

Since the time of Newton, theoretical mechanics has earned the respect of "practical" mechanicians, and has given the impression that the Baconian ideal was at hand. Thanks to reductionism (atomic hypothesis and its derivatives: that the complexity of reality are only manifestations of atoms and their movement) and to the generalization of mechanics from the classical to the quantum (and relativistic), also chemistry has timidly followed the same direction. However neither biology and even less still, the social sciences have followed this pattern. Why ? Is this an inevitable fact, linked to the inability of mankind to dominate on a grand scale, or is it purely accidental, due to a few historical limitations in our development ? Looked at closely the first hypothesis seems unnecessarily pessimistic, based on an assumed incapacity of mankind, while the second, seems much more convincing, at least to the extent that one looks at chemistry and biology, where there are signs of profound transformations bringing these disciplines to resemble the best (theoretical) physics. While, in this field, no hypothesis can be completely proven, all recent developments add credibility to the idea that, soon, chemical and biological procedures will be as controllable as those mechanical. In other words, the dream of theoretical physics to reconstruct the world, which until yesterday appeared inapplicable to the chemistry of materials or to biology, now seems increasingly credible. It seems best then to accept the optimistic hypothesis, and try to understand what primed this process, and what are the limitations of the theory that we are starting to overcome. The idea I wish to demonstrate in the following pages, is that, in the last three hundred years, the missing ingredient in the development of theoretical physics, in the sense of Bacon, has been simply calculating power. Equipped with an open theory (certainly much more refined that that of Newton, but fundamentally the same) and with a growing computing power, we can hope to realize Bacon's dream: to know nature so well as to be able to think of submitting Her to homo sapiens.

Theoretical physics and computing

About three hundred years ago, thanks to the work culminating in the synthesis of Newton, the idea of science as power over the world was fully realized in classical mechanics, which then was promoted, as the most accomplished model of complete knowledge. In ballistics, astronomy, or practical mechanics, the feeling that one had in hand a theoretical instrument capable of going over every difficulty, was considered well founded. However, things were quite different if one left the domain of purely mechanical phenomena. So much so that, at the beginning of the nineteenth century, Auguste Comte felt science should not be classified in a unified way, but rather that each domain should define its own criteria and way of being scientific: thermology and optics being presented as distinct from mechanics, similarly to, but with even greater justification, chemistry or life sciences. The interpretation of acoustic, electromagnetic, and optical phenomena in terms of mechanics (be it of particles or of the continuum, i.e., classical field theory) required about a century. But this was, in a sense, less exhausting than unifying mechanics and thermodynamics. This accomplishment, of the end of the last century, required the conceptually new and remarkable use of the methods of statistics to understand the macroscopic behaviour of systems still fully mechanical. It was from this moment that the unifying ambition of physics ceased to be a chimera, reasonable but provable only in very restricted domains, to become a concrete possibility, both theoretically and practically. It is true that to arrive so far, the laws of physics had to be revised (relativity, and above all quantum mechanics attest to this). However, the revisions were less profound than is often recounted, and did not so much affect the entire edifice of the scientific explanation of the universe, but only the internal consistency of a few presuppositions. The truly important addition to the mechanical ideas of Galileo and Newton was made by Boltzmann, who systematically used statistical methods in mechanics to obtain a unified explanation of macroscopic systems (that include the universe..) from mechanical microscopic ones (the atoms...). To achieve that, a complete new mathematical discipline was created and formalized: the theory of probability, whose axiomatization was given by Kolmogorov in 1933, practically at the same time, as the completion of the construction of the new mechanics by Schroedinger, Pauli and Dirac, to mention a few of the better known names. At this point, the explicative and predictive power of theoretical physics became extremely broad and, unlike what happened at the beginning of the nineteenth century, involved not only all of physics (mechanics, heat, electromagnetism etc), but also the simpler phenomena of chemistry and, at least as a potentiality, the basic phenomena of life. Although from a technical point of view this happened at the beginning of the thirties, from a more general perspective, it was already expected by the great scientists of the end of the nineteenth century, foremost among them Henri Poincare. His writings on the future of physics, written at the beginning of the twentieth century, are still astonishing for their lucidity, clarity and relevance today.

There is however, a but, and not a minor one, in all this gratification. To understand this, it is useful to make a distinction between the virtual and real predictive power of theoretical physics. The former is enormous, but obviously not very satisfying, while the latter is, everything considered, minimum. The difference is entirely due to the lack of capacity and power to calculate, as I will try to show in what follows. And it is not a minor point, because to understand this is to appreciate a major epistemological change. Scientific progress, in these eyes, is no longer the addition of new scientific laws to those already present, but rather the derivation of all of the consequences of the known laws, and only in the eventuality of their deficiency, the updating of the same. That is, the effort (and the value) of research is no more concentrated on the creative activity of the legislator, but on the capacity to rationally reconstruct a domain of phenomena by algorithmic derivation from simple and general laws. Here is the source of the importance acquired by the concept of the model (now sometimes confused with theory) in modern research. A great theoretical physicist, Dirac, seems to have completely missed the point when he maintained that the duty of theoretical physics is to find the laws, the rest being chemistry, because in doing so he practically destroyed the modern, Baconian, concept of science. But let us return to our theme, and try to show the impact of the capacity and power to calculate on the development of science, and on the Baconian dream which corresponds to it.

I will proceed with two extreme examples to place what we are discussing exactly into context. The courageous book of Schroedinger on "What is life" and the comment of Von Neumann at the end of the forties on the problem of meteorological predictions. I will then try to further illustrate the point by comparing the presentation of mechanics in an old, but still excellent and often used book of mechanics, "The variational principles of mechanics" of Cornelius Lanczos, with that of any modern text.

In a book written at the beginning of the forties, and still very famous, Erwin Schroedinger, justly proud of the contribution of quantum mechanics to the development of knowledge, decided to face the question of the importance of the (new) physics for the understanding of the phenomena of life. The book is still today extremely interesting, and yet completely dated. Schrodinger's wish in fact is not to explain in detail (or put more precisely, to calculate) the phenomena of life, but rather to demonstrate that they are not incompatible with the known laws of physics, since, on the contrary, physics alone may even be sufficient to perceive a few biological regularities (laws in the sense of Comte...) without the need of anything else ! In other words, a steady step backwards with respect to the the Newtonian realization of the Baconian programme.

The story of Von Neumann (one of the founding fathers not only of computational physics, but even of the modern computer) is completely different. Von Neumann had discovered and cured a few instabilities in the numerical solutions of partial differential equations, and had decided to apply his algorithms to the equations governing weather prediction. The algorithms were for the epoch (and, to tell the truth, still are) computer intensive, so the calculations could only be done by computer. All of the procedures checked, the calculations took two days to make a two hour forecast. It was clear that either one found faster algorithms, or faster computers, or such "predictions" would remain of no practical interest. We all know how the situation evolved, so much so that today we can produce in a couple of hours a prediction valid for forty eight hours, and we continue to improve, Amen to Dirac's ridiculous comment.

I already said that the Von Neumann example is not a typical one, but an extreme case if very important. The main significance in the power to calculate (in a computer intensive way, not by hand!) lies in the possibility to study the so-called non linear equations, whose qualitative behaviours are totally unexpected since we have no analytical, exact, indication on how they should behave. The first impact of the capacity to calculate introduced by computers into the theory was really here, in the possibility to study the behaviour of systems whose evolution follows laws that we know how to write, but not how to compute, i.e., to solve. This is the typical case in physics, and, even more striking, in mechanics as massive calculations revealed, so creating an important divide between the situation before and after the advent of computers.

The easiest way to characterize the divide is to refer to the book of Lanczos, and to compare it with any modern book on mechanics. The former consists of an elegant, intelligent and profound presentation of the principles of classical mechanics as they have been elaborated over the centuries. It is useful and complete and says much on the various different but equivalent ways to formulate analytically a mechanical problem. However, Lanczos says almost nothing about how to solve a problem once it has been correctly formulated. For him, mechanics formulates, it does not solve. Solving is at the same time both banal, and too difficult. In any event, it is the duty of mathematics, and, if we believe it, we can invoke the infinitely able mathematician of Laplace, otherwise, we can limit ourselves to the few, very few, problems having solutions that we know how to write. This is not only Lanczos, it is the same for any book of mechanics of his generation. Today, instead, the scope of a book on mechanics is to learn how to classify the solutions, including in depth discussions on the possible behaviours of a system, its stability or instability, and according to which criteria one can obtain clues on the behaviour of a given mechanical system. Here numerics plays an essential part, and any astute trick to help solve the problem is welcome. The idea can come from a qualitative study of the differential equations (that govern mechanical behaviour) or from having obtained a great deal of numerical evidence: it does not matter how, one is very tolerant about the methods, but the result must not be the FORMULATION of the problem, but its SOLUTION. Obviously, there are no solutions without exact formulations, but it is important to understand that the emphasis has moved and what counts now is not to find a new formulation that permits one to understand a particular problem better, but to be able to face it with brute force (that is, as we say in the profession, by calculating massively) to extract all possible behaviours, and in the end, to predict concretely, and not virtually the behaviour under given conditions.

We have come to the end of our general discussion of the present situation: the laws of physics until proven otherwise, are true and universally so. One applies and values them always not virtually, but effectively. The world is made of space, time (i.e. motion) and matter (i.e. inertia to movement, or, equivalently, mass, and interactions). Its laws of evolution are known to us, we solve them by calculation (or by finding the way, the algorithm that can do it). After which, if we already have the power to calculate sufficiently, the problem is no more a limit to our power, but a further occasion for the command of Nature, obtained by submitting us to Her own laws (the famous Baconian formula). Otherwise one deals with the problem from many sides, inventing new and more powerful calculating tools, new algorithms and new approaches, further schematizations that could give a solution step by step, and end in controlling Her.

This is the most interesting part of the procedure that we are attempting to describe, and it is on it that we will concentrate in the final part of our discussion.

Computer simulation, and the dream of infinite power of science

The success of the programme that I have tried to describe up to here is based on a characteristic of physics (but it would perhaps be better to say of the world, i.e. of the objects that we would like to know) that has simplified enormously the solution of the reductionist programme that we have posed: reconstruct mathematically the world from the ultimate and simplest elements (before atomic theory I would have said the atoms, but with the philosophical meaning of the term, instead our atoms are not ultimate in any sense, their place having been taken by elementary particles). The point is that little by little, as a system becomes more complex, its "atoms" become larger structures, so as to retain, at least for the problem at hand, the simple character that distinguishes the atoms. Let us try to explain a bit better.

Chemistry is constructed from atoms to form at first molecules, and then molecular complexes and materials as an aggregate state. Having discovered that the atom is not simple but is made of electrons and nucleus, and that the latter is not in fact elementary, but can be broken into fragments that cannot again be considered to be elementary, one finds that the situation of chemistry has not changed greatly. In fact things are more or less the same as before, in the sense that the essential of chemistry comes from the electromagnetic interaction between electrons and nuclei as stable entities, while their complexity, although true, needs only be considered explicitly if one wishes to. Only in this case do the other fundamental interactions become important, for which there are all the conceptual tools of elementary particle physics (and this, when looked at closely, reduces to the same as one uses for electrons and nuclei, except for the simplifying low energy approximations, where the nuclei are stable, which are not valid at high energies, where nuclei can be broken). So we are permitted to solve one problem at a time, and never have to take into account simultaneously all of the possible levels of complexity. Thus, to give an example, to determine the stability and other properties of atoms it is necessary to consider electrons and nuclei. But, they may be treated as material points, with mass, charge, and magnetic moment, devoid of any internal structure, even though we know that this is not true in all possible conditions. However, if we are able to split the nucleus, then the nuclei and the electrons will form not atoms, but rather an anonymous, uninteresting mix of electrons and nuclei (or their fragments). Similarly, if we wish to construct a molecule, we not not need to consider all the nuclei and electrons individually. It is enough to consider some heavy material points (constituted of the nuclei and the most tightly bound electrons), as being even fixed, and, as for the rest, light material points, consisting of the residual electrons. The ensuing objects may be considered as elementary for the problem that we wish to solve. Finally, if one wishes to consider many molecules together and predict the behaviour of such an aggregate (i.e. a piece of ordinary matter), it is sufficient to treat the molecules as material points interacting according to given laws. Once the game is understood, it can be continued ad infinitum.

It is important to realize that the laws which reign over these "elementary particles" are always the same (the famous apple falling on the head of Newton, made him understand universal attraction, and thus the possibility of the moon falling on the earth), they are simply shifted from one spatio-temporal scale to another. This was not unknown in the nineteen thirties, i.e. before it was possible to perform serious calculations, but could not bear fruit on a large scale until one knew how to perform intensive calculations on such scales. Before this, one had to invent simplistic mathematical models containing the essential information of a few levels of complexity. Now, one can not only solve truly realistic models, but above all, systematically calculate the essential information relating adjacent levels of complexity, from the inferior level to the superior (e.g. compute the form of interaction between molecules, using a very detailed model, and then depict molecules as a collection of material points interacting with the computed laws to compute their collective behavior). Thus, one no longer does what in the slang of physicists is called, and with some mild contempt, phenomenology, but true predictive theory or, as one says today in appropriately noble Latin, ab initio.

An interesting cultural by-product of this situation, typical of our times, but one that I do not wish to pursue here, is mathematical modeling running wild for whatever type of phenomenon, even in domains where it is not yet, or even not at all, possible to proceed mathematically (like in the social sciences or the explanation of history, those that someone has called, with a well chosen metaphor, " the formless doctrines"). The consequence is that mathematical toys of little value are called scientific. But let us return to our principal theme.

The success of this programme, over the last fifty years, has been explosive, and has had an effect not only in the ab-initio prediction of already known phenomena, but in the discovery of new phenomena thanks to the more and more cunning management of continuously improving experimental equipment. Consider, for instance, that one can now "see" experimentally spatial structures on atomic scales. As a result, we have now learned how to predict the molecular structure arising from not only a few atoms, but from thousands, and the physical properties of natural and synthetic materials having the complexity of polymers. Little by little we are realizing that biology is of a complexity that we can already hope to deal with really and not only virtually, in our generation, that even life is constructible (not simply understandable !) from matter and movement, that is, with the usual tools of physics. However this is not the physics of Comte but a physics gone beyond the discipline dealing only with physical phenomena (as stated, with amusing logically vicious circles, in many physics textbooks), one that has permeated chemistry and biology, making it ever more difficult to define a physicist as physics is going to be found everywhere, and, ultimately, will no more be characterisable as a separate discipline neighboring others. To content medicine, empirical practice par excellence, perennial nightmare of physicists! Whatever one may think, bionics is less science-fiction, and more premonition for what is happening in front of the eyes of everyone.

IV

Industrial Aspects of Mesoscale Modeling

J.G.E.M. (Hans) Fraaije
University of Leiden, the Netherlands
email: j.fraaije@chem.LeidenUniv.nl

Introduction

In the arena of applied soft-condensed matter physics, mesoscopic dynamics models are receiving increased attention as they form a bridge between fast molecular kinetics and slow thermodynamic relaxations of macroscale properties. The topic is of considerable importance for the understanding of many types of industrial complex liquids. Eventually coarse-grained models for the slow diffusive and hydrodynamic phenomena in phase-separation dynamics may serve as a new simulation tool for chemical engineers in industry... We have all used introductions like this one, they sound nice. But, is there any reality to it? The organizers of the SIMU newsletter asked me to write a paper about my industrial experiences and views. I briefly discuss the background of the EU MesoDyn project we started a few years ago, the current status and where to go in the future. The paper is not a scientific review, but rather a personal collection of views and ideas, and it does not necessarily reflect the opinion of the MesoDyn partners. For details and papers I refer to the MesoDyn pages at
http://www.fwn.rug.nl/mesodyn/index.html

MesoDyn project

The following is a citation from the abstract of the MesoDyn project description. "In this project we aim to provide the chemical industry with general purpose software for mesoscale soft-condensed matter simulations, based on a functional Langevin approach for HPCN-platforms. The prototype of the parallel MesoDyn simulation program produced in Work Package 5 of the CAESAR HPNC-demonstrator project (EP8328) is used as background information" And from the introduction, "In the last decade molecular modeling has grown to an essential part of research and development in the chemicals and pharmaceuticals industries. For a longer time, chemical engineers have analyzed macroscale properties using a variety of continuum mechanics models. Despite the considerable success of both molecular and macroscale modeling, in the past few years it has become more and more apparent that in many materials mesoscale structures determine material properties to a very large extent. Mesoscale structures are typically of the size of 10 to 1000 nm. The emerging industrial relevance of mesoscale modeling is obvious, nevertheless the necessary general purpose computational engineering tools are absent. The MesoDyn project bridges the gap between micro- and macroscale modeling by the development of a new class of models and software modules for the mesoscale chemical engineering of complex industrial polymer liquids. The project is part of the Information Technology Program (ESPRIT) of the European Communities. The project started in January 1997."

The partners of the project are: University of Groningen (my group, responsible for methods development), IBM (Peter Altevogt, parallellisation), MSI (Dave Nicolaides, graphical interface and marketing), Shell (validation), Norsk Hydro (validation) and BASF (Olaf Evers, software, validation and project management). The end of the project is spring 2000, so we are wrapping things up right now.

In the core of the project is a general purpose library of fast numerical routines, such as non-linear equation solvers, stencil operators (these are spatial filters like $\nabla^2(\cdot)$) or convolutions $\int f(\mathbf{r}-\mathbf{r}')(\cdot)d\mathbf{r}'$), noise generators and several types of polymer path integral routines. The routines are written in MPI/C/C++, and can be accessed via a higher-level language (Tcl/Tk). The library runs on any machine which supports MPI, that is all parallel computers, and most low-end workstations and PC's.

In principle, the library lets a modeler compose his or her own model, by combining various library calls. The set of routines as it is now is excellently suited for study of all kinds of non-linear partial equation systems which occur in pattern-formation models, such as meteorological models, reaction-diffusion models or copolymer microphase separation models and even image analysis. In practice, the library has been used mostly for simulation of polymer phase separation, and MSI's graphical interface is also focused on these systems. Since fall 1997 the first version of MesoDyn software has been available on the market. It is one of the packages in MSI's Polymer Consortium 2000.

My group has been responsible for the theoretical background: both the numerical aspects (stencils and solvers), as well as the modeling of the polymer phase separation. The latter is what we have referred to as the dynamic density functional method. The idea is very simple: we imagine that for every real non-equilibrium system one can invent an equilibrium system, balanced by an external potential. The potential is conjugated to the order parameter(s), which in the case of polymer phases are the concentrations of monomers, blocks or entire polymer molecules. The relation between order parameter and external potential is the density functional. The gradient of the external potential is a thermodynamic force, which one can use to drive a dynamical process. As long as the dynamics is (very) slow - which is very often the case in condensed polymer systems - one can neglect elastic contributions from incompletely relaxed polymer conformations. So far we have studied the classical single-chain density functionals (Gaussian chains) in a mean-field environment. As a result the simulation produces the time-evolution of a 3D morphology of a certain (co)polymer mixture on a coarse-grained scale. A typical set of equations to integrate is

$$\begin{aligned}
\frac{\partial \rho}{\partial t} &= M\nabla^2(-U + \left[\frac{\delta F}{\delta \rho}\right]_{MF}) && \text{(IV.1)}\\
\rho &= DF(U) && \text{(IV.2)}
\end{aligned}$$

where the first equation is the dynamic equation, and the second is the density functional equation containing the polymer path integral. These are two equations with two unknowns (the fields U and ρ). The set can be integrated by iteration of U in time. The spirit of the method is very similar to the quantum molecular dynamics methods proposed by Carr and Parinello, and to the methods proposed by Hansen for colloid particle dynamics. Of course, in the case of mesoscale chemical systems one has to take care of the proper mobility coefficients, the hydrodynamics and so on - this seems less of a problem with quantum molecular dynamics.

In the course of the project we have studied a large number of theoretical and numerical aspects for the purpose of making the method more applicable to real industrial systems (papers can be found on the web site). Some problems turned out to be trivial, other turned out to be very, very tough.

The trivial problems are those where one can adapt existing polymer self-consistent field theories to the dynamical case, for example path integrals for branched polymers, path integrals for worm-like polymers (rather than Gaussian models), models for polymers with dissimilar monomer size, mean-field models for Donnan equilibria, boundary methods for geometry constraints and equation-of-state models for compressible systems. Even reactions are relatively easy to model on this level. For a brief moment we also contemplated adapting density functional models for more strongly correlated polymer systems (such as PRISM), but we did not pursue the matter. It seems that the single-chain mean-field model works reasonably well for a large class of problems, and, for practical applications perhaps more important, Flory-Huggins parameters of sufficient accuracy are abundant or can easily be measured. The tough problems either have to do with the numerics or the dynamics; I will discuss these in more detail in the section Challenges.

For my colleagues from the academic community it may be interesting to comment on the organizational aspects of the MesoDyn project. In industry one is accustomed to time-tables, deliverables and milestones. Since the MesoDyn project is in the heart an industrial project, not an academic research project, this holds for the MesoDyn project as well. For someone who believes in academic freedom, and the right of the unexpected, this can create strange problems initially. When I hired people to work on the project, one of my (now) co-workers remarked that in the list of deliverables he could not find the date we were expected to find the Higgs boson. And off he went, wearing a suit and a tie, instead of the usual T-shirt (he had to buy a tie). Another consequence was that I managed to hire some very good people, precisely for the reason of the international industrial dimension. In these times when students are scarce, this is rather important. Another aspect of the industrial setting is the interdisciplinary setting. We have computer scientists, theoreticians, physical chemists and mathematicians in one project. How difficult it still is to start a purely academic research project with such a broad range of expertise!

Challenges

Since the end of the MesoDyn project is near, it seems suited to list a number of tough theoretical challenges for the future, inspired by the project. These are some of the problems we are currently studying.

Numerics

The field equations are discretised on a simple cubic grid by finite differences. One can of course implement other grid-based methods, such as finite elements, but whatever spatial discretisation scheme, the result will always be a large set of non-linear equations which have to be solved each time step. There are as many equations as there are components $\times$ nodes. For a full blown 3D-calculation this may involve $O(10^6)$ equations. Because of the special nature of the differential-algebraic system, we can prove mathematically that each time step only one solution is possible. This does not mean however that the single solution is always easy to find: the problem is ill-posed. We have studied various subspace iteration methods but so far we have not been able to find a satisfactory alternative above the steepest descent method which is now implemented. Yet I am convinced (believe) faster iteration methods can be devised by making special use of the mathematical form of the density functional relation.

Alternatively, how about getting away from the grids? Can one develop an off-lattice integration scheme? There is always some confusion here, since the word 'lattice' seems to have multiple meanings, depending on the particular scientific community one belongs to. In computational polymer physics one uses the word lattice to refer to those theories where a polymer molecule is somehow constrained on fixed positions in space. But in other areas, such as CFD or high energy physics, a lattice simply means that one uses fixed points in space to calculate the fields. In our case too, one must be careful in distinguishing between the 3D continuum theory and the numerics. We use a grid for the fields, not for the molecules. This then, makes one wonder if particle based discretisation schemes can be invented for integrating the same set of field-equations. The idea is not new (compare DPD methods), but...there is no universal approach and I do not have an answer.

Hydrodynamics from meso to macro.

The dynamical model we have studied the most is basically that of non-linear diffusion, such as occurs at the onset of spinodal decomposition, sometimes augmented by external shear fields (diffusion-convection), or simple Darcy hydrodynamics. Thereby we have neglected memory dependent and long-range hydrodynamic contributions. In other words, we have been unsuccessful in attaching to the vast literature on constitutive equations, Computational Fluid Dynamics, or in general the rheology of (complex) polymer liquids. Still, there is a very large number of polymer systems for which internal hydrodynamic effects are not important, either because the system is sheared (in which case the flow field is almost completely imposed from outside), or because the system is gel-like and/or the system has a very inhomogeneous viscosity on a mesoscale (in which case hydrodynamic interactions are completely screened). Yet it would be fascinating to develop a coherent model in which relevant hydrodynamics are reproduced correctly. The answer may be in a proper definition of local stress in an arbitrarily inhomogeneous system. If such an expression can be developed (which is not trivial) than perhaps one can attach to Lattice Boltzmann methods or CFD.

Molecules from micro to meso

On the other end of the spectrum is the mapping problem. How can one find a proper single chain density functional to mimic the behavior of real polymer molecules? So, this is the problem how to get the right chemistry, once the physics is OK. One novel approach we had was to calculate the response functions from a single chain with full molecular detail by Monte Carlo. Once these response functions are known, one can easily test and find the proper Gaussian chain which has the same response. If this is the case, then one can show that on a mesoscale the molecular-detailed polymer density functional behaves in a same way as the much simpler Gaussian chain density functional. In practice the approach has deficiencies, since the Monte Carlo calculations require an enormous amount of computer power for a reasonably sized polymer molecule; and we have not been able to find a Monte Carlo method fast enough for our needs.

The virtual cell.

Suppose one wants to mimic the behavior of a living cell? On a mesoscale? Why not? In fact, although the idea sounds completely crazy, there are several groups now attempting to do just this, with project names such as E-cell or virtual cell. Usually, the approach boils down to the integration of coupled ordinary differential equations, in order to reproduce the complex biochemical pathways. Also in this case, just as in our MesoDyn project, the molecular or atomic detail is integrated out. But now the integration results in a kind of logistics model for the entire cell, rather the spatial-temporal picture one normally associates with molecular or mesoscale models. We are currently trying to attach our knowledge of 3D morphology formation to pathway modeling. Such a connection could result for example in insight in the effect of confinement on the robustness and efficiency of biochemical pathways. The prospects for mesoscale biochemical engineering are staggering, but unfortunately we lack good theory.

Organization

Apart from the purely scientific challenges briefly discussed above, I believe there is also a challenge in the way we have organized the project. Can one do better? And did we really have an impact in the industrial community? To start with the second question: yes I think we have. Since we started the project more than five years ago, a number of other initiatives have popped up around the world, for example the 'seamless-zooming' project of Masao Doi in Japan, or Unilever's mesoscale particle dynamics project. Masao's project (http://www.stat.cse.nagoya-u.ac.jp/˜masao/ , the official name is quite long, in Japan everyone refers to it as Doi's project) is truly spectacular. The ambitious goal is to connect micro to meso and meso to macro, and

provide one uniform simulation environment for all scales. In the US, in a recent assessment of US technology versus European and Japanese technology (sponsored by the International Research Technology Institute), mesoscale modeling was highlighted as one of the key technologies where the US was lagging behind (personal communication P. Westmoreland, see also the workshop
http://itri.loyola.edu/molmodel/amm99.html). In return, the MesoDyn project made it to the cover of Chemical&Engineering News (ACS journal), connected to a feature article describing the bridge between molecular modeling and chemical engineering. I have mentioned before that the MesoDyn code is part of MSI's commercial software, and is now being sold worldwide.

Can we do better? In the MesoDyn project we have constructed a general purpose computational library which in principle can do much more than just polymer phase separation. Unfortunately, the library itself is locked into intellectual property rights, and cannot be made readily accessible to the academic scientific community. It is of course true that any company sponsoring such a project is entitled to an advantage edge, but I would welcome initiatives from the academic community to start construction of a general purpose simulation engine. The challenge here is that we must appreciate the interdisciplinary setting. Perhaps this is something for SIMU to do.

Acknowledgments

The European Union is acknowledged for funding the CAESAR and MesoDyn projects. The following persons are gratefully acknowledged for ideas and suggestions: N.M. Maurits, B.A.C. van Vlimmeren, A.V. Zvelindovsky, G.J.A. Sevink, K.F.L. Michielsen, A.N. Morozov, B. Hess, D. Hekstra (all University of Groningen/Leiden) , O. Evers (BASF), Peter Altevogt (IBM), Jose Brokken and Henk Huinink (Shell), G. Goldbeck-Wood (University of Cambridge), and D. Nicolaides and A. Bick (MSI).

V

Hierarchical Modelling of Polymers

Doros N. Theodorou
Department of Chemical Engineering, University of Patras
and ICE/HT-FORTH, GR 26500 Patras, Greece
and Molecular Modelling of Materials Laboratory,
Institute of Physical Chemistry,
National Research Centre for Physical Sciences "Demokritos",
GR 15310 Ag. Paraskevi Attikis, Greece
email:doros@sequoia.chemeng.upatras.gr
URL: http://tahoe.chemeng.upatras.gr

Polymer modelling and materials design

Polymeric materials are ubiquitous and becoming more important every day in contemporary life, thanks to their processability and to the extremely broad range of properties they exhibit. To control these properties, one can manipulate a very large number of variables, which ultimately determine the molecular composition and morphology of the material. Such variables are the chemical constitution of monomers, the molecular architecture of homopolymer (linear, short-branched, long-branched, tree, star, network) and copolymer (random, alternating, block, graft) chains in the material, the molecular weight distribution, as well as the processing conditions (temperature-pressure history, flow field) and the relative amounts of components in the case of multicomponent materials such as blends and composites.

Materials design problems, as they appear in industrial practice, typically have to do with complex systems whose properties are affected by both synthesis and processing; they are very targeted and have to be solved subject to strong financial and time constraints. For example, one may be seeking the optimal formulation of a pressure-sensitive adhesive, consisting of diblock copolymer, triblock copolymer and tackifier resin, to maximize the work expended when two solid surfaces sticking together across a layer of the adhesive are detached under prescribed conditions of loading and strain rate. Or one may be looking for chemical modifications that would reduce the permeability of a semicrystalline, oriented polymer to carbon dioxide and thus increase the shelf-life of beverage bottles made of this polymer without affecting their mechanical properties. Traditional approaches for solving such problems are based on experimental "screening" of relatively large sets of homologous systems, aided by phenomenological correlations between chemical constitution, morphology and properties. Such correlations have been systematized in convenient algebraic forms[1] and can be valuable in the hands of experienced and inventive materials researchers.

In the mid-1980s the idea of using rigorous quantum and statistical mechanical theory and simulation in addition to, or in place of, phenomenological correlations towards the design of polymeric materials started gaining ground. Rigorous modelling approaches based firmly on the fundamental molecular sciences offer great advantages over phenomenological correlations: they are based on fundamental understanding, and can therefore be used with confidence to explore "what if" scenarios for which experimental data are scarce; they can explain and predict the effects of subtle changes in tacticity and molecular architecture, which phenomenological correlations are simply too crude to capture; and they offer the possibility of addressing a very wide range of properties using a minimal set of models and parameters. The Achilles' heel of rigorous modelling is its excessive demand of computer time. The overly optimistic initial expectation that most polymer design problems would be solved by performing atomistic molecular dynamics (MD) simulations soon met with disappointment and considerable loss of interest in modelling on the part of the industrial sector, as the CPU requirements of MD became apparent.

The challenge of multiple time and length scales

Polymers, perhaps more than any other category of materials, are characterized by a very wide spectrum of length scales in their structure and a very wide spectrum of time scales in their molecular motion. Intramolecular correlations and local packing of chains in the bulk exhibit features on the length scale of bond lengths and atomic radii, i.e. a few Å. The Kuhn segment of a typical synthetic randomly coiled polymer is on the order of 10 Å and can be considerably larger for very stiff polymers. The radius of gyration of entire chains in the amorphous bulk scales as $N^{1/2}$ with the chain length N and is on the order of 100 Å for typical molecular weights; the smallest dimension of microphases (lamellae, cylinders, spheres) in microphase-separated block copolymer systems is on this order of magnitude, while crystallite sizes in semicrystalline polymers and domain sizes in immiscible polymer blends may well be on the order of μm.

Even broader is the range of time scales characterizing the dynamical properties of polymers. While localized vibrational modes of chains have periods on the order of 10^{-14}s, conformational transitions of individual bonds over torsional energy barriers in the melt state exhibit waiting times in excess of 10^{-11}s. Longer and longer sequences of segments along the backbone need longer and longer correlation times to rearrange. The longest relaxation time, required for a chain to diffuse by a length commensurate to its size and thus "forget" its previous conformation, is critical to the viscoelastic response of polymer melts in flow. This time scales as N^2 for low-molecular weight melts in the Rouse regime and as $N^{3.4}$ above a critical molecular weight for entanglements, in the reptation regime; for a C_{800} polyethylene melt at 450K this time is on the order of 3 μs, while it easily exceeds the millisecond time scale for the molecular weights encountered in typical processing operations. The time scales for morphology development through nucleation and growth or spinodal decomposition processes typically exceed 1 s, while the characteristic times for volume and enthalpy relaxation in a glassy polymer just 20°C below the glass temperature T_g are on the order of years. Atomistic MD, on the other hand, typically tracks the evolution of model systems of length scale ca. 100 Å for times up to a few decades of ns. While the length scale can be increased significantly by use of domain decomposition strategies on parallel computers, there is little one can do, even on the fastest machines available today, about the time scale, which falls dramatically short of the times one would wish to address in polymer systems.

There is no reason to despair, however. Recent years have witnessed a growing realization, within the materials modelling community, that theoretical and simulation approaches at different time and length scales can be connected together into hierarchical schemes[2] that are truly reliable and useful as design tools. A modelling hierarchy consists of several levels, each level utilizing a model whose parameters are derived from lower (more fundamental, smaller length- and time scale) levels and providing input to higher (more coarse-grained, larger length- and time scale) levels. Ideally, the hierarchy could span all the way from *ab initio* electronic structure calculations of the geometry and energetics of small structural units of chains to, say, the stress-strain curve, permeability and index of refraction of a finished product consisting of kilograms of polymeric material, the sole input being the monomers, synthesis and processing conditions used for its production. Such complete hierarchical schemes are very rare, and perhaps even unnecessary, as modelling is always accompanied by experimental efforts, which it can use as sources of input as well as guide and interpret. Many partial hierarchies of modelling methods have emerged, however, which provide key connections for understanding structure-property relations and optimizing complex polymeric materials.

Main ingredients of contemporary hierarchical modelling approaches to polymer properties are (a) efficient techniques for sampling polymer configurations and computing free energies; (b) systematic techniques for coarse-graining atomistic polymer models into models involving fewer degrees of freedom; (c) analyses of the paths and rates of infrequent event processes occurring in systems with rugged potential energy terrains, and of sequences of such processes; (d) mesoscopic techniques for the simulation of transport phenomena and morphology development under nonequilibrium conditions. Below we discuss recent developments in each of these fields. The discussion is inevitably brief and tainted by the research interests of the author. The reader is referred to relevant reviews, wherever possible.

Sampling polymer configurations

Although polymeric materials used in practice are most often not in thermodynamic equilibrium, they usually are close to equilibrium at some point in their processing history, and deviations from equilibrium play the role of driving forces for all changes they undergo. Furthermore, equilibrium thermodynamics remains useful as a framework for discussing many properties in configurationally arrested states, such as glasses. Thus, calculation of equilibrium properties (e.g., equation of state and heat capacity, conditions for phase coexistence and phase diagrams, sorption isotherms of small-molecular weight species in polymers, microphase separation morphologies for copolymers, density and conformation profiles for multicomponent polymer systems at interfaces) is a necessary starting point for predicting structure-morphology-performance relations in polymers. Predicting equilibrium properties by simulation requires sampling a sufficiently large number of uncorrelated microscopic configurations, weighted according to the prescription of an equilibrium ensemble. As already pointed out, this "equilibration" challenge cannot be met with MD, at least as regards the long-length scale features of long-chain systems, which decorrelate with characteristic times many orders of magnitude longer than can be tracked by MD. Recent algorithmic developments, most notably time-reversible multiple time step methods based on Trotter factorization of the Liouville operator[3] have greatly enhanced the stability and efficiency of MD methods, but not to the extent of being able to address these long polymeric time scales. On the other hand, spectacular advances in our ability to equilibrate polymer systems have resulted from the development of novel Monte Carlo moves and methods in recent years. These have been reviewed in connection with the problem of calculating phase transitions in complex fluids[4].

By introducing bold changes in the configuration of dense, multichain systems, Monte Carlo moves can circumvent the bottlenecks limiting dynamical progress in real polymeric systems and in MD simulations, thereby accelerating equilibration by many orders of magnitude. The configurational bias (CB) move[5] cuts a terminal section of a chain and regrows it in a bond-by-bond fashion, while avoiding excluded volume overlaps; the bias associated with the regrowth procedure is taken away in the acceptance criteria. It has been used in Gibbs ensemble simulations for the prediction of vapour-liquid phase coexistence curves for alkanes[6] up to C_{48} and for performing biased Widom insertions to estimate chemical potentials in mixed hydrocarbon phases[7]. It has also been adapted to networks[8] and branched molecules[9]. For long-chain systems the efficiency of CB decreases; Recoil-Growth CB MC[10], a modification using retractable "feelers" to explore available space around the growing chain, is likely to help in this respect.

The concerted rotation (CONROT) move brings about local conformational rearrangements which change the torsion angles of seven or eight consecutive bonds and the positions of four or five atoms along the backbone[11]. It has been used very effectively, in combination with CB, to sample conformations of cyclic peptides[12]. The end-bridging (EB) move[13] was developed with the explicit purpose of equilibrating long-length scale features, such as the end-to-end distance, the radius of gyration and the distribution of chain centres of mass in dense phases of long chains. In EB the end of a chain "attacks" the backbone of a neighbouring chain, cutting it in two parts, one of which is annexed to the attacking chain. Connectivity is thus drastically redistributed in the model system. The simulation is carried out in a semigrand ensemble, wherein the total number of chains and the total number of monomer units are kept fixed and the molecular weight distribution is controlled by imposing chemical potentials for all chain species but two, which are taken as reference species. A variety of chain length distributions can be simulated by imposing appropriate profiles of chemical potentials, the algorithm remaining efficient down to polydispersity indices of 1.02 or so. A remarkable attribute of the EB algorithm[14] is that, for fixed shape and polydispersity of the molecular weight distribution, the CPU time required in order for chain centres of mass to move by a length equal to the root mean square end-to-end distance scales *inversely* with the mean chain length N. Thus, the efficiency of the algorithm is *enhanced* as the mean chain length increases. EB has been successful in equilibrating realistic united-atom models of C_{1000} at all length scales and is currently being tried on C_{6000}. Not only long-length scale properties of chains, but also local density fluctuations are sampled more efficiently by an algorithm based on EB, CONROT and reptation moves than with alternative algorithms[14]. When used with detailed models of the bonded geometry of chains, both CONROT and EB rest on determining all (up to 16) solutions to a geometric problem, that of bridging two dimers by a trimer such that the resulting heptamer has prescribed bond lengths and bond angles. An efficient scheme for solving this problem in Cartesian coordinates has been developed[14], and a more general scheme for bridging through a sequence of rigid bodies connected by rotatable bonds has been implemented[12].

A number of new statistical mechanical ensembles have been used in Monte Carlo simulations of polymeric systems in recent years. The motivation behind much of this work was to alleviate the sampling problems associated with insertions of big molecules in dense phases, required by the Widom test particle method for chemical potentials and by grand canonical MC simulations, or with exchanges of big molecules between dense phases, required by the Gibbs ensemble method for calculating phase equilibria. Semigrand Monte Carlo simulations[15], involving identity interchanges between molecules belonging to different chemical species, have been used effectively in conjunction with coarse-grained models to predict the mixing thermodynamics of symmetric polymer blends[16] and in conjunction with atomistic models to simulate polydisperse melts[13],[14] Sorption isotherms of a small-molecular weight species in a polymer matrix are readily calculated in a hybrid isothermal-isobaric/grand canonical ($N_1 f_2 PT$) ensemble, wherein the pressure P, the temperature T, the number of (nonvolatile) polymer molecules N_1, and the fugacity f_2 of the small penetrant are specified[17]; this ensemble is similar to the "osmotic" ensemble proposed for phase equilibria across semipermeable membranes[18]. For the determination of high-pressure phase coexistence properties in binary mixtures of a light solvent and a heavy hydrocarbon, an atomistic simulation scheme involving two boxes simulated in parallel in the $N_1 f_2 PT$ ensemble at common values of P, T, and f_2 has proved useful[7]. The common value of f_2 is revised through a Newton-Raphson iterative scheme leading to equalization of the fugacities of the heavy component in the two boxes. This scheme for simulating phase equilibria of chain systems (SPECS) can be extended to mixtures containing an arbitrary number of light components. Truly polymeric heavy components can be treated by taking advantage of the chain increment Ansatz, which states that the excess chemical potential of a chain inserted in a phase of given temperature, pressure and composition is a linear function of the chain length[19],[7]. SPECS can be considered as a "pseudoensemble" approach, the latter term denoting iterative schemes designed to converge to a desired equilibrium state through successive updates of an intensive parameter, thus circumventing the introduction of moves that would have very low probability of acceptance[4]. For tracing a phase coexistence line, given the properties of coexisting phases at one point of that line, the Gibbs-Duhem integration method has been proposed[20].

Sampling configurations of oriented melts, such as the ones resulting from imposition of a steady-state elongational flow during processing, was made possible by conducting EB MC simulations in the presence of a tensorial thermodynamic field which couples to the end-to-end tensors of chains, inducing orientation[21].

Another way to alleviate problems associated with inserting/deleting large molecules in dense phases for the calculation of phase equilibria is to employ an "expanded ensemble" scheme that inserts or deletes molecules in a gradual manner. In an expanded ensemble simulation configurations are sampled according to the partition function $\sum_{y=1}^{M} Q_y \exp(w_y)$ where y is a parameter in the Hamiltonian of the system, allowed to range over M discrete values; Q_y is a conventional (e.g. canonical) partition function, evaluated at parameter value y; and the w_y are weighting factors modulating the probability of appearance of different y values. The scheme allows calculation of free energy differences between thermodynamic states corresponding to different y and can thus be thought of as an application of the free energy perturbation method "on the fly", within a single simulation[4]. It was originally proposed[22] for the calculation of free energies of solvation at infinite dilution, the parameter y corresponding to the strength of interaction between the solute and solvent molecules. It has been implemented in the context of extended-ensemble MD simulations to calculate the sorption thermodynamics of gases in glassy polymers[23]. It has also been adapted within a CB MC framework for the calculation of chemical potentials of polymers, with y controlling the length of a "tagged" chain which is allowed to fluctuate in size[4].

The parallel tempering technique[24] has recently proven very promising for sampling systems with rugged potential energy functions that tend to make conventional simulation schemes nonergodic. Parallel tempering considers a large ensemble of n systems, each system equilibrated at a different temperature $T_i (i = 1, ..., n)$. The system of interest is the system of lowest temperature; the systems of higher temperature usually have the same Hamiltonian as the system or interest and are added in order to aid in overcoming energy barriers and thereby aid in equilibration. The systems of different temperature are considered as independent of each other, so the partition function sampled is actually the product of the individual partition functions at the different temperatures, i.e. of the form $\prod_{i=1}^{M} Q_i(N, V, T_i)$. There are two types of moves: Regular "configuration" moves, performed at each temperature, and "swapping moves", which exchange configurations between two systems i and j. A swapping move is accepted with probability $\min[1, \exp(\Delta\beta_{ij} \Delta\mathcal{V}_{ij})]$, with $\Delta\beta$ and $\Delta\mathcal{V}$ being the differences in reciprocal temperatures and energies between the two systems. A prerequisite for the scheme to work is that the energy histograms of systems adjacent in the temperature ladder should overlap. Parallel tempering has been used with great advantage in sampling configurations of biological molecules[12] and polymers[25]. In the latter case, an escalation in chemical potential, as well as in temperature, has been used to define the different systems and the method has been coupled to an expanded ensemble scheme.

Histogram reweighting methods[26] analyze results from a limited number of simulation runs in order to extract information about the density of states, which is then used to derive properties at thermodynamic state points other than the ones simulated. These methods are particularly useful for the study of phase transitions in the vicinity of critical points and have been applied to explore the critical properties of polymer solutions using lattice models[27].

Coarse-graining the molecular representation

Coarse-graining is an essential element of any hierarchical modelling approach. It entails replacing a detailed molecular model (e.g., an atomistic model with explicit representation of bond angle bending, torsion, intra- and intermolecular excluded volume, dispersive and Coulombic interactions depending on the positions of atoms and partial charges) with a simpler model, cast in terms of fewer variables, without loss of significant information. The simpler (coarse-grained) model is desirable because it is more manageable computationally in simulations and more amenable to theoretical treatment. The parameters of the coarse-grained model must be determinable from those of the detailed model through a rigorous mapping procedure. Inverse mapping ("fine-graining"), whereby well-equilibrated coarse-grained configurations are used to generate (sets of) detailed configurations is also important for the calculation of properties.

A rigorous framework for coarse-graining is offered by the projection operator formalism of statistical mechanics. For coarse-graining to be successful, the coarse-grained variables must evolve slowly relative to the detailed variables being eliminated from the model description. Interactions at the coarse-grained level are described in terms of the potential of mean force (free energy), derivable by integrating the Boltzmann factor of the detailed model Hamiltonian over all detailed variables being eliminated at each coarse-grained configuration. The efficient sampling techniques discussed above are helpful in extracting such potentials of mean force and in equilibrating the coarse-grained models described thereby. The effects of eliminated detailed variables on the dynamics of the coarse-grained variables are described in terms of stochastic and frictional forces. When there is complete time scale separation between the detailed variables being eliminated and the coarse-grained variables being retained, the in general formidable problem of deriving memory functions for the description of frictional forces is reduced to a calculation of a relatively small number of friction factors. These can be extracted from time correlation functions involving the coarse-grained variables, accumulated in the course of relatively short dynamic simulations of the detailed model.

In practice, rigorous projection operation formalisms are seldom adopted, and coarse-graining of detailed polymer models is performed in a more or less heuristic, nevertheless useful, fashion. A procedure has been developed[28] for mapping polymers, such as polycarbonates, onto the lattice-based bond fluctuation model. This procedure has subsequently been extended to simulating the melt viscosity of polyethylene on the basis of bond fluctuation MC simulations. In an alternative approach, chains represented in terms of a detailed rotational isomeric state model are mapped onto a second-nearest-neighbour diamond lattice[29]. This procedure has been used to look at a number of polymers in the bulk melt and at interfaces. A continuous coarse-grained representation, cast in terms of hard-sphere groups connected by springs, has been employed for polycarbonates[30]. In this work, strategies for both mapping and reverse mapping between the detailed and coarse-grained models are proposed. Coarse-grained bond (spring) stretching and bond angle bending potentials are determined from histograms of the corresponding geometric quantities accumulated in the course of sampling atomistically detailed unperturbed single chains.

An interesting strategy for mapping to an even coarser level, wherein entire polymer chains are represented as soft ellipsoidal particles with dimensions, orientation, and interactions that are governed by their local environment, has been proposed[31]. The ellipsoidal particle shape and density distributions are derived from single-chain bead-spring calculations, and interactions between different ellipsoids are expressed in terms of overlap integrals of their density distributions. The softness of interactions allows for very long effective time steps in dynamic simulations of the coarse-grained model. The soft ellipsoid model has been used to simulate phase separation by spinodal decomposition in a symmetric binary polymer blend.

A coarse-graining approach has been proposed for mapping detailed atomistic polymer melt models onto the dumbbell, Rouse chain and Doi-Edwards tube models invoked in mesoscopic simulations of viscoelastic flow. The free energy of an oriented melt is extracted as a potential of mean force with respect to the conformation tensor (reduced end-to-end tensor) and shown to be of purely entropic origin for long-chain melts subjected to flow fields of low Deborah number[21]. In the case of linear polyethylene, which has been studied so far, the dependence of this elastic free energy on the conformation tensor can be described well in terms of a finitely extensible nonlinear elastic (FENE) model with parameters extracted directly from the unperturbed mean square end-to-end distance and contour length of atomistically detailed chains, while Hookean dumbbell models are less satisfactory. The relation between anisotropy of stress and anisotropy of the refractive index predicted by the simulations obeys the stress optical law with a coefficient very close to that measured experimentally. The EBMC method was of critical importance in enabling these studies of melt orientation and elasticity. The friction factor ζ invoked by the Rouse and reptation models is extracted from atomistic MD simulations initiated at well-equilibrated configurations sampled by EBMC. Friction factor values obtained from the self-diffusivity and from the autocorrelation functions of the two first modes of the chains are consistent; they are chain-length dependent for short chains but assume a constant asymptotic value in the region C_{80} - C_{150}. Zero-shear viscosities estimated from these ζ values on the basis of the Rouse model are in excellent agreement with experimental values for unentangled polyethylene melts, as are the self-diffusivities for all chain lengths[32]. The mapping of atomistic to coarse-grained models of linear chain melts is completed by topological analysis of long-chain atomistic configurations equilibrated by EBMC, leading to the identification of entanglement points and the determination of the molecular weight between entanglements[33]. In this way, it becomes possible to generate coarse-grained networks of entangled chains for the simulation of viscoelastic flow and mechanical failure of amorphous polymers out of detailed atomistic configurations.

Analysis of infrequent event processes

Many dynamical processes in polymers occur as successions of infrequent events, wherein the system is led from one energetically favourable region of configuration space (state) into another, across a bottleneck (hyper)surface separating the states. Typically, a relatively small number of system degrees of freedom are involved in such a transition. Whereas a "brute force" MD simulation would expend most of its time tracking the relatively uninteresting fast in-state motion of the system, dynamically corrected transition-state theory[34] (TST) focusses on the (free) energy barriers (saddle points) that have to be overcome for a transition to occur and calculates rate constants for the transition at a small computational cost. The long-time evolution of the system through a succession of uncorrelated transitions can be tracked by kinetic Monte Carlo simulation (KMC), once the state equilibrium probabilities and interstate transition rates are known. A compilation of recent work on the analysis and simulation of infrequent event processes can be found in Reference [35].

An example of TST-based calculations that has found widespread use is the evaluation of diffusivities of small penetrant molecules in low- temperature amorphous polymer matrices. Gas diffusivities in a polymer glass may be on the order of 10^{-8} to 10^{-9} cm^2/s, and therefore not accessible by MD simulation. A useful TST approach was introduced, which relies upon determination of all minima of the polymer+penetrant free energy in the three-dimensional space of penetrant coordinates and all dividing surfaces for transitions between minima[36]. In this approach, all atoms of the polymer matrix are envisioned as executing isotropic harmonic vibrations around their equilibrium positions. A more refined multidimensional TST approach, in which degrees of freedom of the polymer matrix are incorporated explicitly in the transition path and rate constant calculation[37], starts with geometric analysis of accessible volume in atomistic model configurations of the polymer matrix. This geometric analysis yields initial guesses for the penetrant position at the energy saddle points (bottlenecks), which have to be overcome for elementary jumps of the penetrant between clusters of accessible volume to occur. The set of degrees of freedom with respect to which each saddle point is calculated is progressively augmented by including more and more polymer degrees of freedom, until the saddle point energy becomes asymptotic. The entire transition path for the corresponding jump is mapped out in multidimensional configuration space through a couple of steepest descent constructions initiated at the saddle point. Rate constants for the elementary jumps are used within a KMC scheme to track the long-time diffusive progress of the penetrant.

Infrequent event analysis has also found widespread use in exploring the mechanisms and rates of side-group or main-chain local motions responsible for "Johari-Goldstein"-type local relaxation processes in polymers. TST-based approaches of varying degrees of sophistication have been used to explore skeletal ring flips in glassy bisphenol A polycarbonate[38], side group rotations in methyl acrylate/ethylene copolymers[39], and in PMMA[40], and phenyl group rotations in glassy polystyrene[41]. Predictions are generally in good agreement with solid-state NMR and dielectric spectroscopy measurements.

A challenge in analyzing dynamical processes in systems with rugged potential energy landscapes is the identification of states and transition paths between the states. In some problems, such as diffusion and side-group relaxational motion, this can be guided by geometric arguments; in many other problems, however, it cannot. An elegant method for sampling all relevant transition paths between two given states, termed transition path sampling[42], was proposed recently. For situations where the states are not even known, the recently proposed molecular hyperdynamics method[43] is very promising. This accelerates the progress of molecular dynamics by "filling up" energy wells, using a bias potential that is calculated from local properties of the energy hypersurface. In this way, the system is encouraged to move over barriers, thereby "boosting" the simulation time by a known factor. Efficient numerical techniques for the identification of saddle points which do not require explicit calculation of the Hessian[44] are also likely to help in infrequent event analyses of dynamical processes in polymers.

Mesoscopic simulation

Mesoscopic simulation techniques are designed to fill the gap between molecular simulations and macroscopic analyses based on fluid mechanics and transport phenomena, continuum mechanics and fracture mechanics, electromagnetic theory, and the continuum engineering sciences in general. They focus on length scales of 100 Å to 1 μm and time scales of 0.1μs to 1s and are particularly needed for dealing with issues of complex morphology development, flow and deformation under highly nonequilibrium conditions.

Mesoscopic simulation approaches must necessarily employ a coarse-grained model representation. The dynamic simulations employing a soft ellipsoid model for entire chains, discussed above[31] are an example of a mesoscopic approach. A mesoscopic approach that has been used considerably to analyze viscoelastic flows in complex geometries is CONNFFESSIT[49] (Computation of Non-Newtonian Flows by Finite Elements and Stochastic Simulation Techniques). This employs stochastic simulations of coarse-grained molecular models, such as dumbbells, to track the stress and velocity fields within the finite element regions used to analyze a macroscopic flow, and thus obviates the need for closed- form analytic constitutive equations.

Dissipative Particle Dynamics[45] (DPD) is a stochastic dynamic simulation technique which tracks the evolution of large particles, each particle representing a “packet” of many atomistic degrees of freedom (e.g. fluid molecules or polymer segments). As a result of this coarse-graining, interactions between the particles are very soft and numerical integration can be performed using a long effective time step. An advantage of the method is that it has built-in hydrodynamic interactions. DPD has been used to simulate phase separation and domain growth processes in systems containing low-molecular weight solvents, randomly coiled polymers, rigid rod polymers and copolymers. Predicted phase transitions and morphologies are in qualitative agreement with experiment. Dealing with entangled polymer systems is a challenge, due to the softness of interactions, but recently algorithms have been developed which incorporate uncrossability of interparticle bonds[46]. A more basic challenge is how to extract the soft interparticle interactions of DPD from atomistic interaction potentials. Some promising steps in this direction have been taken for simple fluids[47].

Many mesoscopic techniques constitute numerical solutions of sets of integrodifferential equations, which are derived from a general nonequilibrium thermodynamic formulation and cast in the coarse-grained variables. Although the problem of writing down a general nonequilibrium thermodynamic formulation that can be used to track the spatiotemporal evolution of mesoscopic variables such as mass, momentum, energy density and conformation fields is a very challenging one, recently there have been promising developments in this direction in the area of analyzing polymer flows. One such development is the Poisson bracket formulation[48], another is its generalization, the GENERIC formulation (General Equation for Nonequilibrium Reversible-Irreversible Coupling)[50]. These formulations have been used primarily to test rheological models proposed in the literature for thermodynamic consistency, to modify such models and to explore flow phenomena at interfaces.

In recent years, considerable effort has been devoted to developing a dynamic mean-field density functional method, derived from generalized time-dependent Ginzburg-Landau theory[51]. The time derivative of the local concentration of each species is expressed in terms of gradients in the chemical potentials of all species multiplied by nonlocal Onsager kinetic coefficients, and of a random noise term obeying the requirements of the fluctuation-dissipation theorem. The chemical potential is typically expressed as an ideal part (corresponding to Gaussian single-chain statistics) and a nonideal part (mean field potential resulting from interchain interactions, involving Flory χ factors). The formulation is solved numerically by discretizing space into an array of cubic elements. Applications have been presented for surfactant aggregation in solution and phase separation of quenched block copolymer melts under quiescent conditions and under shear. Predicted morphologies are in qualitative agreement with experimental observations. An independently developed density functional theory approach has been used to track the effects of solid particles in a phase-separating polymer mixture[52].

A promising mesoscopic approach for the simulation of large-scale deformation and fracture in condensed polymer phases is entanglement network modelling. The polymer is represented as a network of chains entangled pairwise at specific points in three-dimensional space. Positions of chain ends and entanglement points are the coarse-grained degrees of freedom with respect to which the simulation is performed. Deformation at a certain strain rate is introduced as a series of stepwise changes in the model "specimen" dimensions. Each such change is followed by (free) energy minimization and KMC simulation of elementary events leading to topological changes in the network, such as slippage of a chain across an entanglement point or breakage of a strand between entanglements. This KMC simulation is carried out according to specific rate expressions involving the local stress state around the nodal points for the time interval that elapses until the next deformation step. Application of such a scheme to polyethylene has allowed the observation of brittle fracture, necking, and homogeneous deformation with strain hardening phenomena as the molecular weight of chains is increased, in good agreement with experimental observations[53]. A simple network of random-walk chains was used for this purpose, although the actual polymer is semicrystalline. Efforts to incorporate crystallinity explicitly have also been undertaken[54]. More recently, methods have been proposed for setting up entanglement networks to represent polymer interfaces in a manner consistent with the composition and conformation profiles yielded by a self-consistent field theory, and for expressing the free energy function and rate coefficients involved in the KMC simulation in terms of interatomic potential parameters and segmental friction factors[55]. These developments, along with techniques for identifying entanglement points through topological analysis of well- equilibrated atomistic long-chain configurations[33], create the possibility of linking this type of entanglement network modelling all the way down to the atomistic level.

Putting the pieces together

Having all the above methodological advances at our disposal, we can start thinking of hierarchical modelling schemes to address design problems such as the ones we mentioned in the introduction. For example, in the case of the pressure-sensitive adhesive consisting of diblock and triblock copolymers and low-molecular weight resin, the material design variables are the chemical constitutions and molecular weight distributions of the copolymer blocks and resin and the composition of the mixture (relative amounts of the three components). The work expended in destroying an adhesive bond across the material under prescribed temperature and strain rate must be maximized as a function of these variables. One can envision a hierarchical scheme which starts with efficient atomistic MC simulations at representative compositions[14], with possible use of coarse-graining and fine-graining[30] to facilitate equilibration, in order to determine equilibrium binary phase diagrams and enthalpies of mixing, from which effective χ interaction parameters could be extracted. Analogous MC simulations at free surfaces and next to the solid substrate of interest could yield equilibrium surface tensions and contact angles, while topological analyses of the well- equilibrated configurations could be used to extract spatial distributions of entanglements and entanglement spacings in the bulk and at interfaces. Atomistic MD simulations initiated at well-equilibrated short-chain configurations generated by MC could be used to extract the friction constant required in Rouse and reptation theory descriptions of the dynamics as a function of temperature and composition. From then on, one could envision two stages of mesoscopic modelling. The first would track morphology development under the conditions of formation and deposition of the adhesive, using an approach such as dynamic density functional theory[51] with coarse-grained chain elasticity parameters, χ factors, and Onsager coefficients based on the atomistic investigations. The second would take representative morphologies from bulk and interfacial regions of the adhesive film, coarse-grain them into networks of entanglement points[55] with the help of atomistic entanglement analyses, and simulate their deformation under a variety of strain states and rates to derive forms and parameters for a constitutive equation describing their rheological behaviour. The thermodynamic and rheological information extracted in this way could be used in a macroscopic analysis of the debonding process, treating the adhesive film as a continuum with position- and deformation history-dependent properties, to simulate all stages of the debonding process (e.g. nucleation of cavities in the adhesive, elongation of cavities and formation of fibrils, extension of fibrils and ultimate breakage or detachment of the fibrils from the solid as the two solid surfaces are pulled apart with the adhesive in-between). In this way, the work required to destroy an adhesive bond would be determined. Validation against experiment could be sought at the level of structure, mixing thermodynamics and equilibrium phase diagrams, chain conformation and linear viscoelastic properties, surface tensions and contact angles estimated from atomistic simulations; at the level of morphology predicted from dynamic density functional theory; at the level of rheological behaviour predicted by the entanglement network modelling; and at the level of mechanism of debonding and stress-strain behavior in actual and simulated adhesion tests.

For our second example problem, that of optimizing the barrier properties of a polymer consisting of oriented glassy and crystalline domains, the chemical constitution of the chains and the morphology are the main design variables. To assess the effect of chain chemical constitution under given morphology, one could envision a hierarchical scheme which first coarse-grains the atomistic representation into one wherein, e.g., rigid aromatic moieties are represented as soft ellipsoidal particles[30]. Simulations at this coarse-grained level in the absence or presence of orienting fields, using an efficient MC algorithm[14],[21], would then yield well- equilibrated melt configurations corresponding to different degrees of orientation, which could be mapped back to the atomistic level. Collections of isotropic and oriented glassy configurations could be generated from the corresponding melt configurations through energy minimization and molecular dynamics. Henry's law constants describing the sorption equilibrium of the gaseous penetrant in each of these configurations could be obtained via Widom insertions, while entire sorption isotherms could be predicted using $N_1 f_2 PT$ MC simulations or expanded-ensemble molecular dynamics[23] atomistic simulations. On the other hand, diffusivity tensors for the penentrant in each (isotropic or oriented) glassy configuration could be obtained through multidimensional TST analysis and KMC simulation[37]. Thus, given the spatial distribution, connectivity and orientation of amorphous regions in the material (crystallites being impermeable) one would be in a position to know the local solubility and the local diffusivity tensor at every point in the material. A macroscopic simulation of the permeation process through a specimen of given morphology by finite difference, finite element or kinetic Monte Carlo methods, using this information as input, would yield the permeability. Validation against experiment could be attempted at the level of structure (experimentally accessible through diffraction), volumetric properties and free volume distribution (experimentally accessible through positron annihilation lifetime spectroscopy) of the atomistically simulated configurations, at the level of predicted sorption isotherms and diffusivities in the amorphous material for various degrees of orientation, and at the level of the permeability of entire specimens of given morphology.

Challenges for the future

Realizing grand hierarchical modelling schemes, such as the ones outlined in the last section, entirely computationally sounds extremely complex and perhaps even unrealistic today; nevertheless, many of the techniques required are already in place. The biggest challenge is in interfacing the different levels of modelling into a coherent hierarchy so as to minimize the loss of information in going from one level to the other, maximize predictive ability and versatility, and minimize computational cost. Global familiarity with efforts and advances at all levels and willingness to work collaboratively towards the development of problem-oriented multilevel approaches would certainly help the scientific community make computer-aided polymeric materials design a reality.

At each level of modelling, comparative studies of the performance of alternative methods on representative benchmark problems would be useful. For example, how do continuum and lattice-based strategies for deriving coarse-grained atomistic models, equilibrating at the coarse-grained level, and fine-graining back to the atomistic level, compare in terms of their computational requirements and in terms of the structural and thermodynamic properties they ultimately predict? Which, among the several MC strategies that have been proposed in recent years, can equilibrate melt models most efficiently, and how could different strategies (e.g. EB and parallel tempering) be combined to achieve even better results? At the mesoscopic level, how do DPD and dynamic density functional theory compare in terms of the morphology predictions they give, e.g. for phase-separation of a binary blend under shear flow conditions, and in terms of their computational requirements?

There are problems for which it is still unclear how one could best proceed to formulate a hierarchical modelling approach, and significant methodological advances are necessary. One such problem is crystallization of polymers, especially under flow conditions. Technologically this is an extremely important problem, as the semicrystalline morphologies one encounters in real-life polymers vary widely with thermal and processing history and have profound effects on properties. Crystallization is a problem in which different length- and time scales seem to be inextricably interwoven, as evidenced by the complex hierarchical structure of a spherulite. Although significant advances have been made, for example in predicting melting temperatures for long-chain alkanes[56], in calculating the dependence of melting temperature on structural defects due to incorporation of comonomers along the chains[57], and in simulating lamellar growth through coarse-grained KMC simulations[58], we are still far from being able to predict semicrystalline morphology from chemical constitution and processing flow history.

Another outstanding problem is how to best model polymer glasses. It is frustrating that generating a computer glass with a history that is both well-defined and realistic (comparable to what is used in applications) is impossible. One can certainly glassify liquid configurations at a well-defined cooling rate of 10^{10} K/s or so with MD; this rate, however, is very far removed from those of typical experiments (ca. 1 K/min). Many simulation studies focus on the region above the calorimetric T_g and present comparisons against the predictions of mode-coupling theory[59]. These simulations, although instructive and leading to very satisfactory agreement with theory, are still of limited utility for predicting T_g or simulating a real-life glass. Atomistic MD simulations of segmental motion above T_g[60] yield strongly temperature-dependent correlation times in good agreement with experimental relaxation (e.g. NMR, QENS) measurements. At low temperatures, the time correlation functions from MD do not decay to zero over the simulation time, but their extrapolation using, e.g., a stretched exponential (KWW) form which seems to be obeyed in the region accessible by MD yields reasonable results. This makes one hope that atomistic MD simulations of low-temperature melts and accumulation of segmental correlation times as a function of T, with appropriate extrapolation, may be a reliable way for estimating T_g through simulation; it does not solve the problem of generating realistic glassy configurations, however. Techniques based on energy minimization and MD, using some form of chain growth procedure based on the rotational isomeric state model to generate initial guess configurations, have been devised to build model polymer glass configurations. An early technique of this kind is the "amorphous cell"[61] method, a more recent one that gives better predictions for chain conformation is "Polypack"[62]. These techniques have the disadvantage that they do not correspond to a well-defined glass formation history. Nevertheless, for some properties, such as elastic constants, they have been shown to yield very satisfactory predictions, provided the glass density is correctly reproduced.

Predicting physical ageing and stress-induced relaxation phenomena in glasses introduces an additional level of difficulty. Although transition-state theory approaches have been used to study local "Johari-Goldstein"-type motions, such as methyl group rotations and aromatic ring flips in polymer glasses, no clear methodology is available yet for connecting these calculations with the main α-relaxation associated with the glass transition, with the volume and enthalpy changes observed over long times in the presence or absence of mechanical load, and with the frequency-dependent dynamic mechanical moduli of polymeric glasses.

Polymer dynamics in confinement and how it affects glass trnsition and relaxation phenomena is another subject, of great importance to the properties of composite materials, where advances in simulation methodology are needed.

Research on these challenging problems is very active today. New, useful ideas are generated every day and the realm of what is computationally possible is constantly expanding. Time is certainly on our side, as large-scale computing becomes ever more powerful and affordable, and bright young people are educated in multiscale modelling of materials. There is every reason to believe that, besides being intellectually fascinating, hierarchical modelling of polymers will be increasingly important for future technological developments.

Four model representations for amorphous polypropylene

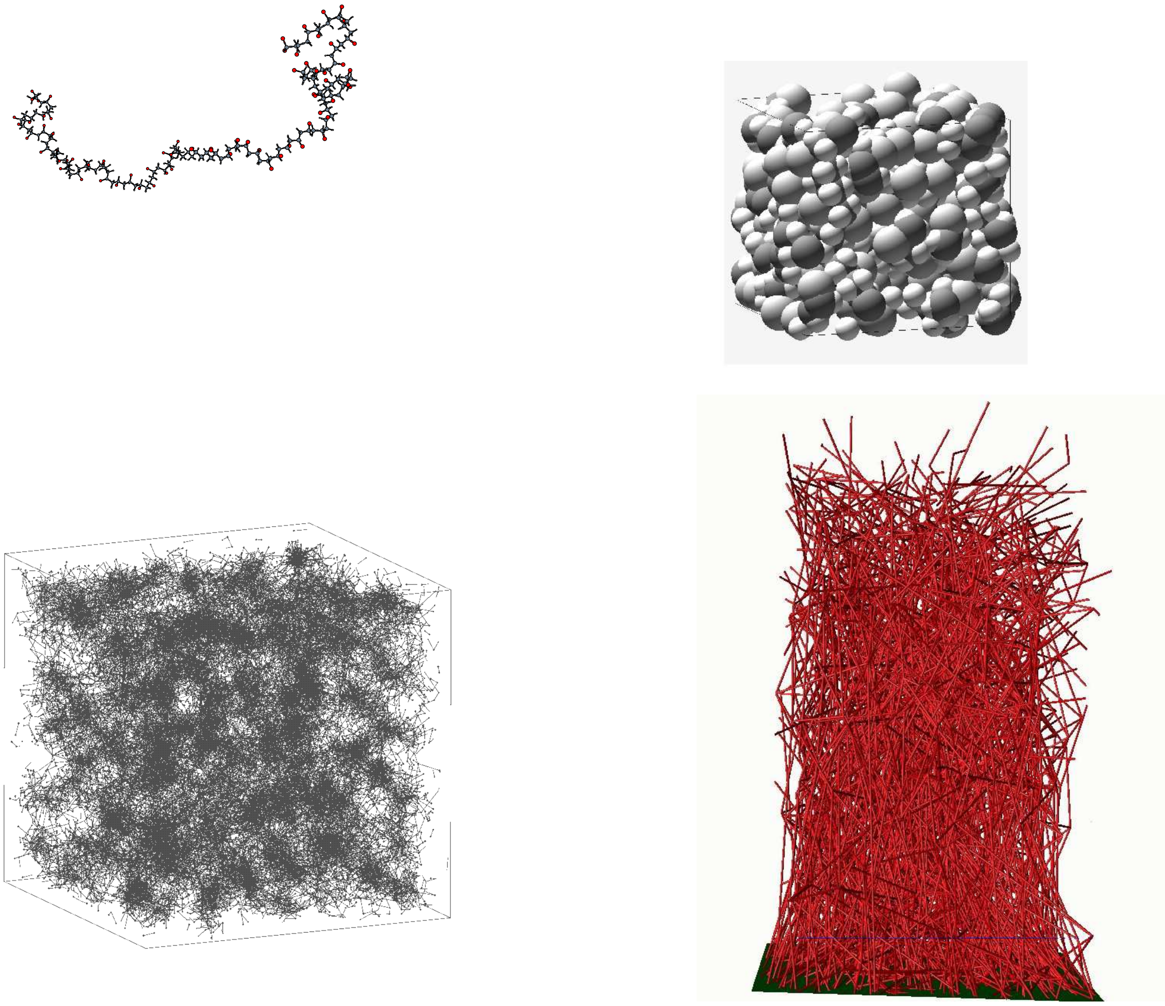

Top left: unperturbed single chain, used in Monte Carlo calculations of intramolecular correlations and chain dimensions in the melt. Top right: atomistic multichain configuration used in extracting PVT properties and segmental dynamics[60] and as a starting point for gas permeability calculations[37]. Bottom left: network of sorption sites, generated on the basis of accessible volume and multidimensional TST analysis of configurations of type (a) and used for KMC simulations of diffusion of methane in glassy atactic polypropylene[37]. Each node represents a site in which a methane penetrant molecule can reside and each line represents a transition path between two sites, to which a forward and a reverse rate constant are assigned. Bottom right: entanglement network model used in simulating interfacial fracture of polypropylene-polyamide interfaces[55]. Nodes are chain ends or entanglement points and lines represent chain strands of known contour length between the nodal points.

Bibliography

[1] D.W. van Krevelen, *Properties of Polymers* (3rd Edition; Elsevier: Amsterdam, 1990). J. Bicerano, *Prediction of Polymer Properties* (Marcel Dekker: New York, 1993).

[2] A. Uhlherr and D.N. Theodorou, Hierarchical simulation approach to structure and dynamics of polymers. Curr. Opin. Solid State and Mat. Sci. **3**, 544-551 (1998).

[3] M.E. Tuckerman, G.J. Martyna, and B.J. Berne, Molecular dynamics algorithm for condensed systems with multiple time scales. J. Chem. Phys. **93** 1287-1291 (1990). M. Tuckerman, B.J. Berne, G.J. Martyna, Reversible time scale molecular dynamics. J. Chem. Phys. **97**, 1990-2001 (1992).

[4] J.J. de Pablo, Q. Yan, and F.A. Escobedo, Simulation of phase transitions in fluids. Ann. Rev. Phys. Chem. **50**, 377-411 (1999).

[5] J.I. Siepmann and D. Frenkel, D. Configurational bias Monte Carlo - A new sampling scheme for flexible chains. Mol. Phys. **75**, 59-70 (1992). J.J. de Pablo, M. Laso, and U.W. Suter, Simulation of polyethylene above and below the melting point. J. Chem. Phys. **96**, 2395-2403 (1992).

[6] B. Smit, S. Karaborni, and J.I. Siepmann, Computer simulations of vapor-liquid phase equilibria of n-alkanes. J. Chem. Phys. **102**, 2126-2140 (1995); ibid. **109**, 352 (1995).

[7] T. Spyriouni, I.G. Economou, and D.N. Theodorou, Thermodynamics of chain fluids from atomistic simulation: a test of the chain increment method for chemical potential. Macromolecules **30**, 4744-4755 (1997). T. Spyriouni, I.G. Economou, D.N. Theodorou, Phase equilibria of mixtures containing chain molecules through a novel simulation scheme. Phys. Rev. Lett. **80**, 4466-4469 (1998).

[8] F.A. Escobedo and J.J. de Pablo, Phase behaviour of model polymeric networks and gels. Mol. Phys. **90**, 437-443 (1997).

[9] M.G. Martin and J.I. Siepmann, Novel configurational-bias Monte Carlo method for branched molecules. Tranferable potentials for phase equilibria. 2. United-atom description of branched alkanes. J. Phys. Chem. B **103**, 4508-4517 (1999). M.D. Macedonia, and E.G. Maginn, A biased grand canonical Monte Carlo method for simulating adsorption using all-atom and branched united atom models. Mol. Phys. **96**, 1375-1390 (1999).

[10] S. Consta, N.B. Wilding, D. Frenkel and Z. Alexandrowicz, Recoil-growth: an efficient simulation method for multi-polymer systems. J. Chem. Phys. **110**, 3220-3228 (1999).

[11] L.R. Dodd, T.D. Boone, and D.N. Theodorou, A concerted rotation algorithm for atomistic Monte Carlo simulation of polymer melts and glasses. Mol. Phys. **78**, 961-996 (1993).

[12] M.W. Deem and J.S. Bader, A configurational bias Monte Carlo method for linear and cyclic peptides. Mol. Phys. **87**, 1245-1260 (1996). M.G. Wu, and M.W. Deem, Analytical rebridging Monte Carlo: application to cis-trans isomerization in proline-containing, cyclic peptides. J. Chem. Phys. **111**, 6625-6632 (1999).

[13] P.V.K. Pant and D.N. Theodorou, Variable connectivity method for the atomistic Monte Carlo simulation of polydisperse polymer melts. Macromolecules **28**, 7224-7234 (1995).

[14] V.G. Mavrantzas, T.D. Boone, E. Zervopoulou, and D.N. Theodorou, End-Bridging Monte Carlo: a fast algorithm for atomistic simulation of condensed phases of long polymer chains. Macromolecules **32**, 5072-5096 (1999).

[15] J.G. Briano and E.D. Glandt, E.D., Statistical Thermodynamics of polydisperse fluids. J. Chem. Phys. **80**, 3336 (1984). D.A. Kofke and E.D. Glandt, Monte Carlo simulation of multicomponent equilibria in a semigrand canonical ensemble. Mol. Phys. **64**, 1105-1131 (1988).

[16] H.P. Deutsch and K. Binder, Critical behavior and crossover scaling in symmetric polymer mixtures - A Monte Carlo investigation. Macromolecules **25**, 6214-6230 (1992).

[17] D.N. Theodorou, Simulations of sorption and diffusion in amorphous polymers, in P. Neogi, Ed. *Diffusion in Polymers* (Marcel Dekker: New York, 1996), pp 67-142.

[18] M. Mehta and D.A. Kofke, Coexistence diagrams of mixtures by molecular simulation. Chem. Eng. Sci. **49**, 2633-2645 (1994).

[19] S.K. Kumar, I. Szleifer, and A.Z. Panagiotopoulos, Determination of the chemical potentials of polymeric systems from Monte Carlo simulations. Phys. Rev. Lett. **66**, 2935-2938 (1991).

[20] D.A. Kofke, Direct evaluation of phase coexistence by molecular simulation via integration along the saturation line. J. Chem. Phys. **98**, 4149-4162 (1993).

[21] V.G. Mavrantzas and D.N. Theodorou, Atomistic simulation of polymer melt elasticity: calculation of the free energy of an oriented polymer melt. Macromolecules **31**, 6310-6332 (1998).

[22] A.P. Lyubartsev, A.A. Martsinovski, S.V. Shevkunov, and P.N. Vorontsov-Velyaminov, New approach to Monte-Carlo calculation of the free energy - Method of expanded ensembles. J. Chem. Phys. **96**, 1776-1783 (1992).

[23] N.F.A. van der Vegt and W.J. Briels, Efficient sampling of solvent free energies in polymers. J. Chem. Phys. **109**, 7578-7582 (1998). N.F.A. van der Vegt, W.J. Briels, M. Wessling, and H. Strathmann, The sorption-induced glass transition in amorphous glassy polymers. J. Chem. Phys. **110**, 11061-11069 (1999).

[24] C.J. Geyer, *Computing Science and Statistics* (American Statistical Association: New York, 1991), pp 156-163. E. Marinari, G. Parisi and J. Ruiz-Lorenzo, in A.P. Young, ed. *Directions in Condensed Matter Physics* (World Scientific: Singapore, 1998), vol 12, pp 59-98.

[25] Prof. Juan J. de Pablo, personal communication.

[26] A.M. Ferrenberg and R.H. Swendsen, New Monte Carlo technique for studying phase transitions. Phys. Rev. Lett. **61**, 2635-2638 (1988). Optimized Monte-Carlo data analysis. Phys. Rev. Lett. **63**, 1195-1198 (1989).

[27] N.B. Wilding, Simulation studies of polymer critical behaviour. J. Phys. Condens. Matter **9**, 585-612 (1997). A.Z. Panagiotopoulos, V. Wong, M.A. Floriano, Phase equilibria of lattice polymers from histogram reweighting Monte Carlo simulations. Macromolecules **31**, 912-918 (1998).

[28] W. Paul and N. Pistoor, A mapping of realistic onto abstract polymer models and an application to two bisphenol polycarbonates. Macromolecules **27**, 1249-1255 (1994). V. Tries, W. Paul, J. Baschnagel, and K. Binder, Modeling polyethylene with the bond fluctuation model. J. Chem. Phys. **106**, 738-748 (1997).

[29] P. Doruker, R. Rapold, and W.L. Mattice, Rotational isomeric state models for polyoxyethylene and polythiacetylene on a high coordination lattice. J. Chem. Phys. **104**, 8742-8749 (1996).

[30] W. Tschöp, K. Kremer, J. Batoulis, J. Bürger, and O. Hahn, Simulation of polymer melts. I. Coarse-graining procedure for polycarbonates. Acta Polymer. **49**, 61-74 (1998). W. Tschöp, K. Kremer, O. Hahn, J. Batoulis, and T. Bürger, Simulation of polymer melts. II. From coarse-grained models back to atomistic description. Acta Polymer. **49**, 75-79 (1998).

[31] M. Murat and K. Kremer, From many monomers to many polymers: soft ellipsoid model for polymer melts and mixtures. J. Chem. Phys. **108**, 4340-4348 (1998).

[32] V.A. Harmandaris, V.G. Mavrantzas, and D.N. Theodorou, Atomistic molecular dynamics simulation of polydisperse linear polyethylene melts. Macromolecules **31**, 7934-7943 (1998).

[33] G. Tsolou, V.G. Mavrantzas, and D.N. Theodorou, Work in progress.

[34] S. Glasstone, K.J. Laidler, and H. Eyring, *The Theory of Rate Processes; the Kinetics of Chemical Reactions, Diffusion, and Electrochemical Phenomena* (McGraw-Hill: New York: New York, 1941). D. Chandler. Statistical Mechanics of isomerization dynamics in liquids and the transition state approximation. J. Chem. Phys. **68**, 2959-2970 (1978) .

[35] B.J. Berne, G. Ciccotti, and D.F. Coker (Eds.) *Classical and Quantum Dynamics in Condensed-Phase Simulations* (World Scientific: Singapore, 1998)

[36] A.A. Gusev and U.W. Suter, Dynamics of small molecules in dense polymers subject to thermal motion. J. Chem. Phys. **99**, 2228-2234 (1993). A.A. Gusev, F. Müller-Plathe, W.F. van Gunsteren, and U.W. Suter, Dynamics of small molecules in bulk polymers. Adv. Polym. Sci. **116**, 207-248 (1994).

[37] M.L. Greenfield and D.N. Theodorou, Molecular modeling of methane diffusion in glassy atactic polypropylene via multidimensional transition state theory. Macromolecules **31**, 7068-7090 (1998).

[38] M. Hutnik, A.S. Argon, and U.W. Suter, Quasi-static modeling of chain dynamics in the amorphous glassy polycarbonate of 4,4'-isopropylidene diphenol. Macromolecules **24**, 5970-5979 (1991).

[39] G.D. Smith and R.H. Boyd, A molecular model for the strength of the dielectric beta-relaxation in methyl acrylate and vinyl acetate polymers. Macromolecules **24**, 2731-2739 (1991).

[40] T.M. Nicholson and J.R. Davies, Modeling of methyl group rotations in PMMA. Macromolecules **30**, 5501-5505 (1997).

[41] R.F. Rapold, U.W. Suter, and D.N. Theodorou, Static atomistic modelling of the structure and ring dynamics of bulk amorphous polystyrene. Macromol. Theory Simul. **3**, 19-43 (1994). R. Khare and M.E. Paulaitis, A study of cooperative phenyl ring flip motions in glassy polystyrene by molecular simulations. **28**, 4495-4504 (1995).

[42] C. Dellago, P.G. Bolhuis, F.S. Csajka, and D. Chandler, Transition path sampling and the calculation of rate constants. J. Chem. Phys. **108**, 1964-1977 (1998). C. Dellago, P.G. Bolhuis, and D. Chandler, On the calculation of reaction rate constants in the transition path ensemble. J. Chem. Phys. **100**, 6617-6625 (1999).

[43] A.F. Voter, Hyperdynamics, Hyperdynamics: accelerated molecular dynamics of infrequent events. Phys. Rev. Lett. **78**, 3908-3911 (1997).

[44] G. Henkelman and H. Jónsson, A dimer method for finding saddle points on high dimensional potential surfaces using only first derivatives. J. Chem. Phys. **111**, 7010-7022 (1999).

[45] P.J. Hoogerbrugge and J.M.V.A. Koelman, Simulating microscopic hydrodynamic phenomena with dissipative particle dynamics. Europhys. Lett. **19**, 155-160 (1992). I. Pagonabarraga, M.H.J. Hagen, and D. Frenkel, Self-consistent dissipative particle dynamics algorithm. Europhys. Lett. **42**, 377-382 (1998). R.D. Groot and P.B. Warren, Dissipative particle dynamics: Bridging the gap between atomistic and mesoscopic simulation. J. Chem. Phys. **107**, 4423-4435 (1997).

[46] Professor W.J. Briels, Personal communication.

[47] E.G. Flekkoy and P.V. Coveney, From molecular dynamics to dissipative particle dynamics. Phys. Rev. Lett. **30**, 1775-1778 (1999).

[48] A.N. Beris and B.J. Edwards, *Thermodynamics of Flowing Systems With Internal Microstructure* (Oxford University Press: Oxford, 1994)

[49] M. Laso and H.C. Öttinger, Calculation of viscoelastic flow using molecular models - the CONNFFESSIT approach. J. Non-Newt. Fluid Mech. **47**, 1-20 (1993). H.C. Öttinger, B.H.A.A. van den Brule, and M. A. Hulsen, Brownian configuration fields and variance-reduced CONNFFESSIT. J. Non-Newt. Fluid Mech. **70**, 255-261 (1997).

[50] M. Grmela and H.C. Öttinger, Dynamics and thermodynamics of complex fluids. I. Development of a general formalism. Phys. Rev. E **56** 6620-6632 (1997). H.C. Öttinger and M. Grmela, Dynamics and thermodynamics of complex fluids II. Illustrations of a general formalism. Phys. Rev. E **56**, 6633-6655 (1997).

[51] J.G.E.M. Fraaije, Dynamic density functional theory for microphase separation kinetics of block copolymer melts. J. Chem. Phys. **99**, 9202-9212 (1993). N.M. Maurits and J.G.E.M. Fraaije, Microscopic dynamics of copolymer melts: from density dynamics to external potential dynamics using nonlocal kinetic coupling. J. Chem. Phys. **107**, 5879-5889 (1997).

[52] V.V. Ginzburg, F. Qiu, M. Paniconi, G. Peng, D. Jasnow, and A.C. Balazs, Simulation of hard particles in a phase-separating polymer mixture. Phys. Rev. Lett. **82**, 4026-4029 (1999). V.V. Ginzburg and A.C. Balazs, Calculating phase diagrams of polymer-platelet mixtures using density functional theory: Implications for polymer/clay composites. Macromolecules **32**, 5681-5688 (1999).

[53] Y. Termonia and P. Smith, Kinetic model for tensile deformation of polymers. 1. Effect of molecular weight. Macromolecules **20**, 835-838 (1987).

[54] J. Bicerano, N.K. Grant, J.E. Seitz, and P.V. K. Pant, Microstructural model for prediction of stress-strain curves of amorphous and semicrystalline elastomers. J. Polym. Sci. B: Polym. Phys. **35**, 2715-2739 (1997).

[55] A. Terzis, D.N. Theodorou and A. Stroeks, Entanglement network of the polypropylene/polyamide interface. 1. Self-consistent field model; 2. Network generation. Macromolecules, in press (2000).

[56] J.M. Polson and D. Frenkel, Numerical prediction of the melting curve of n-octane. J. Chem. Phys. **22**, 1501-1510 (1999).

[57] J. Wendling, A.A. Gusev, and U.W. Suter, Predicting the cocrystallization behavior of random copolymers via free energy calculations. Macromolecules **31**, 2509-2525 (1998).

[58] J.P.K. Doye and D. Frenkel, Mechanism of thickness determination in polymer crystals. Phys. Rev. Lett. **10**, 2160-2163 (1998).

[59] A. van Zon and S. W. de Leeuw, Self-motion in glass-forming polymers: A molecular dynamics study. Phys. Rev. E **60**, 6942-6950 (1999).

[60] S.J. Antoniadis, C.T. Samara and D.N. Theodorou, Molecular dynamics of atactic polypropylene melts. Macromolecules **31**, 7944-7952 (1998).

[61] D.N. Theodorou and U.W. Suter, Detailed molecular structure of a vinyl polymer glass. Macromolecules **18**, 1467-1478 (1985). Atomistic modeling of mechanical properties of polymeric glasses. Macromolecules **19**, 139-154 (1986).

[62] P. Robyr, M. Müller, and U.W. Suter, Atomistic simulations of glassy polystyrenes with realistic chain conformations. Macromolecules **32**, 8681-8684 (1999).

VI

Bridging the time-scale gap: Homogeneous nucleation

Pieter Rein ten Wolde
Present address: Department of Chemistry,
University of California at Berkeley, Berkeley, CA, USA,
and Daan Frenkel
FOM Institute for Atomic and Molecular Physics
Amsterdam, Netherlands.
email: frenkel@amolf.nl

Abstract

Activated processes are a typical example of a physical phenomenon that spans a wide range of timescales. A specific example of such an activated process is homogeneous nucleation. Below we briefly describe some examples that show how computer simulation can now be used to study this elusive phenomenon.

Introduction

Gibbs [1] was the first to realize that the stability of a phase is related to the work that has to be done in order to create a critical nucleus of the new phase. However, the relevance of his work to nucleation remained largely unnoticed until the 1920's and 1930's when Volmer and Weber [2], and Becker and Döring [3] laid the foundations for what is now called classical nucleation theory. In classical nucleation theory (CNT) it is assumed that the nuclei are compact, spherical objects, that behave like small droplets of bulk phase. The free energy of a spherical liquid droplet of radius R in a vapor is then given by

$$\Delta G = 4\pi R^2\gamma + \frac{4}{3}\pi R^3\rho\Delta\mu, \tag{VI.1}$$

where γ is the surface free energy, ρ is the density of the bulk liquid, and $\Delta\mu$ is the difference in chemical potential between bulk liquid and bulk vapor. Clearly, the first term on the right hand side of Eq. VI.1 is the surface term, which is positive, and the second term is the volume term, which is negative; the difference in chemical potential is the driving force for the nucleation process. The height of the nucleation barrier can easily be obtained from the above expression, yielding

$$\Delta G^* = \frac{16\pi\gamma^3}{3\rho^2\Delta\mu^2}. \tag{VI.2}$$

This equation shows that the barrier height depends not only on the surface free energy γ (and the density ρ), but also on the difference in chemical potential $\Delta\mu$. The difference in chemical potential is related to the supersaturation. Hence, the height of the free-energy barrier that separates the stable from the metastable phase depends on the degree of supersaturation. At coexistence, the difference in chemical potential is zero, and the height of the barrier is infinite. Although the system is equally likely in the liquid and vapor phase, once the system is one state or the other, the system will remain in this state; it simply cannot transform into the other state.

Macroscopic thermodynamics dictates that the phase that is formed in a supersaturated system is the one that has the lowest free energy. However, nucleation is an essentially dynamic process, and therefore one cannot expect *a priori* that, on supersaturating the system, the thermodynamically most stable phase will be formed. In 1897, Ostwald [4] formulated his step rule, stating that the crystal phase that is nucleated from the melt need not be the one that is thermodynamically most stable, but the one that is closest in free energy to the fluid phase. Stranski and Totomanow [5] reexamined this rule and argued that the nucleated phase is the phase that has the lowest free-energy barrier of formation, rather than the phase that is globally stable under the conditions prevailing. In experiments on rapidly cooled melt, nucleation of metastable phases is often found [6, 7, 8]. However, all these studies consider the formation of *bulk* phases. The simulation results discussed in this article suggest that even on a *microscopic* scale, something similar to Ostwald's step rule seems to hold.

Homogeneous crystal nucleation from the melt

Alexander and McTague [9] have argued, on the basis of Landau theory, that at least for small supercooling, nucleation of the body-centered cubic (bcc) phase should uniquely be favored in all simple fluids exhibiting a weak first order phase transition. Also a theoretical study by Klein and Levraz [10] suggests that a metastable bcc phase can easily be formed from the undercooled liquid. Experimentally, nucleation of a metastable bcc phase has been observed in rapidly cooled metal melts [6, 7, 8]. However, when attempts were made to investigate the formation of metastable bcc nuclei on a microscopic scale, using computer simulation [11, 12, 13, 14, 1, 16, 17], the picture that emerged gave little support for the Alexander-McTague scenario. For the Lennard-Jones system, which is known to have a stable face-centered cubic (fcc) structure up to the melting curve, the formation of a metastable bcc phase was observed in only one of the simulation studies reported [12], while all other studies [11, 13, 14, 1, 16, 17] found evidence for the formation of fcc nuclei. Of particular interest is the simulation of Swope and Andersen [17] on a system comprising one million Lennard-Jones particles. This study showed that, although both fcc and bcc nuclei are formed in the early stages of the nucleation, only the fcc nuclei grow into larger crystallites. It should be noted however, that in all these simulation studies, large degrees of supercooling (down to 50% of the melting temperature, or lower) had to be imposed to see any crystal formation on the time-scale of the simulation. For such a large undercooling one should expect the free-energy barrier for nucleation into essentially all possible crystal phases to be quite small. It is therefore not obvious that crystal nucleation at large undercooling will proceed in the same way as close to the freezing point.

We have studied homogeneous nucleation in a Lennard-Jones system closer to the freezing point, at 20% of below the melting point. As we show below, at this degree of supercooling the barrier is significant and the "brute-force" approach, where we wait for nuclei to form spontaneously, will not work. Instead, we have used the umbrella-sampling technique [2] to compute the free-energy barrier to crystal nucleation. The umbrella sampling technique can be used even at small (i.e. realistic) undercooling where the straightforward molecular dynamics technique will fail, because the nucleation barrier diverges at coexistence. Moreover, the umbrella-sampling technique allows us to stabilize the critical nucleus and study its structure in detail.

The basic idea of the umbrella-sampling technique is that we can sample states even near the top of the barrier by biasing the sampling of configuration space and correcting for the bias afterwards. We can bias the sampling of configuration space by adding a fictitious potential to the potential-energy function of our model system. In the present case, the biasing potential was taken to be a function of the order parameter Q_6, as introduced by Steinhardt *et al.* [19]. The value of this global order parameter is a measure for the long-range orientational order and hence for the degree of crystallinity in the system. On the other hand, Q_6 is fairly insensitive to the differences between the possible crystalline structures. This implies that by using this order parameter as our reaction coordinate, we do not favor one crystalline structure over the other. Rather, the system is allowed to select its 'own' specific reaction path from the liquid to the solid.

The Gibbs free energy, G, is a function of this order parameter

$$\beta \Delta G(Q_6) = \text{constant} - \ln[P(Q_6)], \tag{VI.3}$$

where $\beta \equiv 1/k_B T$ is the inverse temperature, with k_B Boltzmann's constant and T the absolute temperature, and $P(Q_6)$ is the probability per unit interval to find the order parameter around a given value of Q_6. We have computed the free-energy barrier by measuring the probability distribution function $P(Q_6)$ at two different pressures [20, 21]. Figure VI.1 shows the free-energy barriers computed for these two pressures. Let us now consider the structure of the nuclei. An analysis of the Voronoi signatures and the bond-order parameters as introduced by Steinhardt *et al.* [19], indicated that the small crystallites in the metastable liquid are mainly bcc ordered, whereas the postcritical nuclei are predominantly fcc-ordered [1]. In the metastable liquid we also found some small icosahedral clusters, but these did not grow into larger crystallites. We therefore determined on the basis of the distribution of the local bond-order parameter values, the fraction of particles that are in an fcc, bcc or liquid-like environment, denoted by f_{fcc}, f_{bcc} and f_{liq}, respectively [21].

[1] An examination of the order parameter W_4 revealed that mainly an fcc structure is formed, rather than an hcp structure, although the difference in free energies between the two structures is small. For a more detailed study of the competition of the formation of the fcc phase versus the hcp phase, we to refer to Ref. [22]

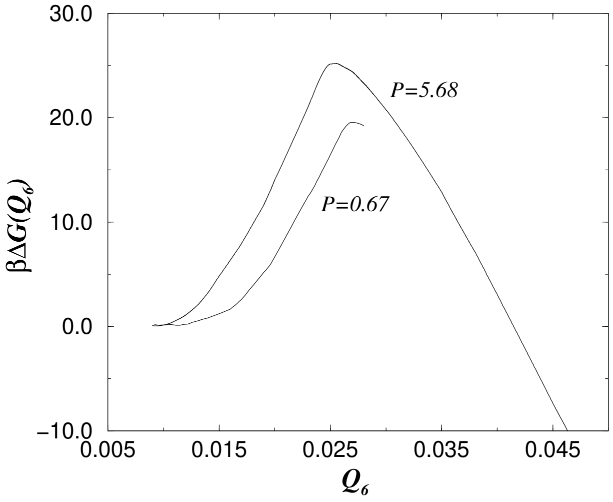

Figure VI.1: The Gibbs free energy of a Lennard-Jones system as a function of crystallinity (Q_6) at 20% undercooling for two different pressures, i.e. $P = 5.68$ ($T = 0.92$) and $P = 0.67$ ($T = 0.6$). The temperatures and pressures are in units of the Lennard-Jones well depth ϵ and the Lennard-Jones diameter σ.

Fig. VI.2 shows the structural "composition" of the largest cluster in the system, as a function of the "reaction coordinate", Q_6.

The figure shows that the pre-critical nuclei are predominantly bcc- and liquid-like. However, near the top of the barrier, at $Q_6 = 0.025$, there is a clear change in the nature of the solid nuclei from bcc- and liquid-like to mainly fcc-like. The fact that the pre-critical nuclei are rather liquid-like is not surprising as they are quite small and consist of nearly only interface. The important point to note is that these nuclei have clearly more bcc than fcc character. This suggests that, at least for small crystallites, we find the behavior predicted by Landau theory [9]. Yet, as the critical and postcritical clusters are predominantly fcc-like, the present results are also compatible with the findings of Swope and Andersen [17], who observed that nucleation proceeded through fcc crystallites.

Still, we note that the critical and postcritical nuclei are not fully fcc ordered. They have both considerable liquid-like and bcc-like character. In fact, it is not surprising that the critical nucleus has some liquid-like character. After all, it consists only of some 642 particles and has therefore a large surface-to-volume ratio. However, the bcc-like character is more intriguing. We have therefore studied the local order of the critical nucleus in more detail.

Visual inspection of the critical and postcritical nuclei showed that the nuclei at this moderate degree of undercooling are fairly compact, more or less spherical objects. Given the spherical shape of the critical nucleus it is meaningful to calculate f_{liq}, f_{bcc} and f_{fcc} in a spherical shell of radius r around the center-of-mass of the cluster. Fig. VI.3 shows the radial profile of the local order of the critical nucleus. As expected, we find that the core of the nucleus is almost fully fcc-ordered and that far away from the center of the nucleus, f_{fcc} decays to zero and f_{liq} approaches unity. More surprisingly however, is that f_{bcc} increases in the interface and becomes even larger than f_{fcc}, before

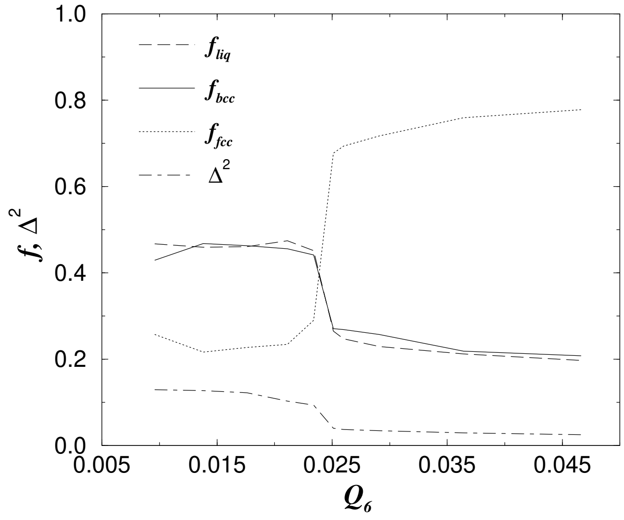

Figure VI.2: Structural composition of the largest cluster in a Lennard-Jones system,indicated by f_{liq}, f_{bcc}, f_{fcc} and Δ^2, as a function of Q_6 (the reaction coordinate) at 20% undercooling ($P = 5.68$, $T = 0.92$). Δ^2 is a measure for the fraction of particles, the structure of which could not be identified as either being liquid-like, bcc-like, or fcc-like.

it decays to zero in the liquid. Hence, the present simulations suggest that the fcc-like core of the equilibrated nucleus is "wetted" by a shell which has more bcc character. This finding explains why Fig. VI.2 shows that even fairly large nuclei do not have a pure fcc signature: there is always a residual bcc signature due to the interface. It also explains the strong bcc character of the small clusters, such as appear on the liquid side of the barrier: they are so small that their structure is strongly surface-dominated.

Coil-globule transition in condensation of polar fluids

The formation of a droplet of water from the vapor is probably the best known example of homogeneous nucleation of a polar fluid. However, the nucleation behavior of polar fluids is still poorly understood. In fact, while classical nucleation theory gives a reasonable prediction of the nucleation rate of nonpolar substances, it seriously overestimates the rate of nucleation of highly polar compounds, such as acetonitrile, benzonitrile and nitrobenzene [23, 24].

In order to explain the discrepancy between theory and experiment, several nucleation theories have been proposed. It has been suggested that in the critical nuclei the dipoles are arranged in an anti-parallel head-to-tail configuration [23, 24], giving the clusters a non-spherical, prolate shape, which increases the surface-to-volume ratio and thereby the height of the nucleation barrier. In the oriented dipole model introduced by Abraham [25], it is assumed that the dipoles are perpendicular to the interface, yielding a size dependent surface tension due to the effect of curvature of the surface on the dipole-dipole interaction. However, in a density-functional study of a weakly polar

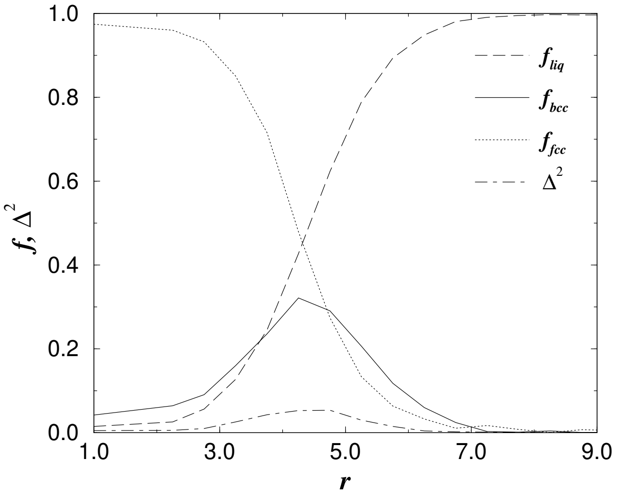

Figure VI.3: Structure of the critical nucleus, indicated by f_{liq}, f_{bcc}, f_{fcc} and Δ^2, as a function of r, the distance to its center-of-mass, at 20% undercooling ($P = 5.68$, $T = 0.92$) in a Lennard-Jones system.

Stockmayer fluid, it was found that on the liquid (core) side of the interface of critical nuclei, the dipoles are not oriented perpendicular to the surface, but parallel [26].

We have studied the structure and free energy of critical nuclei, as well as pre-and postcritical nuclei, of a highly polar Stockmayer fluid [27]. In the Stockmayer system, the particles interact via a Lennard-Jones pair potential plus a dipole-dipole interaction potential

$$\begin{aligned} v(\mathbf{r}_{ij}, \boldsymbol{\mu}_i, \boldsymbol{\mu}_j) &= 4\epsilon \left[\left(\frac{\sigma}{r_{ij}} \right)^{12} - \left(\frac{\sigma}{r_{ij}} \right)^{6} \right] \\ &\quad -3(\boldsymbol{\mu}_i \cdot \mathbf{r}_{ij})(\boldsymbol{\mu}_j \cdot \mathbf{r}_{ij})/r_{ij}^5 + \boldsymbol{\mu}_i \cdot \boldsymbol{\mu}_j / r_{ij}^3. \end{aligned} \qquad \text{(VI.4)}$$

Here ϵ is the Lennard-Jones well depth, σ is the Lennard-Jones diameter, $\boldsymbol{\mu}_i$ denotes the dipole moment of particle i and $\mathbf{r}_{ij}$ is the vector joining particle i and j. We have studied the nucleation behavior for $\mu^* = \mu/\sqrt{\epsilon\sigma^3} = 4$, which is close to the value of water.

We have computed [27] the excess free energy $\Delta\Omega$ of a cluster of size n in a volume V, at chemical potential μ and at temperature T, from the probability distribution function P_n

$$\beta\Delta\Omega(n, \mu, V, T) \equiv -\ln[P(n)] = -\ln[N_n/N]. \qquad \text{(VI.5)}$$

Here β is the reciprocal temperature; N_n is the average number of clusters of size n and N is the average total number of particles. As the density of clusters in the vapor is low, the interactions between them can be neglected. As a consequence, we can obtain the free-energy barrier at any desired chemical potential μ' from the nucleation barrier measured at a given chemical potential μ via

$$\begin{aligned} \beta\Delta\Omega(n, \mu', V, T) &= \beta\Delta\Omega(n, \mu, V, T) - \beta(\mu' - \mu)n \\ &\quad + \ln\left[\rho(\mu')/\rho(\mu)\right], \end{aligned} \qquad \text{(VI.6)}$$

where $\rho = N/V$ is the total number density in the system.

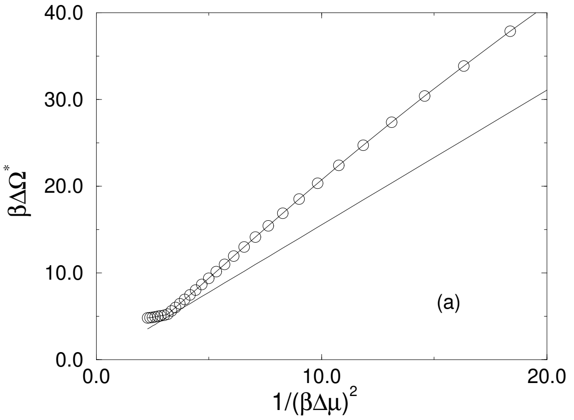

Figure VI.4: Comparison of the barrier height between the simulation results (open circles) and classical nucleation theory (straight solid line) for a Stockmayer fluid with reduced dipole moment $\mu^* = \mu/\sqrt{\epsilon\sigma}^3 = 4$ and reduced temperature $T^* = k_B T/\epsilon = 3.5$. The chemical potential difference $\Delta\mu$ is the difference between the chemical potential of the liquid and the vapor.

Fig. VI.4 shows the comparison between the simulation results and CNT for the height of the barrier. Clearly, the theory underestimates the height of the nucleation barrier. As the nucleation rate is dominated by the height of the barrier, our results are in qualitative agreement with the experiments on strongly polar fluids [23, 24], in which it was found that CNT overestimates the nucleation rate. But, unlike the experiments, the simulations allow us to investigate the microscopic origins of the breakdown of classical nucleation theory.

In classical nucleation theory it is assumed that already the smallest clusters are compact, more or less spherical objects. In a previous simulation study on a typical nonpolar fluid, the Lennard-Jones fluid, we found that this is a reasonable assumption [28], even for nuclei as small as ten particles. However, the interaction potential of the Lennard-Jones system is isotropic, whereas the dipolar interaction potential is anisotropic. On the other hand, the bulk liquid of this polar fluid is isotropic.

We find that the smallest clusters, that initiate the nucleation process, are not compact, spherical objects, but chains, in which the dipoles align head-to-tail. In fact, we find a whole variety of differently shaped clusters in dynamical equilibrium: linear chains, branched-chains, and "ring-polymers". Initially, when the cluster size is increased, the chains become longer. But, beyond a certain size, the clusters collapse to form a compact globule. In order to quantify this behaviour, we have determined the size dependence of the radius-of-gyration, as well as the three eigenvalues of the moment-of-inertia tensor. In Fig. VI.5 we show the square of the radius of gyration, divided by $n^{2/3}$. For a compact, spherical object R_g^2 scales with $n^{2/3}$, whereas for chains R_g^2 scales with n^{α}, where $1.2 < \alpha < 2$, depending on the stiffness of the chain. Hence,

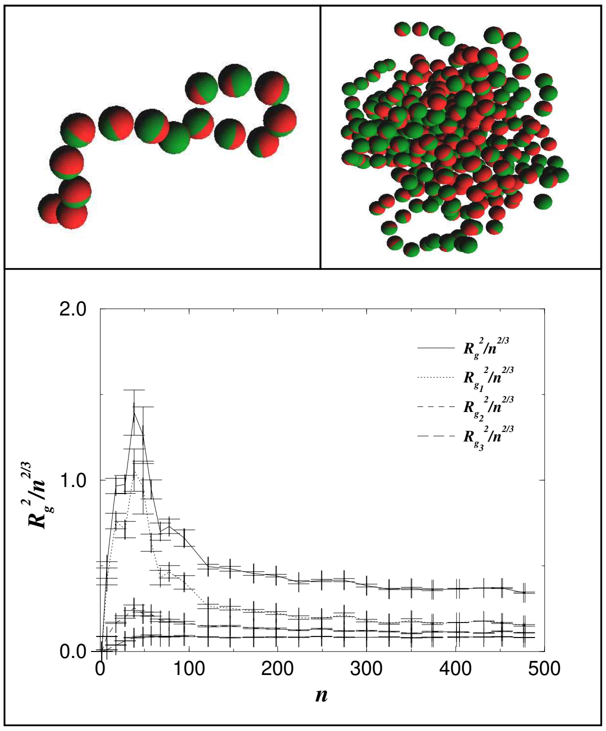

Figure VI.5: Radius of gyration R_g, and the three eigenvalues of the moment-of-inertia tensor, as a function of the size n of a Stockmayer cluster, at supersaturation $S = 1.26$, temperature $T^* = 3.5$ and reduced dipole moment $\mu^* = 4$. Initially, the clusters are chain-like (snapshot top left), but at a cluster size of $n \approx 30$ they collapse to compact, spherical nuclei (snapshot top right

for chain-like clusters $R_g^2/n^{2/3}$ should increase with n, whereas for a globule it should approach a constant value.

Fig. VI.5 shows that initially $R_g^2/n^{2/3}$ increases with the size of the cluster. Moreover, one eigenvalue of the moment-of-inertia tensor is much larger than the other two, indicating the tendency of clusters to form chains. However, at a cluster size of $n \approx 30$, $R_g^2/n^{2/3}$ starts to decrease and approaches a constant value at $n \approx 200$. Analysis of the individual eigenvalues shows that at that point the clusters have collapsed to compact objects that fluctuate around a spherical shape. However, in the interface, traces of the tendency to form chains survive.

The Stockmayer fluid is a simple model system for polar fluids and the mechanism that we describe here might not be applicable for all fluids that have a strong dipole moment. The nucleation behavior of water, for instance, is probably more dominated by hydrogen bonding [29]. Still, our simulations clearly show that the presence of a strong permanent dipole can drastically change the pathway for condensation.

Protein crystallization

Proteins are notoriously difficult to crystallize. The experiments indicate that proteins only crystallize under very specific conditions [30, 31, 32]. Moreover, the conditions are often not known beforehand. As a result, growing good protein crystals is a time-consuming business.

In 1994, George and Wilson [33] proposed that the success of protein crystallization is correlated with the value of B_2, the second osmotic virial coefficient. The second virial coefficient describes the lowest order correction to the van 't Hoff law for the osmotic pressure Π:

$$\frac{\Pi}{\rho k_B T} = 1 + B_2\rho + (\text{terms of order } \rho^2) \tag{VI.7}$$

where ρ is the number density of the dissolved molecules, k_B is Boltzmann's constant, and T is the absolute temperature. The value of the second virial coefficient depends on the effective interaction between a pair of macromolecules in solution [34]:

$$B_2 = 2\pi \int r^2 dr [1 - \exp[-\beta v(r)]] \tag{VI.8}$$

where $\beta \equiv 1/k_B T$ and $v(r)$ is the interaction energy of a pair of molecules at distance r. For macromolecules, B_2 can be determined from static light scattering experiments [35].

George and Wilson measured B_2 for a number of proteins in various solvents. They found that for those solvent conditions that are known to promote crystallization, B_2 was restricted to a narrow range of small negative values. For large positive values of B_2 crystallization did not occur at all, whereas for large negative values of B_2 protein aggregation, rather than crystallization, took place. This correlation has been extended to over 20 distinct proteins with a wide variety of crystal structures and interaction potentials [36].

Subsequently, Rosenbaum, Zamora and Zukoski [36, 37] established a link between the work of George and Wilson and a computer-simulation study by Hagen and Frenkel [38], who studied the phase behaviour of colloid-polymer mixtures. In these mixtures, the polymers induce an effective attraction between the colloids. The range of the attraction depends on the radius-of-gyration of the polymer. Thus, by regulating the effective size of the polymer, the interaction range between the colloids can be tuned. Since the theoretical work of Gast, Hall and Russel [39, 40], it is known that the range of attraction between spherical colloids has a drastic effect on the overall appearance of the phase diagram. If the range of attraction is long in comparison to the diameter of the colloids, the phase diagram of the colloidal suspension resembles that of an atomic substance, such as argon: depending on the temperature and density, the colloids can occur in three phases (Fig. VI.6A) – a dilute colloidal fluid (analogous to the vapor phase), a dense colloidal fluid (analogous to the liquid phase), and a colloidal crystal phase.

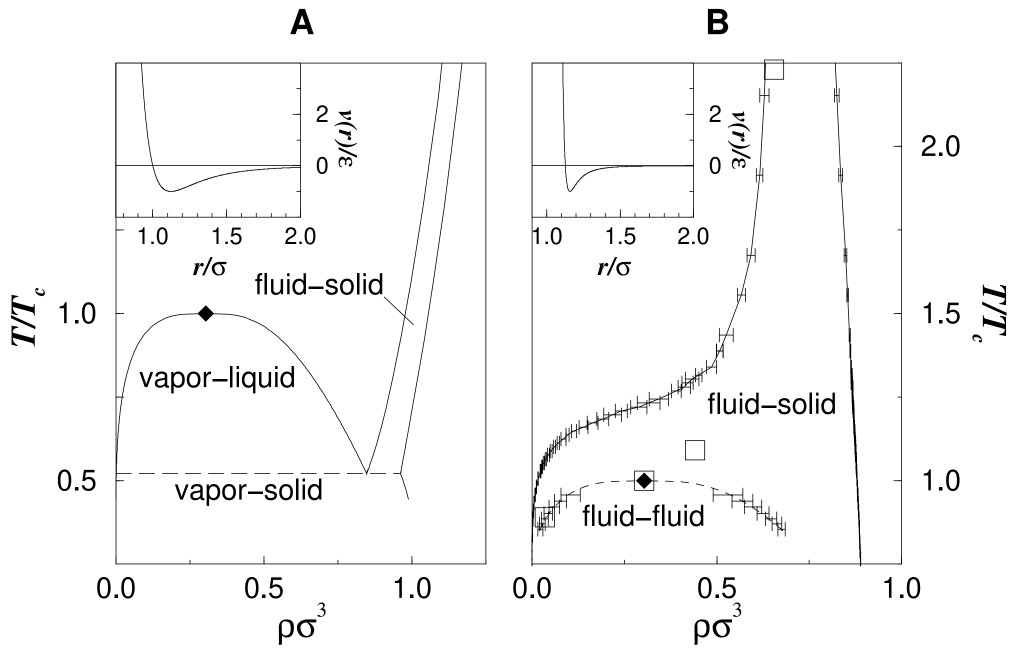

Figure VI.6: (A): Typical phase diagram of a molecular substance with a relatively long-ranged attractive interaction. The phase diagram shown here corresponds to the Lennard-Jones 6–12 potential ($v(r) = 4\epsilon[(\sigma/r)^{12} - (\sigma/r)^6]$ – solid curve in insert). The dashed line indicates the triple point. (B): Typical phase diagram of colloids with short-ranged attraction. The phase diagram was computed for the potential given in Eq. VI.9 (solid curve in insert), with $\alpha = 50$. In both figures, the temperature is expressed in units of the critical temperature T_c, while the number density is given in units σ^{-3}, where σ, the effective diameter of the particles is defined in the expression for $v(r)$. The diamonds indicate the fluid-fluid critical points. In both figures, the solid lines indicate the equilibrium coexistence curves. The dashed curve in B indicates the metastable fluid-fluid coexistence. Crystal-nucleation barriers were computed for the points denoted by open squares.

However, when the range of the attraction is reduced, the fluid-fluid critical point moves towards the triple point, where the solid coexists with the dilute and dense fluid phases. At some point, the critical point and the triple point will coalesce. If the range of attraction is made even shorter (less than some 25% of the colloid diameter), only two stable phases remain: one fluid and one solid (Fig. VI.6B). However, the fluid-fluid coexistence curve survives in the metastable regime below the fluid-solid coexistence curve (Fig. VI.6B). This is indeed found in experiments [41, 42, 43, 44] and simulations [38].

Why is this relevant for protein crystallization? First of all, globular proteins in solution often have short-ranged attractive interactions. In fact, a series of studies [45, 46, 47, 48] show that the phase diagram of a wide variety of proteins is of the kind shown in Fig. VI.6. In addition, Rosenbaum and Zukoski [36, 37], showed that the phase diagrams can be mapped on top of each other when compared on equal footing, ie. on the basis of the density and the second virial coefficient. However, the most interesting observation of Rosenbaum and Zukoski [36, 37] is that the conditions under which a large number of globular proteins can be made to crystallize, map onto a narrow temperature range, or, more precisely, a narrow range in the value of the osmotic second virial coefficient, of the computed fluid-solid coexistence curve of colloids with short-ranged attraction [38]. If the temperature is too high, crystallization is hardly observed at all, whereas if the temperature is too low, amorphous precipitation rather than crystallization occurs. Only in a narrow window around the metastable critical point, high-quality crystals can be formed. Several authors had already noted that a similar crystallization window exists for colloidal suspensions [49, 50]. We have investigated the origin of this crystallization window. We found that the presence of a metastable fluid-fluid critical point is essential [51]. In order to grow high-quality protein crystals, the quench should be relatively shallow, and the system should not be close to a glass transition. Under these conditions, the rate-limiting step in crystal nucleation is the crossing of the free-energy barrier. We have therefore computed the free-energy barrier for homogeneous crystal nucleation for a model "globular" protein. In this model system, the particles interact via a modified Lennard-Jones potential

$$v(r) = \begin{cases} \infty & (r < \sigma) \\ \frac{4\epsilon}{\alpha^2}\left(\frac{1}{[(r/\sigma)^2-1]^6} - \alpha\frac{1}{[(r/\sigma)^2-1]^3}\right) & (r \geq \sigma) \end{cases} \tag{VI.9}$$

where σ denotes the hard-core diameter of the particles and ϵ the well depth. The width of the attractive well can be adjusted by varying the parameter α. Fig. VI.6 shows the phase diagram for $\alpha = 50$. It is clear that the potential in Eq. (VI.9) provides a simplified description of the effective interaction between real proteins in solution: it accounts both for direct and for solvent-induced interactions between the globular proteins. However, the model system reproduces the phase behaviour of proteins in solution. In fact, the phase-diagram can be mapped onto the experimentally determined phase-diagrams of a variety of globular proteins [36, 37].

The free-energy barriers were computed for the four points denoted by open squares in Fig. VI.6. These points were chosen such that on basis of classical nucleation theory the same height of the barrier could be expected. In order to compute the free-energy barrier, we have computed the free energy of a nucleus as a function of its size. However, we first have to define what we mean by a "nucleus". As we are interested in crystallization, it might seem natural to use a crystallinity criterion. However, as mentioned, we expect that crystallization near the critical point is influenced by critical density fluctuations. We therefore used not only a crystallinity criterion, but also a density criterion. We define the size of a high-density cluster (be it solid- or liquid-like) as the number of connected particles, N_ρ, that have a significantly higher local density than the particles in the remainder of the system. The number of these particles that is also in a crystalline environment, which is determined on the basis of the local bond-order parameters [19], is denoted by N_{crys}. In our simulations, we have computed the free-energy "landscape" of a nucleus as a function of the two coordinates N_ρ and N_{crys}. Fig. VI.7 shows the free-energy landscape for $T = 0.89T_c$ and $T = T_c$. The

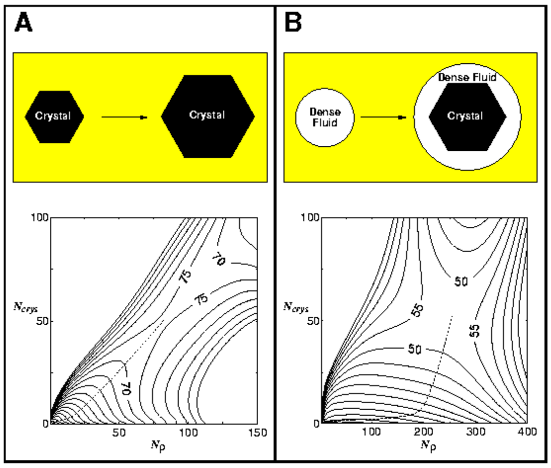

Figure VI.7: Contour plots of the free-energy landscape along the path from the metastable fluid to the critical crystal nucleus, for our system of spherical particles with short-ranged attraction. The curves of constant free energy are drawn as a function of N_ρ and N_{crys} (see text) and are separated by $5k_BT$. (A): The free energy landscape well below the critical temperature ($T/T_c = 0.89$). The lowest free-energy path to the critical nucleus is indicated by a dashed curve. This curve corresponds to the formation and growth of a highly crystalline cluster. (B): As (A), but for $T = T_c$. In this case, the free-energy valley (dashed curve) first runs parallel to the N_ρ axis (formation of a liquid-like droplet), and then moves towards a structure with a higher crystallinity (crystallite embedded in a liquid-like droplet). The free energy barrier for this route is much lower than the one in (A).

free-energy landscapes for the other two points are qualitatively similar to the one for $T = 0.89T_c$ and will not be shown here.We find that away from T_c (both above and below), the path of lowest free energy is one where the increase in N_ρ is proportional to the increase in N_{crys} (Fig. VI.7A). Such behavior is expected if the incipient nucleus is simply a small crystallite. However, around T_c, critical density fluctuations lead to a striking change in the free-energy landscape (Fig. VI.7B). First, the route to the critical nucleus leads through a region where N_ρ increases while N_{crys} is still essentially zero. In other words: the first step towards the critical nucleus is the formation of a liquid-like droplet. Then, beyond a certain critical size, the increase in N_ρ is proportional to N_{crys}, that is, a crystalline nucleus forms inside the liquid-like droplet.

Clearly, the presence of large density fluctuations close to a fluid-fluid critical point has a pronounced effect on the route to crystal nucleation. But, more importantly, the nucleation barrier close to T_c is much lower than at either higher or lower temperatures (Fig. VI.8). The observed reduction in ΔG^* near T_c by some $30k_BT$ corresponds to an increase in nucleation rate by a factor 10^{13}. Finally, let us consider the implications of

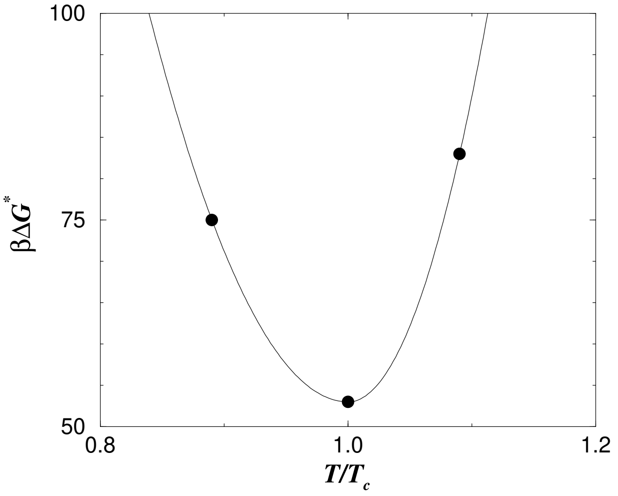

Figure VI.8: Variation of the free-energy barrier for homogeneous crystal nucleation, as a function of T/T_c, in the vicinity of the critical temperature. The solid curve is a guide to the eye. The nucleation barrier at $T = 2.23T_c$ is $128k_BT$ and is not shown in this figure. The simulations show that the nucleation barrier goes through a minimum around the metastable critical point (see text).

this reduction of the crystal nucleation barrier near T_c. An alternative way to lower the crystal nucleation barrier would be to quench the solution deeper into the metastable region below the solid-liquid coexistence curve. However, such deep quenches often result in the formation of amorphous aggregates [33, 36, 37, 42, 43, 44, 48]. Moreover, in a deep quench, the thermodynamic driving force for crystallization ($\mu_{liq} - \mu_{cryst}$) is also enhanced. As a consequence, the crystallites that nucleate will grow rapidly and far from perfectly [31]. Thus the nice feature of crystal nucleation in the vicinity of the metastable critical point is, that crystals can be formed at a relatively small degree of undercooling. This should lead to protein crystals of high quality. It is clear that our model is simplified. However, our model system reproduces the phase behavior of compact proteins in solution. Moreover, the mechanism that we describe here is general, and does not depend on the details of the interaction potential. We expect that when a metastable fluid-fluid coexistence is present below the stable sublimation curve, critical density fluctuations facilitates the formation of ordered structures.

Conclusions

Ostwald formulated his step rule more than a century ago [4] on the basis of macroscopic studies of phase transitions. The simulations suggest that also on a microscopic level, a "step rule" may apply and that metastable phases may play an important role in nucleation. We find that the structure of the pre-critical nuclei is that of a metastable phase (bcc/chains/liquid). As the nuclei grow, the structure in the core transforms into that of the stable phase (fcc/liquid/fcc-crystal). Interestingly, in the interface of the larger nuclei traces of the structure of the smaller nuclei are retained.

Bibliography

[1] J. W. Gibbs, *The Scientific Papers of J. Willard Gibbs*, Dover, New York (1961).

[2] M. Volmer and A. Weber, Z. Phys. Chem. **119**, 227 (1926).

[3] R. Becker and W. Döring, Ann. Phys. **24**, 719 (1935).

[4] W. Ostwald, Z. Phys. Chem. **22**, 289 (1897).

[5] I. N. Stranski and D. Totomanow, Z. Physikal. Chem. **163**, 399 (1933).

[6] R. E. Cech, J. Met. **8**, 585 (1956).

[7] H.-M. Lin, Y.-W. Kim, and T. F. Kelly, Acta Metall. **36**, 2537 (1988).

[8] W. Löser, T. Volkmann, and D. M. Herlach, Mat. Sci. Eng. **A178**, 163 (1994).

[9] S. Alexander and J. P. McTague, Phys. Rev. Lett. **41**, 702 (1978).

[10] W. Klein and F. Leyvraz, Phys. Rev. Lett. **57**, 2845 (1986).

[11] M. J. Mandell, J. P. McTague, and A. Rahman, J. Chem. Phys. **64**, 3699 (1976).

[12] M. J. Mandell, J. P. McTague and A. Rahman, J. Chem. Phys. **66**, 3070 (1977).

[13] C. S. Hsu and A. Rahman, J. Chem. Phys. **71**, 4974 (1979).

[14] R. D. Mountain and A. C. Brown, J. Chem. Phys. **80**, 2730 (1984).

[15] S. Nosé and F. Yonezawa, J. Chem. Phys. **84**, 1803 (1986).

[16] J. Yang, H. Gould, and W. Klein, Phys. Rev. Lett. **60**, 2665 (1988).

[17] W. C. Swope and H. C. Andersen, Phys. Rev. B **41**, 7042 (1990).

[18] G. M. Torrie and J. P. Valleau, Chem. Phys. Lett. **28**, 578 (1974).

[19] P. J. Steinhardt, D. R. Nelson, and M. Ronchetti, Phys. Rev. B **28**, 784 (1983).

[20] P. R. ten Wolde, M. J. Ruiz-Montero, and D. Frenkel, Phys. Rev. Lett. **75**, 2714 (1995).

[21] P. R. ten Wolde, M. J. Ruiz-Montero, and D. Frenkel, J. Chem. Phys. **104**, 9932 (1996).

[22] S. Pronk and D. Frenkel, J. Chem. Phys. **110**, 4589 (1999).

[23] D. Wright, R. Caldwell, C. Moxeley, and M. S. El-Shall, J. Chem. Phys. **98**, 3356 (1993).

[24] D. Wright and M. S. El-Shall, J. Chem. Phys. **98**, 3369 (1993).

[25] F. F. Abraham, Science **168**, 833 (1970).

[26] V. Talanquer and D. W. Oxtoby, J. Chem. Phys. **99**, 4670 (1993).

[27] P. R. ten Wolde, D. W. Oxtoby and D. Frenkel, Phys. Rev. Lett. **81**, 3695 (1998).

[28] P. R. ten Wolde and D. Frenkel, J. Chem. Phys. **109**, 9901 (1998).

[29] I. Kusaka, Z.-G. Wang, and J. H. Seinfeld, J. Chem. Phys. **108**, 3446 (1998).

[30] A. McPherson, *Preparation and analysis of protein crystals*, Krieger Publishing, Malabar (1982).

[31] S. D. Durbin and G. Feher, Ann. Rev. Phys. Chem. **47**, 171 (1996).

[32] F. Rosenberger, J. Crystal Growth **166**, 40 (1996).

[33] A. George and W. W. Wilson, Acta Crytallogr. D **50**, 361 (1994).

[34] T. L. Hill, *An Introduction to Statistical Thermodynamics*, Dover, New York (1986).

[35] E. G. Richards, *An Introduction to physical properties of large molecules in solution*, Cambridge University Press, Cambridge (1980).

[36] D. Rosenbaum, P. C. Zamora, and C. F. Zukoski, Phys. Rev. Lett. **76**, 150 (1996).

[37] D. Rosenbaum and C. F. Zukoski, J. Crystal Growth **169**, 752 (1996).

[38] M. H. J. Hagen and D. Frenkel, J. Chem. Phys. **101**, 4093 (1994).

[39] A. P. Gast, W. B. Russell, and C. K. Hall, J. Colloid Interface Sci. **96**, 251 (1983).

[40] A. P. Gast, W. B. Russell, and C. K. Hall, J. Colloid Interface Sci. **109**, 161 (1986).

[41] H. N. W. Lekkerkerker, W. C. K. Poon, P. N. Pusey, A. Stroobants, and P.B. Warren, Europhys. Lett. **20**, 559 (1992).

[42] S. M. Ilett, A. Orrock, W. C. K. Poon, and P. N. Pusey, Phys. Rev. E **51**, 1344 (1995).

[43] W. C. K. Poon, A. D. Pirie, and P. N. Pusey, Faraday Discuss. **101**, 65 (1995).

[44] W. C. K. Poon, Phys. Rev. E **55**, 3762 (1997).

[45] C. R. Berland, G. M. Thurston, M. Kondo, M. L. Broide, J. Pande, O. O. Ogun, and G. B. Benedek, Proc. Natl. Acad. Sci. USA **89**, 1214 (1992).

[46] N. Asherie, A. Lomakin, and G. B. Benedek, Phys. Rev. Lett. **77**, 4832 (1996).

[47] M. L. Broide, T. M. Tominc, and M. D. Saxowsky, Phys. Rev. E **53**, 6325 (1996).

[48] M. Muschol and F. Rosenberger, J. Chem. Phys. **107**, 1953 (1997).

[49] A. Kose and S. Hachisu, J. Colloid Interface Sci. **55**, 487 (1976).

[50] C. Smits, J. S. van Duijneveldt, J. K. G. Dhont, H. N. W. Lekkerkerker, and W. J. Briels, Phase Transitions **21**, 157 (1990).

[51] P. R. ten Wolde and D. Frenkel, Science **277**, 1975 (1997).

VII

Molecular Modeling and Simulation of a Photosynthetic Reaction Center

Matteo Ceccarelli[1], Marc Souaille[1,2], and Massimo Marchi[3]

[1] **Centre Européen de Calcul Atomique et Moléculaire (CECAM), Ecole Normale Supérieure de Lyon, 46 Allée d'Italie, F-69364 Lyon Cedex 07, France**
[2] **Physical Chemistry Institute, University of Zürich, Winterthurerstrasse 190, CH-8057 Zürich, Switzerland**
[3] **Section de Biophysique des Protéines et des Membranes, DBCM, CEA–Saclay, F-91191 Gif-sur-Yvette Cedex, France**

Abstract

In this paper we give an account of our ongoing effort to understand bacterial photosynthesis at the atomic level. First, we describe earlier simulations which investigate the nuclear motion coupled to the primary donor excitation in bacterial reaction centers (RC). Then, we discuss the molecular modeling of the chromophores of the RC of *rhodobacter sphaeroides*. Finally, we report on our latest molecular dynamics simulation results concerning a RC in a detergent micelle.

Introduction

The bacterial photosynthetic reaction center (RC)[3, 4] is a membrane protein composed of chromophores (bacteriochlorophylls, bacteriopheophytins and quinones) and three protein subunits named L, M and H (see Fig. VII.1). While proteins L and M form two branches of the RC (almost the mirror images of each other) and provide the necessary scaffolding to hold in place bacteriochlorophylls and bacteriopheophytins, the H subunit is in contact with the bacterial cytoplasm and binds the quinones in its interior. In the region of the RC near the pery-plasm is located a bacteriochlorophylls

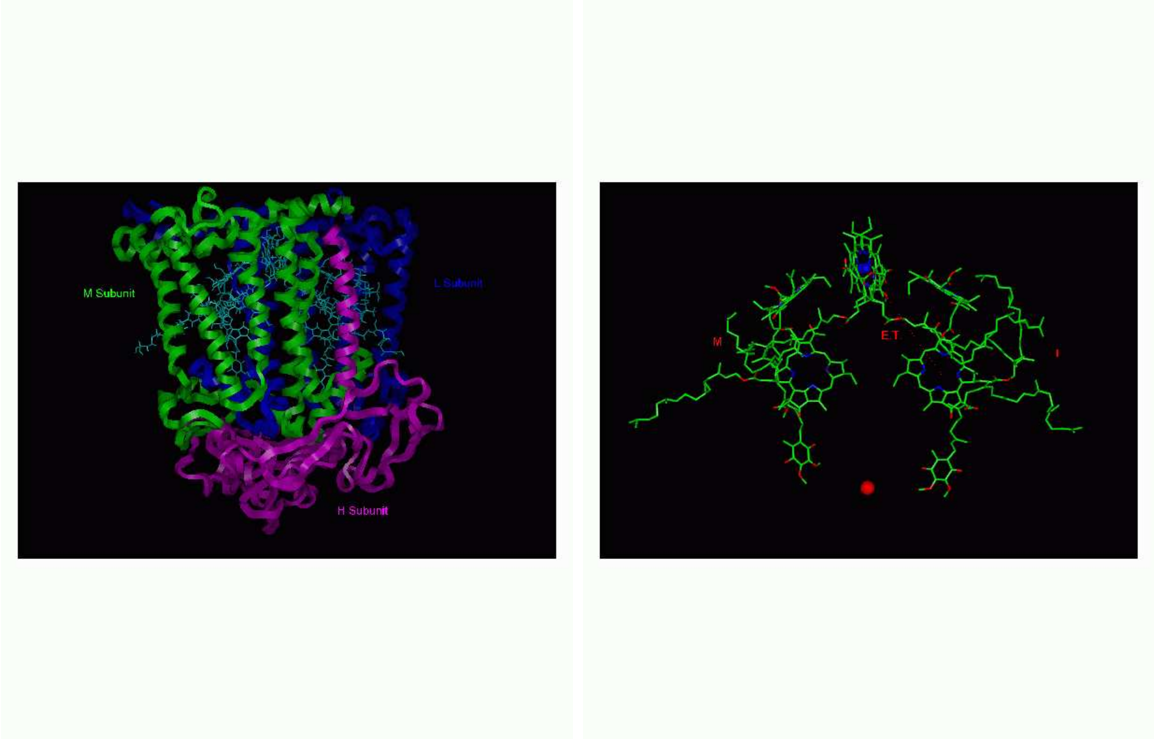

Figure VII.1: Pictorial views of the reaction center of *rb. sphaeroides* (top) and its chromophores (bottom).

dimer, the so–called special pair (P). This chromophore is at the junction point between the L and M branches and is involved directly in the first photosynthetic electron transfer.

Photosynthesis in purple bacteria commences with the excitation of P, the energy for such excitation being transferred directly from surrounding light harvesting proteins. The excited state P^* then decays in a charge transfer state, $P^+ \ H_L^-$, where an electron has been exchanged with the bacteriopheophytins on the L branch (H_L), 17 Å away. The electron transfer (ET), $P^* \ H_L \rightarrow P^+ \ H_L^-$, occurs with a quantum yield of 1 and is called primary charge separation. Experimentally no electron is detected arriving to the bacteriopheophytins on the M branch, H_M. Subsequently, the electron on H_L is first, transferred to the quinone (whose chemical identity changes with the type of RC) on the L side, or Q_A, and second, passed to the quinone on the M side, or Q_B.

The primary ET in RC presents many aspects which are very challenging to understand. Despite the many efforts, as yet unresolved by either experiment or theory are the following features: (a) the remarkably fast rate ($\tau^{-1} \sim 3$ ps) of this electron exchange between two chromophores separated by 17 Å; (b) the fact that the M branch acts as spectator in the reaction, despite structural similarities and quasi-C_2 symmetry between the L and M subunits; (c) the role of the accessory bacteriochlorophyll in Van der Waals contact with P and H_L in the mechanism of ET.

Since the first crystal structures of bacterial photosynthetic RC have been resolved[3], there have been a few investigations of the primary ET in the photosynthetic reaction center by MD simulations[3-6]. All of these investigations are based on a reduced quantum mechanical model whose relevant parameters are derived by running classical MD. This is the so–called spin–boson model[9]. In the last 10 years or so, powerful techniques, derived mostly from this simple model, have been developed to handle linear and non–linear spectroscopy[10]. This entails using the so–called spectral density formalism which relates spectroscopic properties to the fluctuation in the energy gap (i.e., energy difference) function between the ground and the excited states. ET theories derived from the Marcus approach[11] and based on the same spectral density formalism have also been proposed in the past[9]. In that case the energy gap is the energy difference between the neutral and the charge transfer states.

This paper is an account of our continuing effort in the investigation of the primary charge separation in bacterial RC. In the next sections we will describe in some detail our advances in the modeling and understanding of the RC photosynthetic proteins.

Nuclear coupling in the P $\rightarrow$ P* transition

Due to limitations in computational power, the first simulations of RC proteins either ignored[6, 7] or used mean field approximations[5, 8] of the environment surroundings these proteins. In both cases, however, only the atoms closer to the cofactors were actually simulated while the remaining atoms were kept fixed or harmonically restrained. In Ref. [12] we have improved on this model by simulating a RC of *rhodobacter (rb.) sphaeroides* in water. In practice, the simulation box of dimensions a = 65.63 Å , b = 58.0 Å and c = 65.0 Å was composed of a RC protein having its quasi-symmetry axis parallel to the a-direction and of 4104 water molecules which filled in the voids. All the simulation runs in Ref. [12] were carried out by using our in-house molecular dynamics program ORAC[13, 14]. In this earlier work, a spherical cutoff of 9 Å was applied to the non-bonded interactions thus neglecting long range electrostatic effects. The potential parameters and the molecular topology of the system is fully described in Ref. [12]. Simulations of about 100 ps each were carried out at 300 K and 50 K. The latter calculation was done to compare with time resolved data obtained at low temperatures ($\simeq$ 10 K)[15].

Our investigation on a hydrated reaction center was focused on the the dynamics of the P $\rightarrow$ P*, transition which occurs before primary charge separation. In the past, time resolved stimulated emission studies in the P $\rightarrow$ P* region have been carried out on different RC[15, 16]. A common feature obtained in all these studies is that low frequency (less than 200 cm^{-1}) nuclear modes are coupled to this photoexcitation. Although it has been shown that the environment surrounding the special pair is responsible for the coherent oscillations found in the spectra[15], no indication on the atomistic origin of these vibrations has been found.

The principal aim of our study was to gain insights in the coupling mechanism between nuclear modes and electronic transition. To achieve this goal, we computed the time–resolved stimulated emission spectra in different regions of the P* $\rightarrow$ P transition. This involved carrying out molecular dynamic simulations of the hydrated bacterial reaction center of *rb. sphaeroides* in the ground and excited states of the special pair.

Modeling photoexcitation

The spin–boson model is well suited to handle theoretically photoexcitation of a pigment molecule in contact with a dielectric from a ground to an excited state. In this model, the two electronic states of the chromophores are represented by a two–level system which is linearly coupled to a fluctuating dielectric described by harmonic fields. The interaction between dielectric and the photoexcitation is responsible for the broadening of the pigment electronic bands in solution or within a protein. It is worth to point out that even for complex systems the restriction on the harmonicity of the field is not so constraining as it might seem. Indeed, the binding requirement here is that only the nuclear modes coupled to photoexcitation be harmonic[7]. This is in general compatible with very anharmonic systems such as that discussed here.

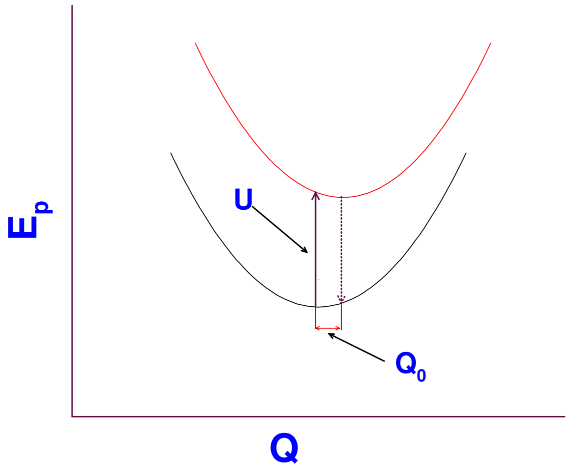

Figure VII.2: Displaced oscillator manifold. E$_p$ is the free energy of obtained by integration of the boson bath.

The underlying Hamiltonian of the spin–boson model is as follows:

$$\begin{aligned} H \;&= |g\rangle H_g \langle g| + |e\rangle \{ H_e - i\hbar\tfrac{\gamma}{2} \} \langle e| + \\ &\quad + |g\rangle H_{ge} \langle e| + |e\rangle H_{eg} \langle g| \end{aligned}$$

where H_α is the diabatic Hamiltonian of the state α (ground or excited), H_{ge} and H_{eg} are the interstate couplings. and γ is the inverse lifetime of the excited state. Only the diabatic Hamiltonians are relevant to electron-nuclear coupling. If only a single harmonic mode of the bath is coupled the two–level system, the Hamiltonians H_g and H_e correspond to a displaced harmonic oscillator system, i.e.

$$\begin{aligned} H_g &= H_B + \frac{1}{2} m\omega_0^2 Q^2 \\ H_e &= H_B + \frac{1}{2} m\omega_0^2 (Q^2 + 2Q_0 Q) + \Delta G \\ U &= m\omega_0^2 Q_0 Q + \Delta G. \end{aligned} \tag{VII.1}$$

Here, ΔG is the electronic energy difference between ground and excited states in the gas phase and H_B is the Hamiltonian of those modes of the boson bath not coupled to the electronic transition. Also, Q_0 is the displacement and U is the energy gap (see Fig. VII.2).

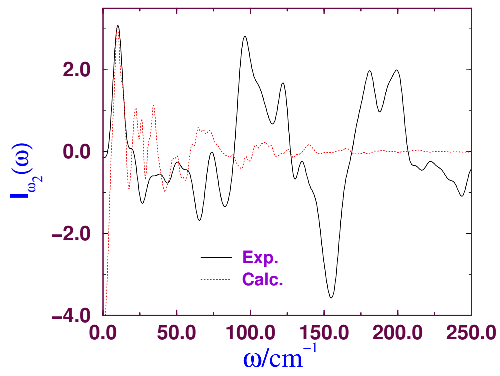

Figure VII.3: Comparison between the experimental and calculated reduced spectral densities. The two spectra are normalized with respect to the intensities of their lowest frequency peak.

In time resolved stimulated emissions experiment[15] the sample is at first pumped to the excited state by a test beam of light of a given frequency ω_1. Then, at variable time delays, a white light continuum beam is shone on the photoexcited sample to probe its absorption spectrum. In the end, the experiment measures the time resolved transmission induced by the photoexciting beam of frequency ω_1 on the absorption at a given frequency ω_2. This transmission is then converted to absorption changes which in turn are proportional to the stimulated emission coefficient $S(\omega_1, \omega_2, t)$. Using a displaced harmonic oscillator model as in Eqs. VII.1, Mukamel[10] has shown that this emission coefficient can be readily computed from the knowledge of the energy gap dynamics. Thus, the major goal of our molecular dynamics investigation was to compute the energy gap for the $P^* \rightarrow P$ transition as a function of time. Although empirical charge distribution was used in our study, *ab initio* data can, in principle, be obtained to model the charge distribution in the P and P^* states. As for the pseudopotential model for the interaction between the special pair and the environment (proteins and water), we used a purely electrostatic model.

Results

After 130 ps of molecular dynamics equilibration and 100 ps of additional run time, the deviation from the X–ray structure (X_{rms}) of the three subunits increased to an average of 3.1 Å for the α carbons. The subunit H had the largest deviations, while the membrane-spanning helices had a relatively low value of X_{rms}. Of the 4101 water molecules solvating the RC, only 304 were trapped near the protein for more than 90 % of the time. They were found more often in the hydrophilic region of the subunits than near the membrane–spanning helices of the L and M subunits.

During the 90 ps run at 50 K in the P^* state, the energy gap or energy difference between the P excited and ground state were accumulated. The energy gap probability distribution derived from this simulation obeyed, to a good approximation, Gaussian statistics. This result gives credibility to our approach in the calculation of the electronic spectra based on a linear response model.

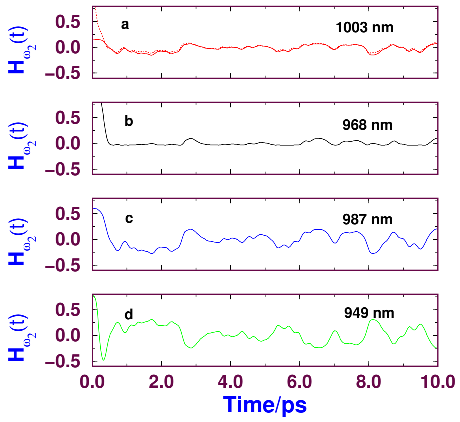

Figure VII.4: Calculated time resolved stimulated emission intensity. From top to bottom the four panels present results for probing frequency ω_2 equal to respectively (a) 1003 , (b) 968, (c) 987 and (d) 949 nm. For comparison, the autocorrelation function of the energy gap has been added on the panel (a) (dotted line).

Our calculation found that the oscillatory part of $S(\omega_1, \omega_2, t)$ at ω_1 (or $H_{\omega_2}(t)$) behaves like the experimental time evolution of the stimulated emission spectra. As shown in From Fig. VII.4, away from the bottom of the emission peak (ω_2 = 968 nm), $H_{\omega_2}(t)$ shows an oscillatory behavior, with a phase change of π between ω_2=987 and 949 nm. Noticeably, at ω_2=968 nm, the maximum of the emission peak, the aspect of $H_{\omega_2}(t)$ changes showing a decrease in the amplitude of the oscillations as well as the appearance of different oscillating features.

For all wavelength, $H_{\omega_2}(t)$ shows coherent oscillations well beyond the 3 ps time mark. This contrasts with experimental results showing an exponential damping of the time correlation function within this time scale. Such a damping might be due to frictional damping or static disorder on the RCs.

The experimental and calculated reduced spectral densities obtained by Fourier transform of $H_{\omega_2}(t)$ are compared in Fig. VII.3. Although the calculation reproduces the first experimental peak at 10 cm^{-1}, the activities of the higher frequency modes is underestimated with respect to experiment. This result and the finding in Ref. [12], that the higher frequency peaks (at 67 and 125 cm^{-1}) in the dimer energy gap spectral density are weakened considerably by solvent effects, may suggest the our simple electrostatic model underestimates the dimer-solvent energy gap with respect to the intra dimer counterpart.

Improving the reaction center model

Starting from the earlier simulation[12] described above, we have in the last few years, achieved major improvements on the modeling of the RC proteins and their environment. Indeed, MD simulations of membrane proteins are challenging for different reasons. First, although force fields for proteins have been steadily improving, *ab initio* based potential models for chromophores such as bacteriochlorophylls and quinones have been lacking. It is clear that in studies of ET realistic modeling of the prosthetic groups is essential. Second, because the coupling between electronic states and the solvent (the surrounding protein) is at the first order electrostatic, electrostatic forces must be computed accurately in MD simulations. Because of the high cost this is not done in standard biomolecular simulations and was not done in our earlier simulation. Third, the large size of the system: the RC protein of *rb. sphaeroides* by itself contains more than 15,000 atoms. The size of the system increases considerably if its natural environment, solvent and phospholipid membrane, is included in realistic simulations. Last but not least, the issue of electronic polarizability in modeling RC's will need to be addressed because it is relevant to electron transfer.

Modeling the chromophores

Deriving a force field for chromophores entails calculations of the electronic structure of these large molecules. In recent times, the density functional theory (DFT)[17] approach has been gaining popularity in the chemical community to investigate on the electronic ground state structure of chemically relevant system. In the past, this technique has been applied by us and others to the study of bacteriochlorophylls molecules[18, 19] and quinones[20]. All our DFT calculations on the chromophores were carried out in the local density plus gradient corrections approximation (LDA+GC), while the Kohn-Sham orbitals were expanded in a basis set of plane waves compatible with the periodic supercell containing the molecule. In this scheme only the valence electrons are included explicitly in the calculation. The effects due to atomic core electrons are taken into account by *ab initio* soft pseudopotentials associated with each atom[21].

In an earlier calculation[18] on a crystal of methyl bacteriopheophorbide (MeBPheo) *a* we have shown the viability of the DFT technique towards the computation of the electronic structure and optimization of molecules important for photosynthesis. In a more recent investigation[19] we have carried out the first (to our knowledge) high quality DFT *ab initio* calculation of the vibrational structure of a bacteriochlorophyll derivative and assigned the in plane frequencies detectable by resonant Raman spectroscopy. The *ab-initio* calculations were performed on an isolated methyl bacteriochlorophyll *a* molecule. Our major result was the determination of a complete set of eigenvalues and eigenvectors which unambiguously identified the fundamental modes. The computed frequencies are in very good agreement with the available experimental data and show a small root mean square deviation (less than 20 cm^{-1}) from experimental modes. In addition, our calculation was able to pin point a strong symmetric behavior of many in–plane vibration similar to results obtained for porphyrines. This is in contrast with results of earlier semiempirical calculations[22], which predicted more localized modes in (bacterio)pheophorbide-type macrocycles.

Based on DFT calculations on chlorophylls and, additionally, on ubiquinone and the RC main detergent, lauryl dimethylamine oxide or LDAO, we have then developed a force field for their classical modelization. Our approach to this undertaking was straightforward. We initially use the DFT optimized structures and the vibrational analysis to determine the bonded part of the potential parameters described by the AMBER potential function. Then, atomic *ab initio* partial charges on the chromophore are used to account for electrostatic effects. At a later stage, experimental data from

X-ray crystallography are used to check the structural properties of the molecule in the condensed state and to refine the intermolecular Lennard-Jones parameters.

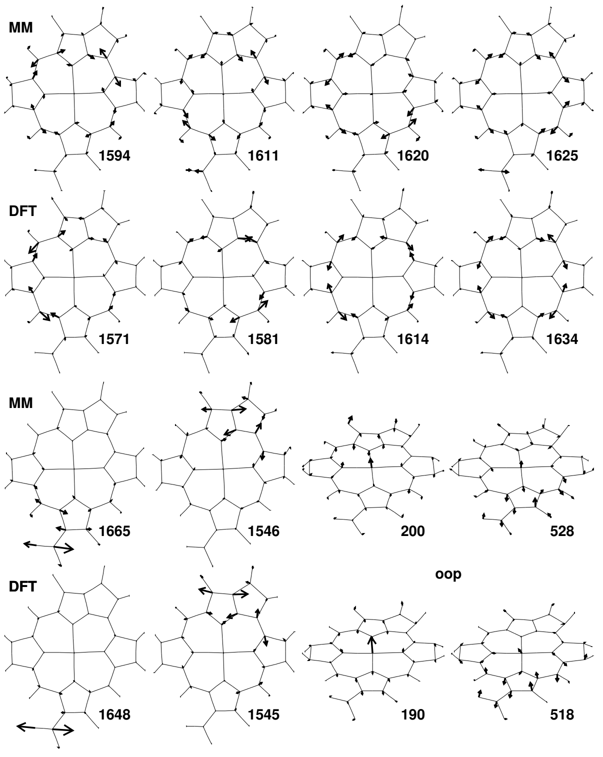

Figure VII.5: Methyl bacteriochlorophyll *a* normal modes. Frequencies are in cm^{-1}

A good starting point for parameter refinement of large molecules are values optimized on small fragments. In the case of bacteriochlorophylls, we started modeling their chemical constituents such as pyrrol, methyl acetate and methylic groups, for which DFT calculations were also made. Subsequently, these parameters were transferred to the larger molecules and refined as much as possible to reproduce the bacteriochlorophylls DFT results. The existing AMBER parameters were used, whenever possible, as a starting point for potential of the fragments. Given the relative smaller size of the quinone and the hydrophilic head of LDAO[1], the force field refinement was done in this case directly on the molecules and not the fragments.

In all our molecular modeling, special care was taken not only to reproduce the DFT frequencies, but also the eigenvectors. Indeed, a great deal of spectroscopic experiments on photosynthetic RC involve directly or indirectly the nuclear dynamics of the chromophores. In Fig. VII.5 we present some typical in–plane and out-of–plane normal modes computed from DFT and molecular mechanics (MM). Its visual inspection shows the good agreement between DFT and MM eigenvectors.

[1]DFT optimization and vibrational analysis were performed on models of ubiquinone and LDAO obtained by cutting and saturating their tails after the first 3 carbon atoms.

Methods for molecular dynamics

Due to the ever increasing power of computers, simulations of solvated proteins for lengths up to hundreds of ps is nowadays becoming routine on desktop workstations. However the simulation of membrane proteins stabilized in membrane or detergent environments is more challenging given the complexity and the large size of such systems. In addition, the dielectric properties of the aqueous solvent are of crucial importance to electron and proton transfer reactions. Consequently, any theoretical investigation of such phenomena must deal with the problem of how to simulate large systems and, at the same time, correctly handle long-range electrostatic interactions.

In the past few years, we have developed new and fast multiple timestep MD algorithms[13, 23, 24] which allow simulations of very large systems and include an accurate representation of the Coulombic interactions for infinite systems. The electrostatic series can be computed in principle *exactly* using the Ewald re-summation technique[25]. This method in its standard implementation, is extremely CPU demanding and scales like N^2, with N being the number of charges with the unfortunate consequence that even moderately large size simulations of inhomogeneous biological systems are not within its reach. Notwithstanding, the rigorous Ewald method, which suffers of none of the inconvenients experienced by the reaction field approach, has very recently regained the spotlight with the particle mesh Ewald (PME) technique[26]. PME, based on older ideas of Hockney's[27], is essentially an interpolation technique which involves charge smearing onto a regular grid and evaluation of the reciprocal lattice energy sums via fast Fourier Transform (FFT). The performance of this technique, both in accuracy and efficiency, is very good. Most importantly, the computational cost scales like $NlogN$ for large N, but it is essentially *linear* for practical application up to 20,000 particles.

The combination of the multiple time step algorithm and PME[28] makes the simulation of large size biomolecular systems such as membrane proteins extremely efficient and affordable even for long time spans. Furthermore, it does not involve any uncontrolled approximation and is entirely consistent with periodic boundary conditions.

Our most recent r-RESPA algorithm in combination with constraints and PME achieves substantial computer savings (more than 10 times) with respect to standard Ewald techniques. In spite of this excellent performance, for a 40,000 atom system 1 ns of simulation takes more than 12 days on a fast Compaq EV5 station. Further improvements can be achieved running simulation on parallel machines. Indeed, a parallelized version of ORAC has been recently developed and each ns of simulation for the same systems now takes 3 days on 8 processors of a Compaq ES232 cluster.

Simulation of a RC in a detergent micelle

To elucidate at the atomic level the asymmetry and the mechanism of the primary charge separation it is advantageous to construct a reliable model of the RC protein and of its environment. Given the latest technical developments in our computational tools[24], we have recently been able to simulate the RC of *rhodobacter sphaeroides* inglobed in a model micelle of detergent lauryl-dimethyl-amine-oxide (LDAO) and hydrated by water for more than 3.4 ns. This hydrated micelle was constructed as follows. First, the isolated RC protein[29] including 9 LDAO molecules and 160 crystallization

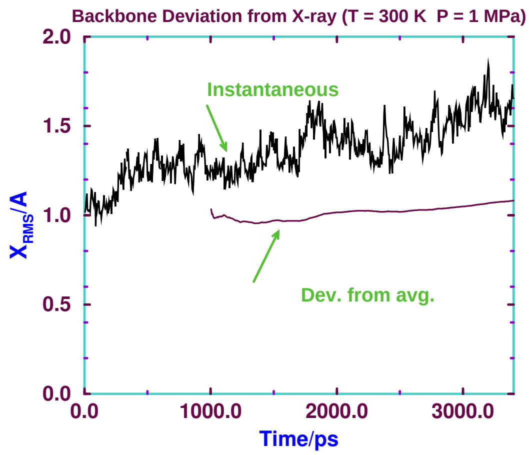

Figure VII.6: Deviation from the crystallographic structure of the RC protein during 3.4 ns of simulation. The upper curve is the instantaneous deviation, while the lower curve is the deviation of the averaged structure.

waters were relaxed at 20 K for about 5 ps to eliminate any accidental stress due to the force field. To this structure we then added 150 LDAO molecules initially disposed around the protein hydrophobic helices in an all–trans conformation and with the polar head pointing away from the protein assembly. From this conformation we ran equilibrations of the LDAO only (i.e. keeping fixed the protein coordinates) for 30 and 230 ps at 250 K and 400 K, respectively. After this step the added LDAO had relaxed to form an aggregate around the RC in which the aliphatic chains were in contact with the transmembrane helices and the polar heads pointed towards the exterior.

Finally, the system was placed in an orthorhombic box of dimension of 76x84x80 Å and hydrated by 6323 additional water molecules to fill the cell voids. A simulation run on our final system, totaling 40,327 atoms, was then started at constant temperature and pressure at T=300 K and P=0.1 MPa.

To achieve full relaxation the simulation box was entirely flexible for the first 300 ps and evolved to a hexagonal–like structure. For the remaining runs only isotropic changes of the box were allowed. With the simulation algorithms in the NPT ensemble described in Ref. [30] and on 32 processors of a T3E parallel computer, 3.4 ns of simulation required 21 days of simulation.

In this report we only provide a brief account of some preliminary results on the structure of the simulated RC. The full account of our results will be given in future publications.

Fig. VII.6 shows the overall deviation (or X_{rms}) of the RC backbone atoms from their X–ray coordinates. We first notice that with respect to our previous, and much shorter, simulations the X_{rms} is twice as small. Moreover, the RC protein shows with time an overall drift towards higher X_{rms}. With additional investigation, we find that this is due essentially to relative motion of subunit H with respect to L and M.

In addition to a low deviation from the crystallographic structure, the experimental Debey–Waller factors are also well reproduced within a constant offset, probably due to disorder (see Fig. VII.7).

In Fig. VII.8 we show a pictorial view of the RC protein surrounded by its deter-

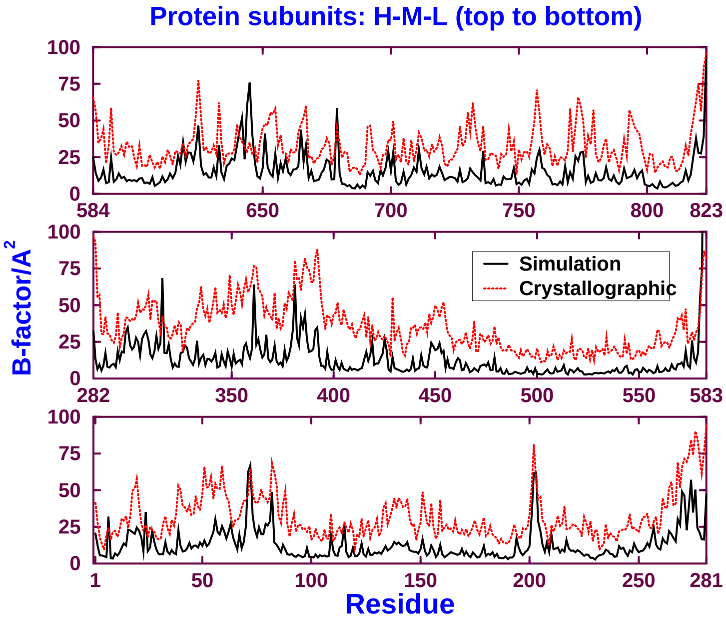

Figure VII.7: Comparison between calculated and crystallographic Debey–Waller factors.

gent. The LDAO molecules are represented by their molecular surface and no water molecules are displayed. This picture is evocative of the detergent micellar structure revealed by the low resolution neutron scattering study of the RC crystal[31]. As in that investigation, our detergent has formed a distinct micelle around the protein. Its thickness along the quasi-C_2 symmetry axis is around 25-30 Å, similar to that observed experimentally. We point out that in the simulation the micelle is a rather dynamics structure with a lateral diffusion constant of 5.6×10^{-10} m^2 s^{-1} which is about 30 times larger than that of the RC protein.

Conclusion and perspectives

Thanks to our ongoing efforts in molecular modeling of RC proteins, we have recently devised a reliable force field and a faithful model for photosynthetic RC proteins in detergent environment. Long simulations (3.4 ns) of a RC protein of *rb. sphaeroides* in its detergent environment have also been possible due our recent technical developments in the MD methodology. The analysis of properties related to the primary ET and its asymmetry is currently underway. Our first task is to compute the average electrostatic field and its dynamics on the bacteriochlorophyll chromophores of the L and M branches to investigate the origin of the ET asymmetry. In this calculation we include both contributions from the fixed charges of the RC and from induction computed from a distributed polarizable model[32]. Investigation of effects from mutations is also underway.

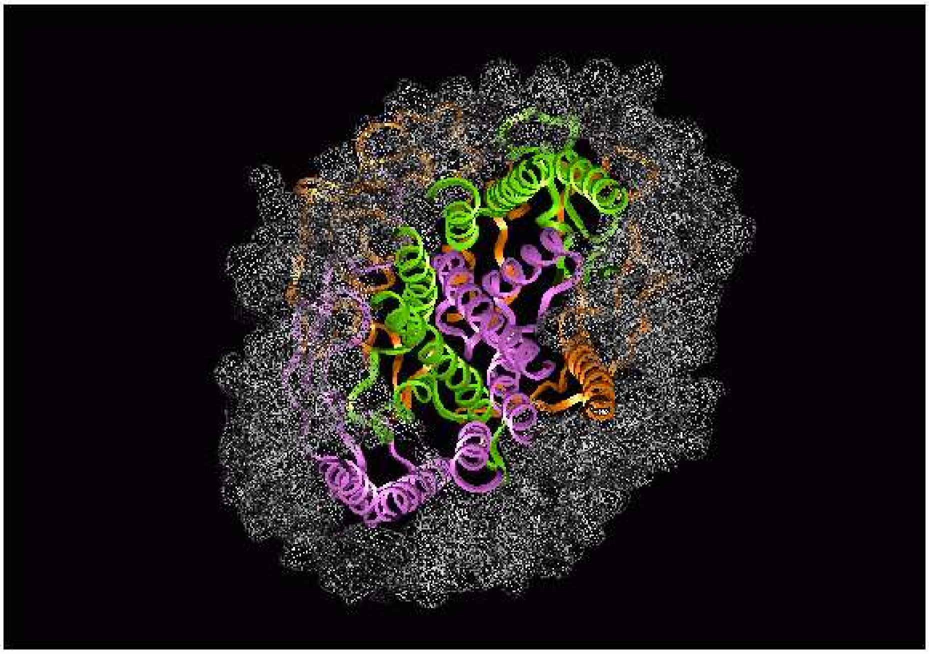

Figure VII.8: Instantaneous view of the RC of *rb. sphaeroides* during the simulation (see text for details).

Bibliography

[1] Nosé, S. *Mol. Phys.* **1986**, *57*, 187–191.

[2] Torrie, G.; Valleau, J. *Chem. Phys. Lett.* **1974**, *28*, 578–581.

[3] Deisenhofer, J.; Epp, O.; Mike, K.; Huber, R.; Michel, H. *J. Mol. Biol.* **1984**, *180*, 385.

[4] Deisenhofer, J.; Michel, H. *Science* **1989**, *245*, 1463.

[5] Creighton, S.; Hwang, J. K.; Warshel, A.; Parson, W. W.; Norris, J. *Biochemistry* **1988**, *27*, 774.

[6] Treutlein, H.; Schulten, K.; Brunger, A.; Karplus, M.; Deisenhofer, J.; Michel, H. *Proc. Natl. Acad. Sci. USA* **1992**, *89*, 75.

[7] Marchi, M.; Gehlen, J. N.; Chandler, D.; Newton, M. *J. Am. Chem. Soc.* **1993**, *115*, 4178.

[8] Parson, W. W.; Chu, Z. T.; Warshel, A. *Photosynthesis Research* **1998**, *55*, 147.

[9] Chandler, D. In *Liquids, Freezing and the glass transition,* Leveque, D.; Hansen, J. P., *edts.* North Holland, 1991, Page 193.

[10] Mukamel, S. *Principles of Nonlinear Optical Spectroscopy.* Oxford University Press, **1995**.

[11] Marcus, R. A.; Sutin, N. *Biochim. Biophys. Acta* **1985**, *811*, 256.

[12] Souaille, M.; Marchi, M. *J. Am. Chem. Soc.* **1996**, *119*, 3948.

[13] Procacci, P.; Darden, T.; Paci, E.; Marchi, M. *J. Comp. Chem.* **1997**, *18*, 1848.

[14] Procacci, P.; Marchi, M. In *Advances in the Computer Simulations of Liquid Crystals,* Zannoni, G.; Pasini, P., *edts*, NATO ASI School (Kluwer Academic publishers, Dodrecht the Netherlands, 1999).

[15] Vos, M. H.; Rappaport, F.; Lambry, J.-C.; Breton, J.; Martin, J.-L. *Nature* **1993**, *363*, 320.

[16] Vos, M. H.; Jones, M. R.; Hunter, C. N.; Breton, J.; Lambry, J.-C.; Martin, J.-L. *Biochemistry* **1994**, *33*, 6750.

[17] Parr, R. G.; Yang, W. *Density Functional Theory of Atoms and Molecules.* Oxford University Press, Oxford **1989**.

[18] Marchi, M.; Hutter, J.; Parrinello, M. *J. Am. Chem. Soc.* **1996**, *118*, 7847.

[19] Ceccarelli, M.; Lutz, M.; Marchi, M. *J. Am. Chem. Soc.* January (2000), . In press.

[20] Nonella, M.; Brändli, C. *J. Phys. Chem.* **1996**, *100*, 14549.

[21] Troullier, N.; Martins, J. L. *Phys. Rev. B* **1991**, *43*, 1993.

[22] Donohoe, R. J.; Frank, H. A.; Bocian, D. F. *Photochem. Photobiol.* **1988**, *48*, 531.

[23] Procacci, P.; Darden, T.; Marchi, M. *J. Phys. Chem.* **1996**, *100*, 10464.

[24] Procacci, P.; Marchi, M. In *Advances in the Computer Simulations of Liquid Crystals,* Zannoni, G.; Pasini, P., *edts*, NATO ASI School (Kluwer Academic publishers, Dodrecht the Netherlands, 1998).

[25] de Leeuw, S. W.; Perram, J. W.; Smith, E. R. *Proc. R. Soc. Lond.* **1980**, *A 373*, 27.

[26] Darden, T.; York, D.; Pedersen, L. *J. Chem. Phys.* **1993**, *98*, 10089.

[27] Hockney, R. W. *Computer Simulation Using Particles.* McGraw-Hill, New York, **1989**.

[28] Procacci, P.; Marchi, M. *J. Chem. Phys.* **1996**, *104*, 3003–3012.

[29] Ermler, U.; Fritzsch, G.; Buchanan, S. K.; Michel, H. *Structure* **1994**, *2*, 925.

[30] Marchi, M.; Procacci, P. *J. Chem. Phys.* **1998**, *109*, 5194.

[31] Roth, M.; Lewit-Bentley, A.; Michel, H.; Deisenhofer, J.; Huber, R.; Oesterhelt, D. *Nature* **1989**, *340*, 659.

[32] Thole, B. T. *Chem. Phys.* **1981**, *59*, 341.

VIII

From Molecular Dynamics to Dissipative Particle Dynamics

Peter V. Coveney[1], Gianni De Fabritiis[1],
Eirik G. Flekkøy[2] and James Christopher[1]
[1]Centre for Computational Science, Queen Mary and Westfield College,
University of London, London E1 4NS, United Kingdom
[2]Department of Physics, University of Oslo
P.O. Box 1048 Blindern, 0316 Oslo 3, Norway

Abstract

We describe a mesoscopic modeling and simulation technique that is very close to the technique known as dissipative particle dynamics. The model is derived from molecular dynamics by means of a systematic coarse-graining procedure. Thus the rules governing this form of dissipative particle dynamics reflect the underlying molecular dynamics; in particular all the underlying conservation laws carry over from the microscopic to the mesoscopic descriptions. Whereas previously the dissipative particles were spheres of fixed size and mass, now they are defined as cells on a Voronoi lattice with variable masses and sizes. This Voronoi lattice arises naturally from the coarse-graining procedure which may be applied iteratively and thus represents a form of renormalisation-group mapping. It enables us to select any desired local scale for the mesoscopic description of a given problem. Indeed, the method may be used to deal with situations in which several different length scales are simultaneously present. Simulations carried out with this scheme show good agreement with theoretical predictions for the equilibrium behavior.

Introduction

The non-equilibrium behavior of fluids continues to present a major challenge for both theory and numerical simulation. In recent times, there has been growing interest in the study of so-called 'mesoscale' modeling and simulation methods, particularly for the description of the complex dynamical behavior of many kinds of soft condensed matter, whose properties have thwarted more conventional approaches. As an example, consider the case of complex fluids with many coexisting length and time scales, for which hydrodynamic descriptions are unknown and may not even exist. Such fluids include multi-phase flows, particulate and colloidal suspensions, polymers, and amphiphilic fluids, including emulsions and microemulsions. Fluctuations and Brownian motion are often key features controlling their behavior.

From the standpoint of traditional fluid dynamics, a general problem in describing such fluids is the lack of adequate continuum models. Such descriptions, which are usually based on simple conservation laws, approach the physical description from the macroscopic side, that is in a 'top down' manner, and have certainly proved successful for simple Newtonian fluids [1]. For complex fluids, however, equivalent phenomenological representations are usually unavailable and instead it is necessary to base the modeling approach on a microscopic (that is on a particulate) description of the system, thus working from the bottom upwards, along the general lines of the program for statistical mechanics pioneered by Boltzmann [2]. Molecular dynamics (MD) presents itself as the most accurate and fundamental method [3] but it is far too computationally intensive to provide a practical option for most hydrodynamical problems involving complex fluids. Over the last decade several alternative 'bottom up' strategies have therefore been introduced. Hydrodynamic lattice gases [4], which model the fluid as a discrete set of particles, represent a computationally efficient spatial and temporal discretization of the more conventional molecular dynamics. The lattice-Boltzmann method [5], originally derived from the lattice-gas paradigm by invoking Boltzmann's *Stosszahlansatz*, represents an intermediate (fluctuationless) approach between the top-down (continuum) and 'bottom-up' (particulate) strategies, insofar as the basic entity in such models is a single particle distribution function; but for interacting systems even these lattice-Boltzmann methods can be subdivided into bottom-up [6] and top-down models [7].

A recent contribution to the family of bottom-up approaches is the dissipative particle dynamics (DPD) method introduced by Hoogerbrugge and Koelman in 1992 [8]. Although in the original formulation of DPD time was discrete and space continuous, a more recent re-interpretation asserts that this model is in fact a finite-difference approximation to the 'true' DPD, which is defined by a set of continuous time Langevin equations with momentum conservation between the dissipative particles [9]. Successful applications of the technique have been made to colloidal suspensions [10], polymer solutions [11] and binary immiscible fluids [12]. For specific applications where comparison is possible, this algorithm is orders of magnitude faster than MD [13]. The basic elements of the DPD scheme are particles that represent rather ill-defined 'mesoscopic' quantities of the underlying molecular fluid. These dissipative particles are stipulated to evolve in the same way that MD particles do, but with different inter-particle forces: since the DPD particles are pictured to have internal degrees of freedom, the forces between them have both a fluctuating and a dissipative component in addition to the conservative forces that are present at the MD level. Newton's third law is still satisfied, however, and consequently momentum conservation together with mass conservation produce hydrodynamic behavior at the macroscopic level.

Dissipative particle dynamics has been shown to produce the correct macroscopic (continuum) theory; that is, for a one-component DPD fluid, the Navier-Stokes equations emerge in the large scale limit, and the fluid viscosity can be computed [14, 15].

However, even though dissipative particles have generally been viewed as clusters of molecules, no attempt has been made to link DPD to the underlying microscopic dynamics, and DPD thus remains a foundationless algorithm, as is that of the hydrodynamic lattice gas and *a fortiori* the lattice-Boltzmann method. It is the principal purpose of the present paper to provide an atomistic foundation for dissipative particle dynamics. Among the numerous benefits gained by achieving this, we are then able to provide a precise definition of the term 'mesoscale', to relate the purely phenomenological parameters in the algorithm to the transport coefficients of the fluid, and thereby to formulate DPD simulations for *specific* physicochemical systems, defined in terms of their molecular constituents. The DPD that we derive is a representation of the underlying MD. Consequently, to the extent that the approximations made are valid, the DPD and MD will have the same hydrodynamic descriptions, and no separate kinetic theory for, say, the DPD viscosity will be needed once it is known for the MD system. Since the MD degrees of freedom will be integrated out in our approach the MD viscosity will appear in the DPD model as a parameter that may be tuned freely.

In our approach, the 'dissipative particles' (DP) are defined in terms of appropriate weight functions that sample portions of the underlying conservative MD particles, and the forces between the dissipative particles are obtained from the hydrodynamic description of the MD system: the microscopic conservation laws carry over directly to the DPD, and the hydrodynamic behavior of MD is thus reproduced by the DPD, albeit at a coarser scale. The mesoscopic (coarse-grained) scale of the DPD can be precisely specified in terms of the MD interactions. The size of the dissipative particles, as specified by the number of MD particles within them, furnishes the meaning of the term 'mesoscopic' in the present context. Since this size is a freely tunable parameter of the model, the resulting DPD introduces a general procedure for simulating microscopic systems at any convenient scale of coarse graining, provided that the forces between the dissipative particles are known. When a hydrodynamic description of the underlying particles can be found, these forces follow directly; in cases where this is not possible, the forces between dissipative particles must be supplemented with the additional components of the physical description that enter on the mesoscopic level.

The DPD model which we derive from molecular dynamics is formally similar to conventional, albeit foundationless, DPD [14]. The interactions are pairwise and conserve mass and momentum, as well as energy [16, 17]. Just as the forces conventionally used to define DPD have conservative, dissipative and fluctuating components, so too do the forces in the present case. In the present model, the role of the conservative force is played by the pressure forces. However, while conventional dissipative particles possess spherical symmetry and experience interactions mediated by purely central forces, our dissipative particles are defined as space-filling cells on a Voronoi lattice whose forces have both central and tangential components. These features are shared with a model studied by Español [18]. This model links DPD to smoothed particle hydrodynamics [19] and defines the DPD forces by hydrodynamic considerations in a way analogous to earlier DPD models. Español *et al.* [20] have also carried out MD simulations with a superposed Voronoi mesh in order to measure the coarse grained inter-DP forces.

While conventional DPD defines dissipative particle masses to be constant, this feature is not preserved in our new model. In our first publication on this theory [21], we stated that, while the dissipative particle masses fluctuate due to the motion of MD particles across their boundaries, the average masses should be constant. In fact, the DP-masses vary due to distortions of the Voronoi cells, and this feature is now properly incorporated in the model.

The magnitude of the thermal forces is given by a fluctuation-dissipation relation which we obtain by making use of a Fokker-Planck equation We show that the DPD system is described in an approximate sense by the isothermal-isobaric ensemble. Simulations confirm that, with the use of the fluctuating forces, the measured DP temperature is equal to the MD temperature which is provided as input. This is an important finding in the present context as the most significant approximations we have made underlie the derivation of the thermal forces.

Coarse-graining molecular dynamics: from micro to mesoscale

The essential idea motivating our definition of mesoscopic dissipative particles is to specify them as clusters of MD particles in such a way that the MD particles themselves remain unaffected while *all* being represented by the dissipative particles. The independence of the molecular dynamics from the superimposed coarse-grained dissipative particle dynamics implies that the MD particles are able to move between the dissipative particles. The stipulation that all MD particles must be fully represented by the DP's implies that while the mass, momentum and energy of a single MD particle may be shared between DP's, the sum of the shared components must always equal the mass and momentum of the MD particle.

Definitions

Full representation of all the MD particles can be achieved in a general way by introducing a sampling function $f_k(\mathbf{x}) = s(\mathbf{x}-\mathbf{r}_k)/\sum_l s(\mathbf{x}-\mathbf{r}_l)$. Here the positions $\mathbf{r}_k$ and $\mathbf{r}_l$ define the DP centers, $\mathbf{x}$ is an arbitrary position and $s(\mathbf{x})$ is some localized function, which we choose as a Gaussian $s(\mathbf{x}) = \exp\left(-x^2/a^2\right)$. The mass, momentum and internal energy E of the kth DP are then defined as

$$\begin{aligned} M_k &= \sum_i f_k(\mathbf{x}_i) m, \\ \mathbf{P}_k &= \sum_i f_k(\mathbf{x}_i) m \mathbf{v}_i, \\ \frac{1}{2} M_k U_k^2 + E_k &= \sum_i f_k(\mathbf{x}_i) \left(\frac{1}{2} m v_i^2 + \frac{1}{2} \sum_{j \neq i} V_{MD}(r_{ij}) \right) \\ &\equiv \sum_i f_k(\mathbf{x}_i) \epsilon_i, \end{aligned} \tag{VIII.1}$$

where $\mathbf{x}_i$, $\mathbf{v}_i$ and ϵ_i are respectively the position, velocity and total energy of the ith MD particle, which are all assumed to have identical masses m, $\mathbf{P}_k$ is the momentum of the kth DP and $V_{MD}(r_{ij})$ is the potential energy of the MD particle pair ij, separated a distance r_{ij}. The kinematic condition

$$\dot{\mathbf{r}}_k = \mathbf{U}_k \equiv \mathbf{P}_k / M_k \tag{VIII.2}$$

completes the definition of our dissipative particle dynamics.

In the following sections, we shall use the notation $\mathbf{r}$, M, $\mathbf{P}$ and E with the indices k, l, m and n to denote DP's while we shall use $\mathbf{x}$, m, $\mathbf{v}$ and ϵ with the indices i and j to denote MD particles.

Derivation of dissipative particle dynamics

We now need to draw on a hydrodynamic description of the underlying molecular dynamics and construct a statistical mechanical description of our dissipative particle dynamics. For concreteness we shall take the hydrodynamic description of the MD system in question to be that of a simple Newtonian fluid [1]. This is known to be a good description for MD fluids based on Lennard-Jones or hard sphere potentials, particularly in three dimensions [3]. Here we shall carry out the analysis for systems in two spatial dimensions; the generalization to three dimensions is straight forward, the main difference being of a practical nature as the Voronoi construction becomes more involved.

We shall begin by specifying a scale separation between the dissipative particles and the molecular dynamics particles by assuming that

$$|\mathbf{x}_i - \mathbf{x}_j| << |\mathbf{r}_k - \mathbf{r}_l| \, , \tag{VIII.3}$$

where $\mathbf{x}_i$ and $\mathbf{x}_j$ denote the positions of neighbouring MD particles. Such a scale separation is in general necessary in order for the coarse-graining procedure to be physically meaningful. Although for the most part in this paper we are thinking of the molecular interactions as being mediated by short-range forces such as those of Lennard-Jones type, a local description of the interactions will still be valid for the case of long-range Coulomb interactions in an electrostatically neutral system, provided that the screening length is shorter than the width of the overlap region between the dissipative particles. Indeed, as we shall show here, the result of doing a local averaging is that the original Newtonian equations of motion for the MD system become a set of Langevin equations for the dissipative particle dynamics. These Langevin equations admit an associated Fokker-Planck equation. An associated fluctuation-dissipation relation relates the amplitude of the Langevin force to the temperature and damping in the system.

With the mesoscopic variables now available, we need to define the correct average corresponding to a dynamical state of the system. Many MD configurations are consistent with a given value of the set $\{\mathbf{r}_k, M_k, \mathbf{U}_k, E_k\}$, and averages are computed by means of an ensemble of systems with common *instantaneous* values of the set $\{\mathbf{r}_k, M_k, \mathbf{U}_k, E_k\}$. This means that only the time derivatives of the set $\{\mathbf{r}_k, M_k, \mathbf{U}_k, E_k\}$, i.e. the forces, have a fluctuating part. In the end of our development approximate distributions for the $\mathbf{U}_k$'s and E_k's will follow from the derived Fokker-Planck equations. These distributions refer to the larger equilibrium ensemble that contains all fluctuations in $\{\mathbf{r}_k, M_k, \mathbf{U}_k, E_k\}$.

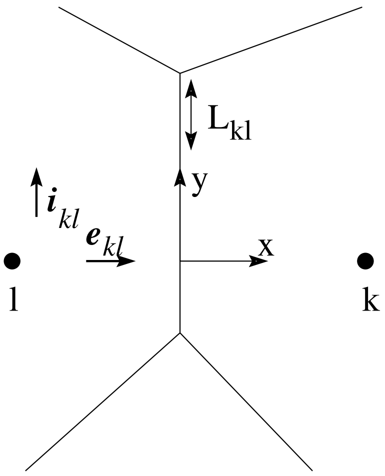

Figure VIII.1: Two interacting Voronoi cells. The length of the intersection between DP's k and l is l_{kl}, the shift from the center of the intersection between $\mathbf{r}_{kl}$ and l_{kl} is L_{kl} ($L_{kl} = 0$ when $\mathbf{r}_{kl}$ intersects l_{kl} in the middle) and the unit vector $\mathbf{i}_{kl}$ is normal to $\mathbf{e}_{kl}$. The coordinate system x-y used for the integration has its origin on the intersection.

It is necessary, to compute the average MD particle velocity $\langle \mathbf{v} \rangle$ *between* dissipative particle centers, given $\{\mathbf{r}_k, M_k, \mathbf{U}_k, E_k\}$. This velocity depends on all neighboring dissipative particle velocities. However, for simplicity we shall employ a "nearest neighbor" approximation, which consists in assuming that $\langle \mathbf{v} \rangle$ interpolates linearly between the two nearest dissipative particles.

Equations of motion for the dissipative particles based on a microscopic description

The fact that all the MD particles are represented at all instants in the coarse-grained scheme is guaranteed by the normalization condition $\sum_k f_k(\mathbf{x}) = 1$. This implies directly that $\sum_k M_k = \sum_i m$, $\sum_k \mathbf{P}_k = \sum_i m\mathbf{v}_i$ and $\sum_k E_k^{tot} = \sum_i \epsilon_i$, so that if mass, momentum and energy are conserved at the MD level, they are also conserved at the DP level.

In order to obtain the equations of motion for the DPD we now take the time derivatives of Eqs. (VIII.1). The Gaussian form of s makes it possible to write the time derivative $\dot{f}_k(\mathbf{x}_i) = f_{kl}(\mathbf{x}_i)(\mathbf{v}_i' \cdot \mathbf{r}_{kl} + \mathbf{x}_i' \cdot \mathbf{U}_{kl})$ where the overlap function f_{kl} is defined as $f_{kl}(\mathbf{x}) \equiv (2/a^2) f_k(\mathbf{x}) f_l(\mathbf{x})$ and we have rearranged terms so as to get them in terms of the centered variables $\mathbf{v}_i' = \mathbf{v}_i - (\mathbf{U}_k + \mathbf{U}_l)/2$, $\mathbf{x}_i' = \mathbf{x}_i - (\mathbf{r}_k + \mathbf{r}_l)/2$, $\mathbf{U}_{kl} = \mathbf{U}_k - \mathbf{U}_l$ and $\mathbf{r}_{kl} = \mathbf{r}_k - \mathbf{r}_l$. After some algebra and averaging [22] the microscopic equations of motion then take the form

$$
\begin{aligned}
\frac{\mathrm{d}M_k}{\mathrm{d}t} &= \sum_l \dot{M}_{kl} \equiv \sum_{li} f_{kl}(\mathbf{x}_i) m \left(\mathbf{v}'_i \cdot \mathbf{r}_{kl} + \mathbf{x}'_i \cdot \mathbf{U}_{kl}\right) \\
\frac{\mathrm{d}\mathbf{P}_k}{\mathrm{d}t} &= M_k \mathbf{g} + \sum_l \dot{M}_{kl} \frac{\mathbf{U}_k + \mathbf{U}_l}{2} + \sum_{li} f_{kl}(\mathbf{x}_i) \langle \Pi'_i \rangle \cdot \mathbf{r}_{kl} \qquad \text{(VIII.4)} \\
&+ \sum_{li} f_{kl}(\mathbf{x}_i) m \mathbf{v}'_i \mathbf{x}'_i \cdot \mathbf{U}_{kl} + \sum_l \tilde{\mathbf{F}}_{kl} \\
\frac{\mathrm{d}E_k}{\mathrm{d}t} &= \sum_l \frac{\dot{M}_{kl}}{2} \left(\frac{\mathbf{U}_{kl}}{2}\right)^2 + \sum_{li} f_{kl}(\mathbf{x}_i) \left(\langle \mathbf{J}'_{\epsilon i} \rangle - \langle \Pi'_i \rangle \cdot \frac{\mathbf{U}_{kl}}{2} \right) \cdot \mathbf{r}_{kl} \\
&+ \sum_{li} f_{kl}(\mathbf{x}_i) \left(\epsilon'_i - m \mathbf{v}'_i \cdot \frac{\mathbf{U}_{kl}}{2} \right) \mathbf{x}'_i \cdot \mathbf{U}_{kl} + \sum \tilde{q}_{kl} \qquad \text{(VIII.5)}
\end{aligned}
$$

where we have defined the general momentum-flux tensor $\Pi'_i = m\mathbf{v}'_i\mathbf{v}'_i + (1/2)\sum_j \mathbf{F}_{ij}\Delta\mathbf{x}_{ij}$ and the microscopic energy flux vector

$$
\mathbf{J}'_{\epsilon i} = \epsilon_i \mathbf{v}'_i + (1/4) \sum_{i \neq j} \mathbf{F}_{ij} \cdot (\mathbf{v}'_i + \mathbf{v}'_j) \Delta\mathbf{x}_{ij},
$$

$m\mathbf{g}$ is the external force on an MD particle and $\tilde{\mathbf{F}}_{kl}$, $\tilde{q}_{kl}$ are the fluctuating components of the momentum and energy. We note that Eq. (VIII.5) has been derived by sampling MD particles over the Voronoi volume and considering the average and fluctuating components of mass, momentum and energy, without any other approximation.

All the interaction terms in the above transport equations are weighted by the overlap function $f_{kl}(\mathbf{x})$. If only two DP's, k and l say, are present it may be shown that $f_{kl}(\mathbf{x}) = (1/(2a^2)) \cosh^{-2}\left((\mathbf{x} - (\mathbf{r}_k + \mathbf{r}_l)/2) \cdot (\mathbf{r}_k - \mathbf{r}_l)/a^2\right)$. This function is shown in Fig. VIII.2. Dissipative particle interactions only take place where the overlap function is non-zero. This happens along the dividing line which is equally far from the two particles. The contours of non-zero f_{kl} thus define a Voronoi lattice with lattice segments of length l_{kl}. This Voronoi construction is shown in Fig. VIII.3 in which MD particles in the overlap region defined by $f_{kl} > 0.1$, are shown, though presently not actually simulated as dynamic entities. The volume of the Voronoi cells will in general vary under the dynamics. However, even with arbitrary dissipative particle motion the cell volumes will approach zero only exceptionally, and even then the identities of the DP particles will be preserved so that they subsequently re-emerge.

When additional DP's are present their contribution to the $\cosh^{-2}$ result may be shown to be negligible in the vicinity of the dividing line, except at the corners, where dividing lines meet. In the end the DPD equations of motion will be a-independent, and only the length l_{kl} shown in Fig. VIII.3 will enter. At this point it suffices to construct the Voronoi lattice itself, and there is no need to evaluate the overlap functions.

Note that since the right hand side terms of Eq. (VIII.5) are all odd under the exchange $l \leftrightarrow k$ the DP's interact in a pairwise and explicitly conservative fashion.

Finally, we need to compute the average of the pressure tensor and the heat flux in Eq. (VIII.5) over the overlap region using the corresponding constitutive equations. We note that all terms involving $\langle \mathbf{v}'_i \rangle$ are zero since the linear assumption of the average MD velocity implies this is equal to zero in the overlap region. It can be shown [22]

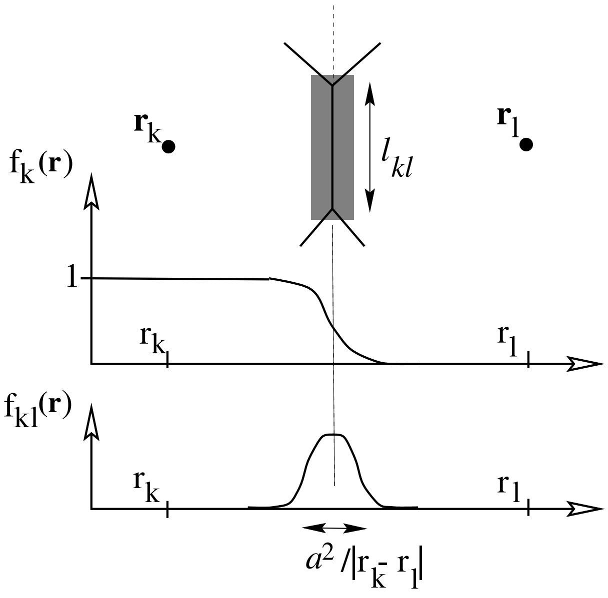

Figure VIII.2: The overlap region between two Voronoi cells is shown in grey. The sampling function $f_k(\mathbf{r})$ is shown in the top graph and the overlap function $f_{kl}(\mathbf{r}) = f_k(\mathbf{r})f_l(\mathbf{r})$ in the bottom graph. The width of the overlap region is $a^2/|\mathbf{r}_k - \mathbf{r}_l|$ and its length is denoted by l.

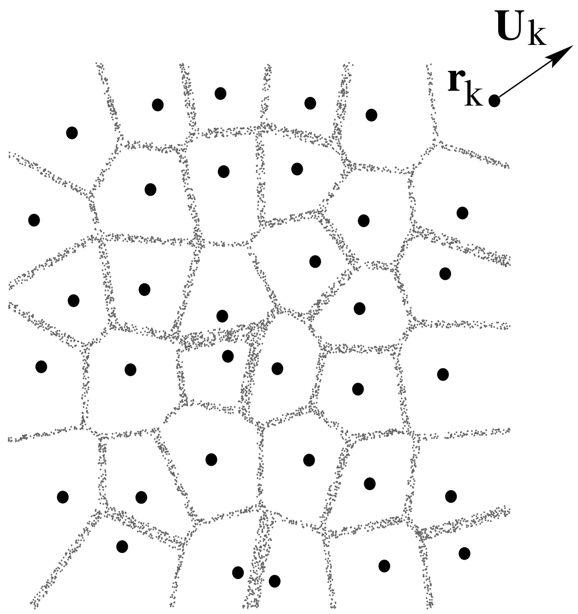

Figure VIII.3: The Voronoi lattice defined by the dissipative particle positions $\mathbf{r}_k$. The grey dots which represent the underlying MD particles are drawn only in the overlap region.

that this gives the final equations of motion as

$$\dot{M}_k = \sum_l (\langle \dot{M}_{kl} \rangle + \dot{M}_{kl}) \,, \tag{VIII.6}$$

where

$$\begin{aligned}
\langle \dot{M}_{kl} \rangle &= \frac{l_{kl}}{2r_{kl}} L_{kl} \frac{\rho_k + \rho_l}{2} \mathbf{i}_{kl} \cdot \mathbf{U}_{kl} \\
\frac{\mathrm{d}\mathbf{P}_k}{\mathrm{d}t} &= M_k \mathbf{g} + \sum_l (\langle \dot{P}_{kl} \rangle + \sum_l \tilde{\mathbf{F}}_{kl}) \\
\langle \dot{P}_{kl} \rangle = \sum_l \langle \dot{M}_{kl} \rangle \frac{\mathbf{U}_k + \mathbf{U}_l}{2} &- \sum_l l_{kl} \left(\frac{p_{kl}}{2} \mathbf{e}_{kl} + \frac{\eta}{r_{kl}} \left(\mathbf{U}_{kl} + \left(\mathbf{U}_{kl} \cdot \mathbf{e}_{kl} \right) \mathbf{e}_{kl} \right) \right)
\end{aligned} \tag{VIII.7}$$

and

$$\begin{aligned}
\dot{E}_k = &- \sum_l l_{lk} \lambda \frac{T_{kl}}{r_{kl}} \\
&- \sum_l l_{lk} \left(\frac{p_k + p_l}{2} \mathbf{e}_{kl} - \frac{\eta}{r_{kl}} (\mathbf{U}_{kl} + (\mathbf{U}_{kl} \cdot \mathbf{e}_{kl}) \mathbf{e}_{kl}) \right) \cdot \frac{\mathbf{U}_{kl}}{2} \\
&+ \sum_l \frac{1}{2} \langle \dot{M}_{kl} \rangle \left(\frac{\mathbf{U}_{kl}}{2} \right)^2 + \frac{l_{kl}}{4r_{kl}} L_{kl} \mathbf{i}_{kl} \cdot \mathbf{U}_{kl} \left(\frac{E_k}{V_k} + \frac{E_l}{V_l} \right) \\
&- \sum_l \tilde{\mathbf{F}}_{kl} \cdot \frac{\mathbf{U}_{kl}}{2} + \tilde{q}_{kl} \,.
\end{aligned} \tag{VIII.8}$$

The fluctuation of mass can be shown [22] to be of the order of $1/N_k$ where N_k is the number of MD particles in the region k. Thus for large N_k the mass fluctuations can be neglected.

Statistical mechanics of dissipative particle dynamics

In this section we discuss the statistical properties of the DP's with the particular aim of obtaining the magnitudes of $\tilde{\mathbf{F}}_{kl}$ and $\tilde{q}_{kl}$. We follow the conventional Fokker-Planck description of DPD[16].

It is not straightforward to obtain a general statistical mechanical description of the DP-system. The reason is that the DP's, which exchange mass, momentum, energy and volume, are not captured by any standard statistical ensemble. For the grand canonical ensemble, the system in question is defined as the matter within a fixed volume, and in the case of the isobaric ensemble the particle number is fixed. Neither of these requirements hold for a DP in general.

A system which exchanges mass, momentum, energy and volume without any further restrictions will generally be ill-defined as it will lose its identity in the course of time. The DP's of course remain well-defined by virtue of the coupling between the momentum and volume variables: the DP volumes are defined by the positions of the DP-centers and the DP-momenta govern the motion of the DP-centers. Hence the quantities that are exchanged with the surroundings are not independent and the ensemble must be constructed accordingly.

However, for present purposes we shall leave aside the interesting challenge of designing the statistical mechanical properties of such an ensemble, and derive the magnitude of $\tilde{\mathbf{F}}_{kl}$ and $\tilde{q}_{kl}$ from the approximation of a Fokker-Planck description of the DP system. The approximation is justifiable from the assumption that $\tilde{\mathbf{F}}_{kl}$ and $\tilde{q}_{kl}$ have a negligible correlation time. It follows that their properties may be obtained from the DP behavior on such short time scales that the DP-centers may be assumed fixed in space. As a result, we may take either the DP volume or the system of MD-particles fixed for the relevant duration of time. Hence for the purpose of getting $\tilde{\mathbf{F}}_{kl}$ and $\tilde{q}_{kl}$ we may use either the isobaric ensemble, applied to the DP system, or the grand canonical ensemble, applied to the MD system. We shall find the same results from either route. The analysis of the DP system using the isobaric ensemble follows the standard procedure using the Fokker-Planck equation, and the result for the equilibrium distribution is only valid in the short time limit. This analysis is given below. We note that the analysis of the MD system corresponding to the grand canonical ensemble could be conducted along similar lines.

We consider the system of $N_k \gg 1$ MD particles inside a given DP$_k$ at a given time. At later times it will be possible to associate a certain volume per particle with these particles, and by definition the system they form will exchange volume and energy but not mass. We consider all the remaining DP's as a thermodynamic bath with which DP$_k$ is in equilibrium. The system defined in this way will be described by the Gibbs free energy and the isobaric ensemble. Due to the diffusive spreading of MD-particles, this system will only initially coincide with the DP; during this transient time interval, however, we may treat the DP's as systems of fixed mass and describe them by the approximation $\langle \dot{M}_{kl} \rangle = 0$. The magnitudes of $\tilde{q}$ and $\tilde{\mathbf{F}}$ follow in the form of fluctuation-dissipation relations from the Fokker-Planck equivalent of our Langevin equations. The mathematics involved in obtaining fluctuation-dissipation relations is essentially well-known from the literature [9], and our analysis parallels that of Avalos and Mackie [16]. However, the fact that the conservative part of the conventional DP forces is here replaced by the pressure and that the present DP's have a variable volume makes a separate treatment enlightening.

The probability $\rho(V_k, \mathbf{P}_k, E_k)$ of finding DP$_k$ with a volume V_k, momentum $\mathbf{P}_k$ and internal energy E_k is then proportional to $\exp(S_T/k_B)$ where S_T is the entropy of all DP's given that the values $(V_k, \mathbf{P}_k, E_k)$ are known for DP$_k$[26]. Since there is nothing special about DP$_k$ it immediately follows that the the full equilibrium distribution has the form

$$\rho^{\text{eq}} = Z^{-1}(T_0, p_0) \exp\left(-\beta_0 \sum_k \frac{P_k^2}{2M_k} + G_k \right) , \tag{VIII.9}$$

where $\beta_0 = 1/(k_B T_0)$ and the Gibbs free energy has the standard form $G_k = E_k + p_0 V_k - T_0 S_k$. The temperature $T_k = (\partial S_k / \partial E_k)^{-1}$ and pressure $p_k = T_k(\partial S_k/\partial V_k)$ will fluctuate around the equilibrium values T_0 and p_0. The above distribution is analyzed by Landau and Lifshitz [27] who show that the fluctuations have the magnitude

$$\langle \Delta P_k^2 \rangle = \frac{k_B T_0}{V_k \kappa_S}, \ \ \langle \Delta T_k^2 \rangle = \frac{k_B T_0^2}{V c_v} \tag{VIII.10}$$

where the isentropic compressibility $\kappa_S = -(1/V)(\partial V/\partial P)_S$ and the specific heat capacity c_v are both intensive quantities. Comparing our expression with the distribution postulated by Avalos and Mackie, we have replaced the Helmholtz by the Gibbs free energy in Eq. (VIII.9). This is due to the fact that our DP's exchange volume as well as energy.

We write the fluctuating force as

$$\tilde{\mathbf{F}}_{kl} = \boldsymbol{\omega}_{kl||} W_{kl||} + \boldsymbol{\omega}_{kl\perp} W_{kl\perp} \tag{VIII.11}$$

where, for reasons soon to become apparent, we have chosen to decompose $\tilde{\mathbf{F}}_{kl}$ into components parallel and perpendicular to $\mathbf{e}_{kl}$. The W's are defined as Gaussian random variables with the correlation function

$$\langle W_{kl\alpha}(t) W_{nm\beta}(t') \rangle \;\; = \;\; \delta_{\alpha\beta}\delta(t-t')(\delta_{kn}\delta_{lm} + \delta_{km}\delta_{ln}) \tag{VIII.12}$$

where α and β denote either $\perp$ or $||$. The product of δ factors ensures that only equal vectorial components of the forces between a pair of DP's are correlated, while Newton's third law guarantees that $\boldsymbol{\omega}_{kl} = -\boldsymbol{\omega}_{lk}$. Likewise the fluctuating heat flux takes the form

$$\tilde{q}_{kl} = \Lambda_{kl} W_{kl} \tag{VIII.13}$$

where W_{kl} satisfies Eq. (VIII.12) without the $\delta_{\alpha\beta}$ factor and energy conservation implies $\Lambda_{kl} = -\Lambda_{lk}$.

It is a standard result in non-equilibrium statistical mechanics that a Langevin description of a dynamical variable has an equivalent probabilistic representation in terms of the Fokker-Planck equation. Using the above definitions and $\langle \dot{M}_{kl} \rangle = 0$ it is a standard matter [9] to obtain the Fokker-Planck equation and show that its steady-state solution is given by Eq. (VIII.9). Following conventional procedures we can obtain the fluctuation-dissipation relations for $\boldsymbol{\omega}$ and Λ by inserting ρ^{eq} into the Fokker-Planck equation corresponding to the Langevin equations VIII.7-VIII.8and show that detailed balance [28] holds only to order $1/N_k$. We may write down the sizes of the fluctuation in momentum and energy as

$$\begin{aligned} \omega^2_{kl||} \;\; &= \;\; 2\omega^2_{kl\perp} = 4\eta k_B \Theta_{kl} \frac{l_{kl}}{r_{kl}} \\ \Lambda^2_{kl} \;\; &= \;\; 2k_B T_k T_l \lambda \frac{l_{kl}}{r_{kl}} \, , \end{aligned} \tag{VIII.14}$$

where $\Theta^{-1}_{kl} = (1/2)(T^{-1}_k + T^{-1}_l)$.

The fluctuation-dissipation relations Eqs. (VIII.14) complete our theoretical description of dissipative particle dynamics, which has been derived by a coarse-graining of molecular dynamics. All the parameters and properties of this new version of DPD are related directly to the underlying molecular dynamics, and properties such as the viscosity which are emergent from it.

Simulations

Relaxation towards equilibrium

We have carried out simulations to test the equilibrium behavior of the model in the case of the isothermal model. This is a crucial test as the derivation of the fluctuating

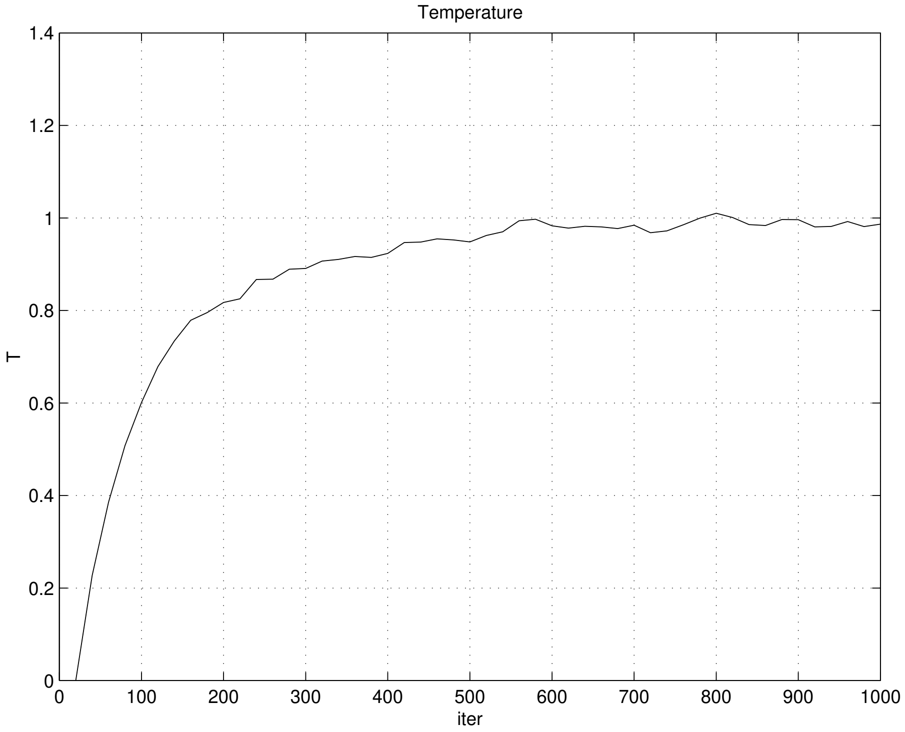

Figure VIII.4: The DPD temperature (energy units) averaged over 5000 dissipative particles as a function of time (iteration number in the integration scheme), showing good convergence to the underlying molecular dynamics temperature which was set at one. This simulation provides strong support for the approximations used to derive the fluctuation-dissipation relations in our DPD model from molecular dynamics.

forces relies on the most significant approximations. The simulations are carried out using a periodic Voronoi tesselation described in detail elsewhere [29]. Figure VIII.4 shows the relaxation process towards equilibrium of an initially motionless system. The DP temperature is measured as $\langle \mathbf{P}_k^2/(2M_k) \rangle$ for a system of DPs with internal energy equal to unity. The simulations were run for 1000 iterations of 5000 dissipative particles and a timestep $\mathrm{d}t = 0.0005$ using an initial molecular density $\rho = 5$ for each DP. The molecular mass was taken to be $m = 1$, the viscosity was set at $\eta = 1$, the expected mean free path is 0.79, and the Reynolds number (See Sec. VIII) is Re=2.23. The mass of the DP's was taken to be constant, as in the derivation of the magnitude of the fluctuations. It is seen that the convergence of the DP system towards the MD temperature is good, a result that provides strong support for the fluctuation-dissipation relations of Eq. (VIII.14). These simulations are run using the sequential code on a standard PC.

Parallel performance

The performance analysis of the code is presented on both Cray T3E (256 processors Alpha 600MHz) and SGI Origin 2000 (64 processors MIPS R12000 300MHz) in Figure VIII.5, Table VIII.1 and Figure VIII.6, Table VIII.2 respectively. All the benchmarks are run with the same configuration for both machines: 128000 particles (Npart), the same simulation box 100×100 $(space\ unit)^2$, 50 iterations.

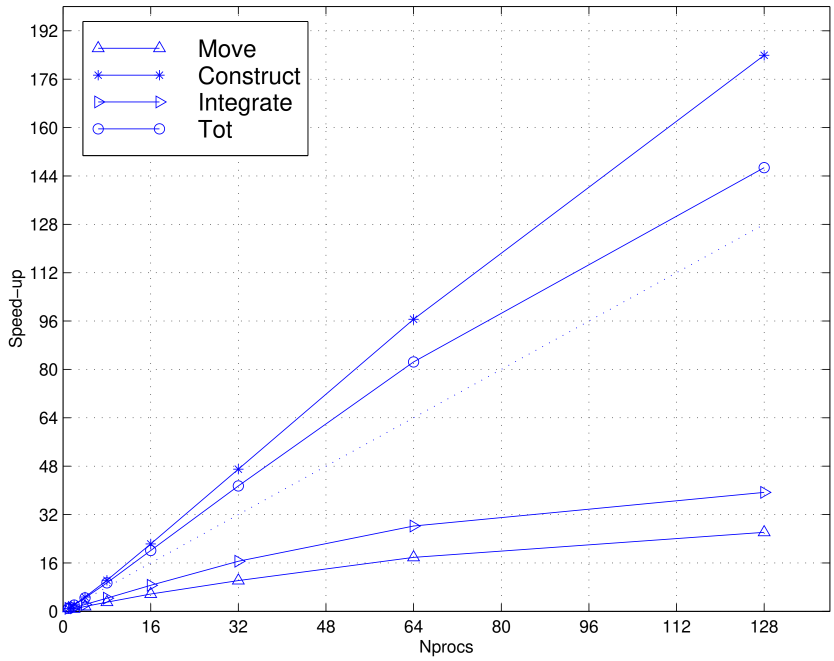

Figure VIII.5: Speed-up index on Cray T3E. The dotted line indicates the linear speed-up.

Nprocs	Npart/NProcs	Move	Construct	Integration	Comm	Total
1	128000	4.50	395.17	19.38	0	427.73
2	64000	5.45	180.96	16.54	1.49	206.99
4	32000	2.76	83.42	8.46	1.43	96.52
8	16000	1.48	38.48	4.43	1.02	45.34
16	8000	0.78	17.70	2.24	0.67	21.24
32	4000	0.44	8.40	1.16	0.44	10.31
64	2000	0.25	4.09	0.68	0.38	5.18
128	1000	0.17	2.14	0.49	0.47	2.91

Table VIII.1: Timings in seconds of the main routines on the Cray T3E. Comm measures the total time for communication, while the other timings are inclusive of the communication time. The number of iterations is 50.

Nprocs	Npart/NProcs	Move	Construct	Integration	Comm	Total
1	128000	1.94	307.77	17.90	0	334.24
2	64000	3.15	124.44	13.16	0.56	143.53
4	32000	1.78	50.03	5.94	0.69	58.95
8	16000	0.90	22.89	3.44	1.89	27.86
16	8000	0.59	11.20	1.77	1.25	13.88
32	4000	0.71	6.66	1.75	2.73	9.51

Table VIII.2: Timings in seconds of the main routines on the SGI Origin 2000. Comm measures the total time for communication, while the other timings are inclusive of the communication time. The number of iterations is 50.

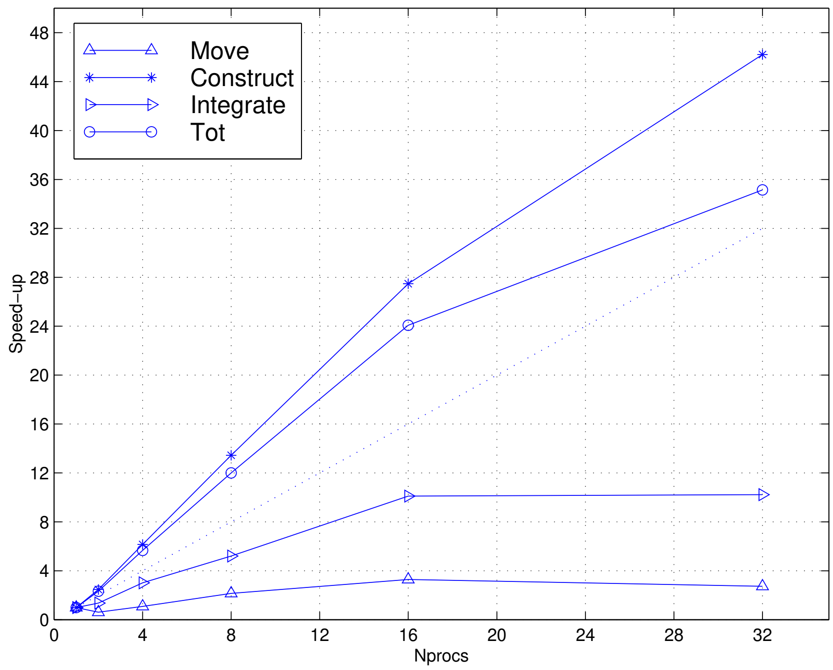

Figure VIII.6: Speed-up index on SGI Origin 2000. The dotted line indicates the linear speed-up.

The simulation is a relaxation towards equilibrium of the isothermal model starting from a random initial configuration. The timings have been taken measuring the CPU-clock time for the routines: *move* that updates the position and communicates the particle outside the boundary, *construct* that constructs the tessellation, *integration* that integrates the Langevin's equation and communicates the stochastic force, *comm* that is the total time of communication without the time for buffering and *total* that measures the total time without Input-Output. All the times measured are inclusive of communication, which is reported separately for comparison; the time for one processor is the time of the sequential version without any overhead due to buffering.

Looking at the speed-up index, it is worth noting that the super-linearity shown was expected because the algorithmic complexity of the construction is not linear, but $Nlog(N)$. The construction of the tessellation for $N/2$ takes less than half of the time spent for N dissipative particles.

Applications

Dissipative particle dynamics has been successfully applied to many hydrodynamical problems involving complex fluids. For example, Boek *et al.* [10] have successfully simulated colloidal suspensions at low to intermediate solids volume fractions, using the original DPD model developed by Hoogerbrugge and Koelman [8]. The colloidal particles are modelled by freezing together a spherical cluster of DP's and considering the total mass and momentum of the cluster as an effective single object. In this way, the interactions are computed using the standard DPD scheme for both the DP colloidal clusters and the DP fluid particles. Applications to polymeric fluids have been made by Schlijper *et al.* [11] who successfully reproduced the essential physical phenomena of such systems. The polymer chains are introduced into the fluid as a linear chain of DPD particles connected by Fraenkel springs. Novik and Coveney [12] have reported simulations of binary immiscible fluids in agreement with expectations. The fluids are modelled by assigning to different molecules a different 'color'. Individual molecules then attract similar and repel dissimilar coloured molecules. Laplace's law is shown to be satisfied in a series of bubble experiments, confirming the existence of a surface tension between the two phases. We now discuss some possible applications of our new DPD model.

Multiscale phenomena

For most practical applications involving complex fluids, additional interactions and boundary conditions need to be specified. These too must be deduced from some suitable meso-description of the microscopic dynamics, just as we have done for the interparticle forces. This may be achieved by considering a particulate description of the boundary itself and including molecular interactions between the fluid MD particles and other objects, such as particles or walls. Appropriate modifications can then be made on the basis of the momentum-flux tensor of Eq. (VIII.5), which is generally valid. Consider for example the case of a colloidal suspension, which is shown in Fig. VIII.7. Beginning with the hydrodynamic momentum-flux tensor Eq. (VIII.5), it is evident that we also need to define an interaction region where the DP–colloid forces act: the

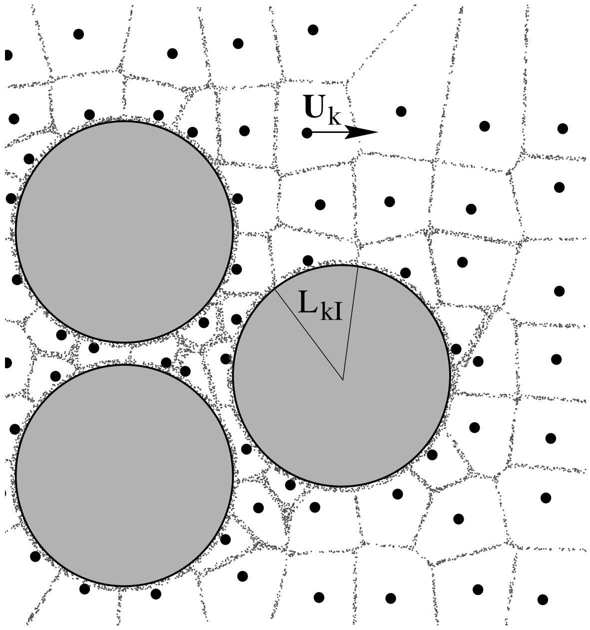

Figure VIII.7: **Multiscale modeling of colloidal fluids.** As usual, the dissipative particles are defined as cells in the Voronoi lattice. Note that there are four relevant length scales in this problem: the scale of the large, gray colloid particles, the two distinct scales of the dissipative particles in between and away from the colloids and finally the molecular scale of the MD particles. These mediate the mesoscopic interactions and are shown as dots on the boundaries between dissipative and colloidal particles.

DP–colloid interaction may be obtained in the same form as the DP–DP interaction by making the replacement $l_{kl} \rightarrow L_{kI}$, where L_{kI} is the length (or area in 3D) of the arc segment where the dissipative particle meets the colloid (see Fig. VIII.7) and the velocity gradient $r_{kl}^{-1}((\mathbf{U}_{kl}\cdot\mathbf{e}_{kl})\mathbf{e}_{kl}+\mathbf{U}_{kl})$ is that between the dissipative particle and the colloid surface. The latter may be computed using $\mathbf{U}_k$ and the velocity of the colloid surface together with a no-slip boundary condition on this surface. In Eq. (VIII.14) the replacement $l_{kl} \rightarrow L_{KI}$ must also be made.

Although previous DPD simulations of colloidal fluids have proved rather successful [10] at low to intermediate solids volume fractions, they break down for dense systems whose solids volume fraction exceeds a value of about 40% because the existing method is unable to handle multiple lengthscale phenomena. However, our new version of the algorithm provides the freedom to define dissipative particle sizes according to the local resolution requirements as illustrated in Fig. VIII.7. In order to increase the spatial resolution where colloidal particles are within close proximity it is necessary and perfectly admissible to introduce a higher density of dissipative particles there; this ensures that fluid lubrication and hydrodynamic effects are properly maintained. After these dissipative particles have moved it may be necessary to re-tile the DP system; this is easily achieved by distributing the mass and momentum of the old dissipative particles on the new ones according to their area (or volume in 3D). Considerations of space prevent us from discussing this problem further in the present paper, but we plan to report in detail on such dense colloidal particle simulations using our method in future publications. We note in passing that a wide variety of other complex systems exist where modeling and simulation are challenged by the presence of several simultaneous length scales, for example in polymeric and amphiphilic fluids, particularly in confined geometries such as porous media [30]. For instance, a simulation involving a polymeric fluid could be set up with a large number of dissipative particles for the solvent and sets of 100-1000 dissipative particles for each polymer molecule. The polymer is modelled by different polymer-fluid and polymer-polymer interactions more the standard fluid-fluid interaction. When a fluid dissipative particle is interacting with the polymer, the Delaunay triangulation handles the individuation of the monomers (polymer particles) to interact with (see Figure VIII.8).

The low viscosity limit and high Reynolds numbers

In the kinetic theory derived by Marsh, Backx and Ernst [15] the viscosity is explicitly shown to have a kinetic contribution $\eta_K = \rho D/2$ where D is the DP self diffusion coefficient and ρ the mass density. The kinetic contribution to the viscosity was measured by Masters and Warren [31] within the context of an improved theory. How then can the viscosity η used in our model be decreased to zero while kinetic theory puts the lower limit η_K to it?

To answer this question we must define a physical way of decreasing the MD viscosity while keeping other quantities fixed, or, alternatively rescale the system in a way that has the equivalent effect. The latter method is preferable as it allows the underlying microscopic system to remain fixed. In order to do this we non-dimensionalize the DP momentum equation.

For this purpose we introduce the characteristic equilibrium velocity, $U_0 = \sqrt{k_B T/M}$, the characteristic distance r_0 as the typical DP size. Then the characteristic time

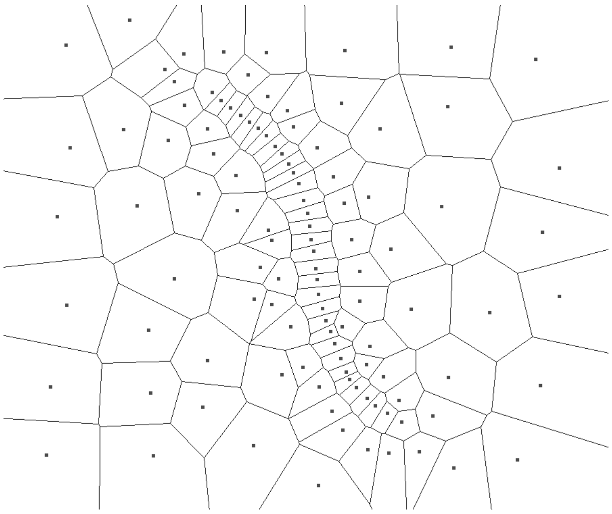

Figure VIII.8: Structure of a polymeric fluid according to the multiscale dissipative particle dynamics method. The resolved length scale of the polymer is much finer than that of the fluid.

$t' = r_0/U_0$ follows.

Neglecting gravity for the time being, the DP momentum equation takes the form

$$\frac{\mathrm{d}\mathbf{P}'_k}{\mathrm{d}t'} = -\sum_l l'_{kl}\left(\frac{p'_{kl}}{2}\mathbf{e}_{kl} + \frac{1}{\mathrm{Re}}\left(\mathbf{U}'_{kl} + (\mathbf{U}'_{kl}\cdot\mathbf{e}_{kl})\mathbf{e}_{kl}\right)\right)$$
$$+ \sum_l \frac{l'_{kl}L'_{kl}}{2r'_{kl}}\frac{\rho'_k + \rho'_l}{2}\mathbf{i}_{kl}\cdot\mathbf{U}'_{kl}\frac{\mathbf{U}'_k + \mathbf{U}'_l}{2} + \sum_l \tilde{\mathbf{F}}'_{kl}\ , \tag{VIII.15}$$

where $\mathbf{P}'_k = \mathbf{P}_k/(MU_0)$, $p'_{kl} = p_{kl}r_0^2/(MU_0^2)$, $M = \rho r_0^2$ in 2d, the Reynolds number $\mathrm{Re} = U_0 r_0 \rho/\eta$ and $\tilde{\mathbf{F}}'_{kl} = (r_0/MU_0^2)\tilde{\mathbf{F}}_{kl}$ where $\tilde{\mathbf{F}}_{kl}$ is given by Eqs. (VIII.11) and (VIII.14). A small calculations then shows that if $\tilde{\mathbf{F}}'_{kl}$ is related to ω'_{kl} and t' like $\tilde{\mathbf{F}}_{kl}$ related to ω_{kl} and t, then

$$\omega'^2_{kl} \approx \frac{1}{\mathrm{Re}}\frac{k_B T}{MU_0^2} \approx \frac{1}{\mathrm{Re}} \tag{VIII.16}$$

where we have neglected dimensionless geometric prefactors like l_{kl}/r_{kl} and used the fact that the ratio of the thermal to kinetic energy by definition of U_0 is one.

The above results imply that when the DPD system is measured in non-dimensionalized units everything is determined by the value of the mesoscopic Reynolds number Re. There is thus no observable difference in this system between increasing r_0 and decreasing η.

Returning to dimensional units again the DP diffusivity may be obtained from the Stokes-Einstein relation [32] as

$$D = \frac{k_B T}{a r_0 \eta} \tag{VIII.17}$$

where a is some geometric factor ($a = 6\pi$ for a sphere) and all quantities on the right hand side except r_0 refer directly to the underlying MD. As we are keeping the MD system fixed and increasing Re by increasing r_0, it is seen that D and hence η_K vanish in the process.

We note in passing that if D is written in terms of the mean free path λ: $D = \lambda\sqrt{k_B T/(\rho r_0^2)}$ and this result is compared with Eq. (VIII.17) we get $\lambda' = \lambda/r_0 \sim 1/r_0$ in 2d, i.e. the mean free path, measured in units of the particle size decreases as the inverse particle size. This is consistent with the decay of η_K. The above argument shows that decreasing η is equivalent to keeping the microscopic MD system fixed while increasing the DP size, in which case the mean free path effects on viscosity is decreased to zero as the DP size is increased to infinity. It is in this limit that high Re values may be achieved.

Note that in this limit the thermal forces $\tilde{\mathbf{F}}_{kl} \sim \mathrm{Re}^{-1/2}$ will vanish, and that we are effectively left with a macroscopic, fluctuationless description. This is no problem when using the present Voronoi construction. However, the effectively spherical particles of conventional DPD will freeze into a colloidal crystal, i.e. into a lattice configuration [8,9] in this limit. Also while conventional DPD has usually required calibration simulations to determine the viscosity, due to discrepancies between theory and measurements, the viscosity in this new form of DPD is simply an input parameter. However, there may still be discrepancies due to the approximations made in going from MD to DPD. These approximations include the linearization of the inter-DP velocity fields, the Markovian assumption in the force correlations and the neglect of a DP angular momentum variable.

None of the conclusions from the above arguments would change if we had worked in three dimensions instead of two.

Conclusions

We have introduced a systematic procedure for deriving the mesoscopic modeling and simulation method known as dissipative particle dynamics from the underlying description in terms of molecular dynamics. Figure VIII.9 illustrates the structure of the theoretical development of DPD equations from MD as presented in this paper. The initial coarse graining leads to equations of essentially the same structure as the final DPD equations. However, they are still invariant under time-reversal. The development we have made which is shown in Fig.VIII.9 does not claim to derive the irreversible DPD equations from the reversible ones of molecular dynamics in a rigorous manner, although it does illustrate where the transition takes place with the introduction of molecular averages. The kinetic equations of this new DPD satisfy an H-theorem, guaranteeing an irreversible approach to the equilibrium state.

This is the first time that any of the various existing mesoscale methods have been put on a firm 'bottom up' theoretical foundation, a development which brings with it numerous new insights as well as practical advantages. One of the main virtues of this procedure is the capability it provides to choose one or more coarse-graining lengthscales to suit the particular modeling problem at hand. The relative scale between molecular dynamics and the chosen dissipative particle dynamics, which may be defined as the ratio of their number densities $\rho_{\mathrm{DPD}}/\rho_{\mathrm{MD}}$, is a free parameter within the theory. Indeed, this rescaling may be viewed as a renormalisation group procedure under which the fluid viscosity remains constant: since the conservation laws hold ex-

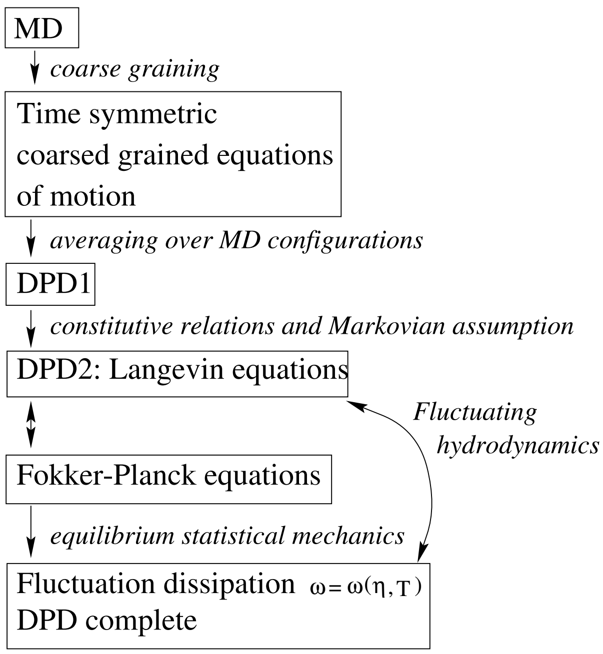

Figure VIII.9: Outline of the derivation of dissipative particle dynamics from molecular dynamics as presented in the present paper. The MD viscosity is denoted by η and ω is the amplitude of the fluctuating force $\tilde{\mathbf{F}}$ as defined in Eq. (VIII.11)

actly at every level of coarse graining, the result of doing two rescalings, say from MD to DPDα and from DPDα to DPDβ, is the same as doing just one with a larger ratio, i.e. $\rho_{\mathrm{DPD}\beta}/\rho_{\mathrm{MD}} = (\rho_{\mathrm{DPD}\beta}/\rho_{\mathrm{DPD}\alpha})(\rho_{\mathrm{DPD}\alpha}/\rho_{\mathrm{MD}})$.

The present coarse graining scheme is not limited to hydrodynamics. It could in principle be used to rescale the local description of any quantity of interest. However, only for locally conserved quantities will the DP particle interactions take the form of surface terms as here, and so it is unlikely that the scheme will produce a useful description of non-conserved quantities.

In this context, we note that the bottom-up approach to fluid mechanics presented here may throw new light on aspects of the problem of homogeneous and inhomogeneous turbulence. Top-down multiscale methods and, to a more limited extent, ideas taken from renormalisation group theory have been applied quite widely in recent years to provide insight into the nature of turbulence [33, 34]; one might expect an alternative perspective to emerge from a fluid dynamical theory originating at the microscopic level, in which the central relationship between conservative and dissipative processes is specified in a more fundamental manner. From a practical point of view it is noted that, since the DPD viscosity is the same as the viscosity emergent from the underlying MD level, it may be treated as a free parameter in the DPD model, and thus high Reynolds numbers may be reached. In the $\eta \to 0$ limit the model thus represents a potential tool for hydrodynamic simulations of turbulence. However, we have not investigated the potential numerical complications of this limit.

The dissipative particle dynamics which we have derived is formally similar to the conventional version, incorporating as it does conservative, dissipative and fluctuating forces. The interactions are pairwise, and conserve mass and momentum as well as energy. However, now all these forces have been derived from the underlying molecular dynamics. The conservative and dissipative forces arise directly from the hydrodynamic description of the molecular dynamics and the properties of the fluctuating forces are determined via a fluctuation–dissipation relation.

The simple hydrodynamic description of the molecules chosen here is not a necessary requirement. Other choices for the average of the general momentum and energy flux tensors may be made and we hope these will be explored in future work. More significant is the fact that our analysis permits the introduction of specific physico-chemical interactions at the mesoscopic level, together with a well-defined scale for this mesoscopic description.

While the Gaussian basis we used for the sampling functions is an arbitrary albeit convenient choice, the Voronoi geometry itself emerged naturally from the requirement that all the MD particles be fully accounted for. Well defined procedures already exist in the literature for the computation of Voronoi tesselations [35] and so algorithms based on our model are not computationally difficult to implement. Nevertheless, it should be appreciated that the Voronoi construction represents a significant computational overhead. This overhead is of order $N \log N$, a factor $\log N$ larger than the most efficient multipole methods in principle available for handling the particle interactions in molecular dynamics. However, the prefactors are likely to be much larger in the particle interaction case.

Finally we note the formal similarity of the present particulate description to existing continuum fluid dynamics methods incorporating adaptive meshes, which start out from a top-down or macroscopic description. These top-down approaches include in particular smoothed particle hydrodynamics [19] and finite-element simulations. In these descriptions too the computational method is based on tracing the motion of elements of the fluid on the basis of the forces acting between them [36]. However, while such top-down computational strategies depend on a macroscopic and purely phenomenological fluid description, the present approach rests on a *molecular* basis.

Bibliography

[1] L. D. Landau and E. M. Lifshitz, *Fluid Mechanics* (Pergamon Press, New York, 1959).

[2] L. Boltzmann., *Vorlesungen über Gastheorie* (Leipzig, 1872).

[3] J. Koplik and J. R. Banavar, Ann. Rev. Fluid Mech. **27**, 257 (1995).

[4] U. Frisch, B. Hasslacher, and Y. Pomeau, Phys. Rev. Lett. **56**, 1505 (1986).

[5] G. McNamara and G. Zanetti, Phys. Rev. Lett. **61**, 2332 (1988).

[6] X. W. Chan and H. Chen, Phys. Rev E **49**, 2941 (1993).

[7] M. R. Swift, W. R. Osborne, and J. Yeomans, Phys. Rev. Lett. **75**, 830 (1995).

[8] P. J. Hoogerbrugge and J. M. V. A. Koelman, Europhys. Lett. **19**, 155 (1992).

[9] P. Español and P. Warren, Europhys. Lett. **30**, 191 (1995).

[10] E. S. Boek, P. V. Coveney, H. N. W. Lekkerkerker, and P. van der Schoot, Phys. Rev. E **54**, 5143 (1997).

[11] A. G. Schlijper, P. J. Hoogerbrugge, and C. W. Manke, J. Rheol. **39**, 567 (1995).

[12] P. V. Coveney and K. E. Novik, Phys. Rev. E **54**, 5143 (1996).

[13] R. D. Groot and P. B. Warren., J. Chem. Phys. **107**, 4423 (1997).

[14] P. Español, Phys. Rev. E **52**, 1734 (1995).

[15] C. A. Marsh, G. Backx, and M. Ernst, Phys. Rev. E **56**, 1676 (1997).

[16] J. B. Avalos and A. D. Mackie, Europhys. Lett. **40**, 141 (1997).

[17] P. Español, Europhys. Lett **40**, 631 (1997).

[18] P. Español, Phys. Rev. E **57**, 2930 (1998).

[19] J. J. Monaghan, Ann. Rev. Astron. Astophys. **30**, 543 (1992).

[20] P. Español, M. Serrano, and I. Zuñiga, Int. J. Mod. Phys. C **8**, 899 (1997).

[21] E. G. Flekkøy and P. V. Coveney, Phys. Rev. Lett. **83**, 1775 (1999).

[22] E. G. Flekkøy, P. V. Coveney, and G. De Fabritiis (submitted to Phys. Rev. E).

[23] P. V. Coveney and O. Penrose, J. Phys A: Math. Gen. **25**, 4947 (1992).

[24] O. Penrose and P. V. Coveney, Proc. R. Soc. **447**, 631 (1994).

[25] P. V. Coveney and R. Highfield, *The Arrow of Time* (W. H.Allen, London, 1990).

[26] F. Reif, *Fundamentals of statistical and thermal physics* (Mc Graw-Hill, Singapore, 1965).

[27] L. D. Landau and E. M. Lifshitz, *Statistical Physics* (Pergamon Press, New York, 1959).

[28] C. W. Gardiner, *Handbook of stochastic methods* (Springer Verlag, Berlin Heidelberg, 1985).

[29] G. De Fabritiis, P. V. Coveney, and E. G. Flekkøy, in *Proc. 5th European SGI/Cray MPP Workshop, Bologna, Italy 1999.*

[30] P. V. Coveney, J. B. Maillet, J. L. Wilson, P. W. Fowler, O. Al-Mushadani and B. M. Boghosian, Int. J. Mod. Phys. C **9**, 1479 (1998).

[31] A. J. Masters and P. B. Warren, *preprint* cond-mat/9903293 (http://xxx.lanl.gov/) (unpublished).

[32] A. Einstein, Ann. Phys. **17**, 549 (1905).

[33] U. Frisch, *Turbulence* (Cambridge University Press, Cambridge, 1995).

[34] A. Bensoussan, J. L. Lions, and G. Papanicolaou, *Asymptotic Analysis for Periodic Structures* (North-Holland, Amsterdam, 1978).

[35] D. E. K. L. J. Guibas and M. Sharir, Algorithmica **7**, 381 (1992).

[36] B. M. Boghosian, Encyclopedia of Applied Physics **23**, 151 (1998).

IX

The_elements: A Beowulf class Computer

Stavros C. Farantos
Institute of Electronic Structure and Lasers,
FORTH, Iraklion, Crete, 711 10, Greece, and
Department of Chemistry, University of Crete, Iraklion,
Crete, 711 10, Greece

Abstract

The_elements is a Beowulf-Type computer for supporting the project in Classical and Quantum Mechanical Molecular Dynamics of Theoretical and Computational Chemistry in Crete. This distributed parallel system is an effort to create large computational power by accumulating low cost CPUs, memory and hard discs for data storage using open software as far as possible. The current composition of The_elements is eight dual Pentium II systems with CPUs at 350 and 450 MHz, total memory 5GBytes, total hard discs 76 GBytes and all these connected with a fast Ethernet switch of 100 Mbits/s.

Introduction

The Beowulf-class era has dawned and this species of computers is rapidly multipling all over the world. The first book on how to build a Beowulf system [1] has been published and several documents have been written by those who have experienced the construction of a Beowulf computer
(http://beowulf.gsfc.nasa.gov/). It is amazing that with today's technology, low cost PCs and open software, scientists in fields other than the computer science are capable of building a parallel system with memory and performance met in supercomputers just a few years ago.

Scientists from physics and chemistry are ravenous for CPU time and memory when trying to solve problems related to simulations of matter. There are several advantages with the Beowulf-class parallel computers [1]. However, the freedom of designing and constructing a system which is tailored to solving specific computational problems does not come easily. Decisions about how to split the budget among the number of CPUs, the memory or the size of hard discs, the kind and the speed of the connecting network in a parallel system depend on the applications one has in mind.

In our laboratory the main computational projects are in the areas:

1. Molecular Potential Energy Surfaces and Clusters [2,3].
2. Non-Linear Classical Mechanical Analysis of Molecular Systems: Periodic Orbit Multiple Shooting Algorithms [4].
3. Molecular Quantum Dynamics: Periodic Orbit Assisted Grid Solutions of Time Dependent Schrödinger Equation [5].
4. Molecular Electronic Structure Calculations (Quantum Chemistry) [6].

Parallelized codes are available for locating minima and transition states on multidimensional Potential Energy Surfaces and for solving the Time Dependant Schrödinger Equation. The latter is greatly facilitated by employing high order Finite Difference algorithms [5]. For electronic structure quantum chemistry type calculations a parallelized packet, NWCHEM, [1] is that from EMSL-PNNL. The above projects are memory and CPU time intensive. Therefore, we have built the following Beowulf-class system.

Technical Characteristics

The system was built in two phases.

PHASE 1 (JULY 1998)

Dual Nodes: / Fire / Water / Air / Earth /

- CPUs: Eight Pentium II CPUs at 350 MHz - Cash Memory 512 KBytes
- Motherboards: QDI Brilliant V, Chipset INTEL 440 BX 100MHz
- Memory: 2.048 GBytes (4x512) (100 MHz SDRAM)
- Discs: 21 GBytes (5x4.2) (WESTERN DIGITAL ULTRA WIDE SCSI)
- Network: Bay 350T, 100 Mbits Switch, Backbone 1Gbits, 16 ports

PHASE 2 (APRIL 1999)

Dual Nodes: / Hydrogen / Helium / Nitrogen[*] / Oxygen[*] /

- CPUs: Eight Pentium II CPUs at 450 MHz - Cash Memory 512 KBytes
- Motherboards: P2B-D, ASUS, Chipset INTEL 440 BX 100MHz
- Memory: 3.072 GBytes (2x512+2x1024[*]) (100 MHz SDRAM)
- Discs: 54.6 GBytes (6x9.1) (IBM, ULTRA WIDE2 SCSI)

In total the hardware consists of Sixteen Pentium II CPUs, 5 GBytes Memory and 76 GBytes Hard Discs. Each system has 0.5 GBytes memory but two of 1 GByte. Special care was taken for the cooling of the computers. Two more fans were added to each case which contains the CPUs.

[1] http://www.emsl.pnl.gov:2080/docs/nwchem/nwchem.html

Software

- Operational System: Linux, Distributor Red Hat 6.1 (Cartman) (Kernel 2.2.13) (O)
- Communication Programs: Message Passing Interface (MPI) Argonne MPI (O)
- Batch Queuing Program: Generic NQS (Network Queuing System 3.50.6) - Sterling Software Incorporated (O)
- Compilers: /High Performance Fortran (HPF) / Fortran 90 / Fortran 77 / C / C++ / Portland Group 3.1 (C)
- Libraries: Numerical Recipes (C) - PETSc (Portable, Extensible Toolkit for Scientific Computations) (O)

O = Open software, C = Commercial software, L = Local software.

Communication mode

The eight dual PCs connected by the fast Ethernet consist an isolated local area network (ILAN). The mode of accessing The_elements from the outside world is what is called **"the Guarded Beowulf"** [1]. In this scheme only one of the nodes has an IP address recognizable from machines outside The_elements. The **"worldly-node"** is Fire which has been upgraded to a 450 MHz dual Pentium II. Fire is protected by a firewall software. Each node has a local hard disc but a raid of 17 GBytes is supported my the server (Fire).

Cost and Performance

The cost of The Elements was: Phase 1: $25000, Phase 2: $17000. These prices of course are relevant with the time of purchase of the systems mentioned above. The stability and reliability of the cluster is unquestionable. This has been tested by running two jobs in each CPU simultaneously in the scientific fields mentioned above. Comparisons of the performance per CPU have been made with a HP-Exemplar system with eight CPUs and 1GByte memory. The speed is the expected for an INTEL processor at 350 MHz or 450 MHz (approximately 2:1) for classical Molecular Dynamics calculations. However, the compilers of PGgroup, especially of FORTRAN 90, are highly efficient for matrix-vector multiplication. Some tests as well as other information for our applications in The_elements can be found in the URL address:
http://TCCC.iesl.forth.gr/AMS_EPEAEK/the_elements/the_elements_profile.html.

Discussion

Parallel systems of Beowulf-Type with a small number of CPUs are distinguished from the massively parallel systems, and should be compared with the similar size shared memory parallel servers commercially available by SUN, SGI and HP. The latter have the advantage of having a common memory accessible by all CPUs simultaneously, something which simplifies the programming. In a Beowulf-class computer the memory is distributed among the nodes and the programmer must take care to transfer data from one computer to the other. This is achieved by using the Message Passing Interface (MPI) library which provides subroutines in C or FORTRAN programming languages to facilitate the transfer of data. The task of writing the proper codes or as in most cases of modifying existing ones, is sometimes considerable and this is only compensated by the low cost of a Beowulf-Type computer. The prices may differ even by an order of magnitude.

Using MPI itself is relatively simple and in most applications a small number of subroutines are used. However, a serious planning is needed when we have to restructure the code in order to parallelize our program. At present, we have acquired limited experience by parallelizing a code for solving the time-dependent Schrödinger equation which involves matrix-vector multiplications. Libraries with parallelized codes for numerical analysis applications using MPI exist such as PETSc. To the best of our knowledge efficient open software for converting a distributed memory system to a shared memory type is not yet available, but it is likely to appear in the future.

The amount of work for the administration of a parallel system depends, of course, on its size. In our case we have adopted a master-slave scheme where the shared software is stored and maintained in the server. Software for batch queuing and statistics of memory and CPU utilization by the running jobs is available, both commercial and public. The one that we use (Generic NQS) achieves a good balance in distributing the jobs among the CPUs. Generic NQS allows to define batch queues with different priorities and memory needs.

We have adopted two batch queues, the **large** with unlimited CPU time but maximum memory for each running job up to 250 MBytes, and the **mlarge** with unlimited CPU time and maximum memory of 500 MBytes, restricted only to those systems with one GByte memory. Also, the number of jobs running in each node is one per CPU, i.e. two jobs in each dual system. The administrator can easily reconfigure Generic NQS to achieve the most efficient use of memory and CPU time to a dynamically varying environment. Interactive use of the system is not encouraged, except for parallelized codes which utilize MPI.

The stability of the whole system has been tested under conditions where single jobs (mainly of quantum chemistry type) and parallel jobs using MPI are executed simultaneously. The system can be run for several days without observing any error in the connecting network. Up to now we have a positive experience from the performance of The_Elenents, but the elaborate task of writing efficient parallel codes remains and this is the value to be paid for having a low cost powerful distributed computer.

Bibliography

[1] T. L. Sterling, J. Salmon, D. J. Becker and D. F. Savarese.
How to Build a Beowulf: A guide to the implementation and application of PC clusters. *The MIT Press, Cambridge, Massachusetts*, 1999.

[2] J. Papadakis, G. S. Fanourgakis, M. Founargiotakis and S. C. Farantos.
Comparison of Line Search Minimization Algorithms for Exploring Topography of Multidimensional Potential Energy Surfaces: $Mg^{+}Ar_n$ case. *J. Comput. Chem.*, 18:1011, 1997.

[3] S. Stamatiadis, R. Prosmiti and S. C. Farantos.
AUTO_DERIV: Tool for automatic differentiation of a FORTRAN code. *Comp. Phys. Comm.*, in press, 2000.

[4] S. C. Farantos.
POMULT: A Program for Computing Periodic Orbits in Hamiltonian Systems Based on Multiple Shooting Algorithms. *Comp. Phys. Comm.*, 108:240, 1998.

[5] R. Guantes and S. C. Farantos.
High Order Finite Difference Algorithms for Solving the Schrödinger Equation in Molecular Dynamics. *J. Chem. Phys.*, 111:10827, 1999.

[6] G. S. Fanourgakis, S. C. Farantos, M. Velegrakis and S. S. Xantheas.
Photofragmentation Spectra and Structures of $Sr^{+}Ar_n, n = 2 - 8$ Clusters: Experiment and Theory. *J. Chem. Phys.*, 109:108, 1998.

X

Did you see ?

We wish to have on the simu web site (http://simu.ulb.ac.be/) a list of books, newsletters, websites, programmes, in fact anything which coincides with the goals of *SIMU*, provided that each item is either striking, or very useful. We would like each of you, as a reader of this newsletter, to play the role of an expert filter, selecting and channeling information to the site, so that it can be distributed to everyone. The following sections are only an attempt to "set the ball rolling" and are by no means complete.

Computer clusters and parallel computing

1. The Message Passing Interface (MPI) standard. Description of the MPI parallel library, manuals and examples
   http://www-unix.mcs.anl.gov/mpi/index.html

2. The MPICH implementation of MPI. A public domain library.
   http://www-unix.mcs.anl.gov/mpi/mpich

3. The LAM-MPI implementation of MPI. A public domain library
   http://www.mpi.nd.edu/lam/

4. The Beowulf pages. Description of Linux clusters to do distributed computations: recommendations, software, documentation, etc
   http://www.beowulf.org/
   http://www.beowulf-underground.org/

5. Parallel Mac cluster description: technical details on building and running codes on the cluster are available in Viktor K. Decyk, Dean E. Dauger, and Pieter R. Kokelaar, Appleseed: A Parallel Macintosh Cluster for Numerically Intensive Computing
   http://exodus.physics.ucla.edu/appleseed/appleseed.html

6. Other Macintosh cluster information is at
   http://exodus.physics.ucla.edu/appleseed/appleseedsites.html

Physics

1. The XXX-LANL article depository. French mirror
   http://xxx.lpthe.jussieu.fr/

2. The SISSA (Trieste) information web site for condensed matter, a treasure trove
   http://www.sissa.it/~furio/cminfo.html

Chemistry

1. A URL for departments of chemistry is
   http://www.ch.cam.ac.uk/ChemSitesIndex.html

2. An article about Beowulf-Class Computers used by chemists, available at
   http://TCCC.iesl.forth.gr/AMS_EPEAEK/the_elements/articles/ACS_Jan10.html

Scientific software

1. FFTW: An efficient FFT library for sequential and parallel computers
   http://www.fftw.org/

2. Numerical Recipes on Line. PostScript and PDF files of the NR C/Fortran books
   http://www.ulib.org/webRoot/Books/Numerical_Recipes/

3. List of web references on numerical methods (benchmarks, fortran courses, books, sites etc...)
   http://tonic.physics.sunysb.edu/docs/num_meth.html

4. A general-purpose molecular dynamics simulation program called Moldy. It is sufficiently flexible that it ought to be useful for a wide range of simulation calculations of atomic, ionic and molecular systems.
   http://www.earth.ox.ac.uk/~keith/moldy.html

5. For a library of software on molecular dynamics, Monte Carlo, Lattice statistics and Lattice dynamics containing the programmes of the book, see the web site of the UK CCP5 group,
   http://www.daresbury.ac.uk/CCP/CCP5/librar.html

6. Quantum Simulations of Condensed Matter Systems, the NCSA Condensed Matter Physics home page of David Ceperley containing lots of free software,
   http://www.ncsa.uiuc.edu/Apps/CMP/cmp-homepage.html

7. LASSP Tools:A great variety of scientific visualization programmes
   http://www.lassp.cornell.edu/LASSPTools/LASSPTools.html

Books and associated sites on molecular simulation

1. Understanding Molecular Simulation: From Algorithms to Applications Daan Frenkel and Berend Smit, Academic Press (1996). For new additions, exercises, programmes and associated courses see
   http://molsim.chem.uva.nl/frenkel_smit/

2. Computer Simulation of liquids, M.P. Allen and D.J. Tildesley, Oxford Science Publications, 1997, one of the bibles of simulators. The programmes of the book, are available on the CCP5 group web site, http://www.daresbury.ac.uk/CCP/CCP5/librar.html
   The web site of an associated summer school is
   http://molsim.ch.umist.ac.uk/CCP5SS/

3. Classical and Quantum Dynamics in Condensed Phase Systems, Editors: Bruce J. Berne, Giovanni Ciccotti and David F. Coker.
   For associated material, check out the web site of Giovanni Ciccotti
   http://mefisto.phys.uniroma1.it/cgi-bin/wrap/ciccotti/Public/LERICI/

4. Monte Carlo and Molecular Dynamics of Condensed Matter Systems, Kurt Binder and Giovanni Ciccotti, Italian Physical Society, 1995

5. Monte Carlo Simulation in Statistical Physics, An Introduction, Kurt Binder and Dieter W. Heermann, Springer, 1988

Newsletters and associated web sites

1. The Ψ_k newsletter, Ab-initio (from electronic structure) calculation of complex processes in materials, which is supported by the European Science Foundation,
   http://psi-k.dl.ac.uk/

2. The webserver of the European Science Foundation, also our sponsor is
   http://www.esf.org/

3. The CCP3 Surface Science newsletter, see
   http://www.cse.clrc.ac.uk/Activity/CCP3

XI

Conferences, Schools, Workshops, Tutorials and *SIMU* fellowships

Upcoming activities supported completely or in part by *SIMU*

Detailed information on the following activities is available at the URL:
http://simu.ulb.ac.be/activities/activities.html

Conference

SIMU conference on Bridging the time scale gap, Konstanz, Germany, September 11-15, 2001.

Workshops

1. Planning meeting on "Universal Statistics in Correlated Systems", Lyon, France, March 29-31, 2000
Peter Holdsworth, Ecole Normale Supérieure de Lyon, France;
Jean François Pinton, Ecole Normale Supérieure de Lyon, France;
Steven T. Bramwell, University College London.

2. Characterizing and Studying Transition Mechanisms and States in High Dimensional Systems Lyon, France, May 4-6, 2000.
Peter Bolhuis , Department of Chemistry, Cambridge University UK;
Christoph Dellago , Department of Chemistry, University of Rochester, USA;
David Chandler , Department of Chemistry, University of California, Berkeley, USA.

3. Multiscale Modeling of Macromolecular Systems , Max Planck-Institute for Polymer Research, Mainz, Germany, September 4-6, 2000.
Dr. Ralf Everaers, Dr. Burkhard Dünweg Max-Planck-Institut für Polymerforschung, Mainz, Germany;
Dr. Wolfgang Paul, Dr. Walter Kob Institut für Physik, Johannes Gutenberg-Universität, Mainz, Germany;

4. Statistical Mechanics of Materials with Extreme Nonequilibrium Constraints Lyon, France, August 28-31,2000.
Siegfried Hess, Techniche Universität; Berlin, Germany;
Malek Mansour Université Libre de Bruxelles, Belgium.

5. *SIMU*lations of long time scale dynamics, molecular and continuum descriptions, Rejkavik, Iceland, 26-30 July 2000.
Hannes Jónsson, Chemistry Department, University of Washington Seattle, USA;
Giovanni Ciccotti, Dipartimento di Fisica, Università "La Sapienza", Rome, Italy.

6. Across the Length Scales II: Applications MML2000 , Oxford University, UK, 2000.
Prof David G. Pettifor, Prof Adrian P. Sutton, Dr Robert E. Rudd, Dr Steven D. Kenny; Department of Materials, University of Oxford, UK.

Schools

Methods in Molecular Simulation, summer 2000, to be held in UMIST, Manchester, UK.

Tutorials

1. *SIMU-CECAM* tutorial on Computational Stochastic Methods for Mesoscale Dynamics, Lyon, May 22-24, 2000.
Alejandro L. Garcia Department of Physics, San Jose State University; Florence Baras Center for Nonlinear Phenomena and Complex Systems, Université Libre de Bruxelles.

2. *SIMU-CECAM* tutorial on Car-Parinello molecular dynamics, Lyon, 11-15 September 2000.
Jürg Hutter University of Zurich, Switzeland;
Michiel Sprik University of Cambridge, U.K.

3. *SIMU-CECAM* tutorial on Advanced Monte Carlo simulation techniques, Lyon, 16-20 October 2000.
Berend Smit and Thijs Vlugt, Universiteit van Amsterdam, Netherlands.

Short Visits and Fellowships

The *SIMU* Programme supports individual short visits of up to one week (mainly for senior researchers) and fellowships for younger researchers to spend up to three months in a research group involved in the *SIMU* Programme in a different European country. Either the institute of origin or the receiving institute should be in a countryin which a funding agency contributes to the *SIMU* Programme (currently Belgium, Denmark, Finland, France, Germany, Italy, The Netherlands, Norway, Portugal, Sweden, Switzerland, United Kingdom). All applications for support of a short visit or a fellowship should be made with the attached latex template. Grants for short visits and fellowships are awarded every three months, the dates for 2000 are March 31, June 30, November 15 and December 31. Applications should be sent to:
Professor Michel Mareschal

email: Michel.Mareschal@cecam.fr
CECAM, ENS-Lyon
46, allée d'Italie
69364 Lyon cedex 7
France.

Activities relevant to *SIMU*, organised by other organisations/programmes.

1. Eilat Workshops on: Multiscale Computational Methods in Chemistry, April 5-11, 2000. Interdisciplinary forum of computational mathematicians, physicists and chemists, to study basic computational obstacles in chemistry and advanced multiscale approaches for treating them. For scientific background, general information, current participant list and registration forms, see:
http://www.wisdom.weizmann.ac.il/ achi/conf00/index.html

2. For *CECAM* and *CECAM*-Ψ_k Workhops, see http://www.cecam.fr/

3. "Molecular Simulation IN THE 21st CENTURY", the EPSRC CCP5 Annual Meeting, 2nd-5th July 2000, University of Surrey Guildford, UK. For further information see http://www.dl.ac.uk/CCP/CCP5/meetings/ann2000.html

XII

Jobs, Grants and Fellowships

For more recent information please consult the *SIMU* newsgroup on our web site where most of these offers are available. Feel free to use our site to advertise offers as well.

Post-docs

In the Condensed Matter Theory Sector of the International School for Advanced Studies in Trieste (Italy)

A postdoctoral position is available, starting immediately, for 1 year on a on a project entitled: "Density-functional theory-based molecular dynamics of biological systems." The work will involve applications of the Car-Parrinello to systems of pharmaceutical relevance, such as targets for anti-AIDS and anti-cancer therapy. Candidates should hold a Ph.D in Physics or Chemistry or have equivalent research experience and have good computing and physical modeling skills. Further information can be obtained from Dr. Paolo Carloni, International School for Advanced Studies, SISSA, via Beirut 4, 34014 Trieste, Italy http://www.sissa.it/cm/bc/
email: carloni@sissa.it Phone: +39-040-3787407, Fax:+39-040-3787528

PhD fellowships

Opportunities for research with the Atomistic Simulation Group at Queen's University, Belfast.

QUB expects to be offering studentships for research leading to a PhD starting in October. There may be funding for E.U. students as well as for U.K. students. For more information visit the web site http://titus.phy.qub.ac.uk
or contact Professor Lynden-Bell or Professor Finnis
r.lynden-bell@qub.ac.uk m.finnis@qub.ac.uk